Laboratory of Virology

Department of Virology, Immunology and Parasitology

Faculty of Veterinary Medicine

Ghent University

Interactions of Pseudorabies Virus and Swine Influenza Virus with Porcine Respiratory Mucus

Xiaoyun Yang

Dissertation submitted in fulfillment of the requirement for the degree of

Doctor in Veterinary Sciences, 2015

Promoters: Prof. dr. Hans J. Nauwynck

Prof. dr. Kristien Van Reeth

Yang X. (2015). Interactions of Pseudorabies Virus and Swine Influenza Virus with Porcine Respiratory Mucus

ISBN: 9789058644206

Xiaoyun Yang was supported by a Concerted Research Action of the Research Council of Ghent University

Table of Contents

List of abbreviations

AFM	atomic force microscopy
ASL	airway surface liquid
BoHV-1 and 5	bovine herpesvirus 1 and 5
BRDC	bovine respiratory disease complex
BRSV	bovine respiratory syncytial virus
CHV-1	canine herpesvirus 1
CMC	carboxymethylcellulose
D_a	apparent diffusion coefficient
DABCO	1,4-diazobicyclo-(2,2,2)-octane
Dio	3,3′-Dioctadecyloxacarbocyanine perchlorate
ECM	extracellular matrix
EHV-1 and 4	equine herpesvirus 1 and 4
FHV-1	feline herpesvirus 1
GalNAc	N-acetylgalactosamine
Gal	galactose
HA	hemagglutinin
Hap	haemagglutinin/protease
HI	hemagglutination inhibition
HIV	human immunodeficiency virus
HPLC	high-performance liquid chromatography
HSV	herpes simplex virus
IPMA	immunoperoxidase monolayer assay
IPS	image processing software
M1	matrix 1 proteins
MAA	*Maackia amurensis* agglutinin
MALDI-TOF-MS	matrix-assisted laser desorption/ionization time-of-flight
MDCK	Madin Darby Canine Kidney

MDV	marek's disease virus
MEM	maximum entropy method
MSD	mean squared displacements
MU-NANA	4-methylumbelliferyl-N-acetylneuraminic acid
NA	neuraminidase
Neu5Ac	N-acetylneuraminic acid
Neu5Gc	N-glycolylneuraminic acid
NP	nucleoprotein
ORF	open reading frame
PBS	phosphate buffered saline
PEGylated	polyethylene glycol coupled
PFU	plaque forming units
PRDC	porcine respiratory disease complex
PrV	pseudorabies virus
PVA	pattern of viral attachment
RBS	receptor binding site
RNP	ribonucleoprotein
ROI	region of interest
RSV	respiratory syncytial virus
SA	sialic acid
SHV-1	suid herpes virus 1
sIgA	secretory immunoglobulin A
SIV	swine influenza virus
SNA	*Sambucus nigra* agglutinin
SP-D	Surfactant protein D
SPT	single particle tracking
ST	swine testicular
$TCID_{50}$	mean tissue culture infectious dose
TLC	thin layer chromatography

TRS	terminal repeat sequence
UL	unique long
US	unique short
VCNA	*Vibrio cholerae* neuraminidase
VZV	varicella-zoster virus

Chapter 1

1. Introduction

1.1. Viruses

1.1.1. Pseudorabies virus

1.1.1.1. Classification of pseudorabies virus

Pseudorabies virus (PrV), also called Aujeszky's disease virus or suid herpes virus 1 (SHV-1), is a member of the *Herpesviridae* family. Herpesviruses have a double-stranded DNA genome, similar virion size (200 to 250 nm) and structure (capsid, tegument, and envelope). Based on the host range, replication cycle, genome content and organization, most herpesviruses can be subdivided into three subfamilies including the *Alphaherpesvirinae*, *Betaherpesvirinae*, and *Gammaherpesvirinae*. Alphaherpesviruses are distinguished by the rapid lytic growth, neurotropism, latency in neurons and broad host range (Cohrs & Gilden, 2011; Mettenleiter, 2000; Roizman, 2001). Besides PrV, several other animal pathogens are classified within this subfamily: equine herpesvirus 1 and 4 (EHV-1 and EHV-4), avian Marek's disease virus (MDV), bovine herpesvirus 1 and 5 (BoHV-1 and BoHV-5), canine herpesvirus 1 (CHV-1) and feline herpesvirus 1 (FHV-1). By comparison of deduced amino acid sequences of homologous proteins, PrV was found to be most closely related to BoHV-1, EHV-1, and varicella-zoster virus (VZV) (Daikoku, 2000; McGeoch, 1987).

1.1.1.2. Virion structure

The mature virion or infectious viral particle consists of four morphologically distinct structures (as shown in Figure 1): a linear double-stranded DNA genome, a protective icosahedral capsid forming a nucleocapsid surrounding the DNA, a tegument in which the capsid is embedded and a lipid envelope surrounding the tegument.

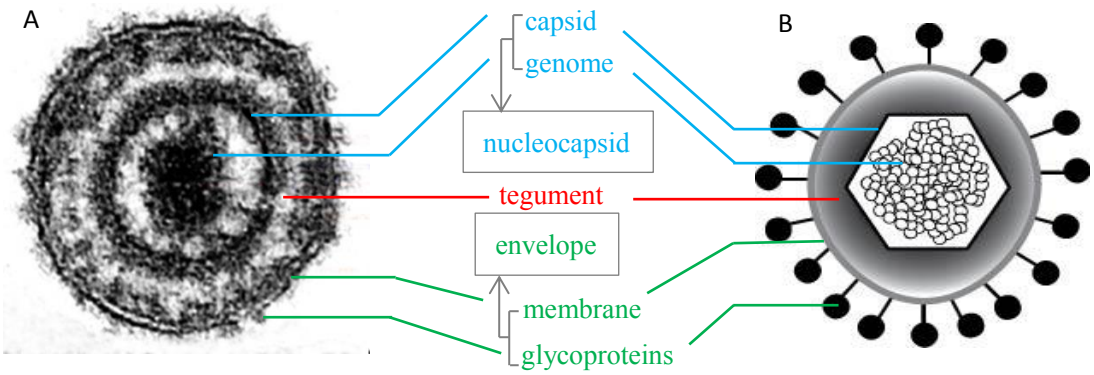

Figure 1. Structure of a pseudorabies virion. (A) Electron microscopy view of a PrV particle. Adapted from (Enquist). (B) Schematic structure of a virion. A PrV viron contains a linear double-stranded DNA genome, a icosahedral capsid forming a nucleocapsid, a tegument in which the capsid is embedded and a lipid envelope surrounding the tegument.

Alphaherpesvirus genomes have a partial colinear arrangement of genes encoding similar proteins in the function. Based on the overall arrangement of repeat sequences and unique regions, the herpesvirus genomes are divided into six classes, designated by the letters A to F. The genome of PrV belongs to the class D genomes of the herpesviruses. The PrV genome is constituted of a unique long (UL) segment and a unique short (US) region bracketed by inverted repeat sequences, an internal repeat sequence (IRS) and a terminal repeat sequence (TRS) (Ben-Porat T., 1985; Klupp *et al.*, 2004). The genome contains 72 open reading frames (ORFs) which encode 70 different proteins. These different genes are designated by a two letter code UL or US depending on its position in the genome unique regions, followed by a number. The number indicates the location of the gene within each specific region.

Most of what is known about the PrV capsid is inferred from detailed studies of the prototypical HSV-1 virion. The major capsid protein (MCP or VP5) is encoded by UL19 and assembles into 162 capsomers arranged in a T=16 icosahedral lattice (Newcomb *et al.*, 1999; Newcomb *et al.*, 1993). The resulting capsid has a diameter of approximately 125 nm. The capsid, together with the enclosed genome forms the nucleocapsid. Each mature capsid contains 955 molecules of UL19(VP5), 900 molecules of UL35(VP26), 640 molecules of UL18(VP23), 320 molecules of

UL38(VP19C), and 12 molecules of UL6 (portal protein) (Homa & Brown, 1997).

The space between the capsid and the envelope is filled with tegument, which consists of viral tegument proteins. At least fourteen tegument proteins have been identified (Guo *et al.*, 2010). Tegument proteins are important during entry, priming the cell for virus replication (Mettenleiter, 2002). Following the fusion of the viral envelope with the plasma membrane, the tegument proteins enter the cell with the capsid and assist in taking over the metabolism of the host cell. The tegument is composed of two distinct structures: an inner layer that is associated with capsid proteins and an outer layer that interacts with the cytoplasmic domains of viral membrane proteins (Grunewald *et al.*, 2003).

The envelope derived from the cell membrane during assembly at trans-Golgi vesicles, is a bilayered phospholipid membrane. It contains 10 glycoproteins (gB, gC, gD, gE, gH, gI, gK, gL, gM, gN) and at least 2 nonglycosylated proteins (p(UL43), p(US9)). gB forms homodimers, and gE/gI, gH/gL and gM/gN form hetero-oligomers (Mettenleiter, 2000). The envelope glycoproteins play an important role in binding, internalization, envelopment, egress, cell-associated spread, induction of protective immunity and immune evasion. Different domains in both the extra- and intra-envelope regions are important for these functions.

1.1.1.3. PrV entry into cells: ligands and receptors

Binding of PrV to cells occurs primarily through an interaction of viral glycoprotein C (gC) with cell surface heparan sulphate. This was discovered by the observation that heparin, a soluble molecule resembling heparan sulphfate, inhibits the adsorption of PrV virions to their target cells (Mettenleiter *et al.*, 1990). Glycoprotein gB is also involved in this binding step, albeit to a lesser extent (Nixdorf *et al.*, 1999). The binding between gC and cellular heparan sulphate is efficient, however, not absolutely essential for the virus infection (Karger *et al.*, 1995; Mettenleiter *et al.*, 1990; Shukla & Spear, 2001). Following this binding, entry requires an interaction of viral gD with one or several cell surface co-receptors (Spear & Longnecker, 2003). These entry receptors that associate with alphaherpesvirus gD can be grouped into three classes:

herpesvirus entry mediator, a member of the tumor necrosis factors (TNF) receptor family; nectin-1 and nectin-2, members of the immunoglobulin superfamily; and specific sites in heparan sulphate generated by certain 3-O-sulfotransferases (Geraghty *et al.*, 1998; Heldwein & Krummenacher, 2008; Montgomery *et al.*, 1996; Shukla *et al.*, 1999; Warner *et al.*, 1998). Up till now, several PrV entry receptors, including herpesvirus entry mediator B (HevB, nectin 2), HveC (nectin-1) and HevD (CD155), have been identified, with nectin-1 being the most effective (Campadelli-Fiume *et al.*, 2000; Geraghty *et al.*, 1998; Mettenleiter, 2002; Nixdorf *et al.*, 1999; Spear *et al.*, 2000; Spear & Longnecker, 2003).

Nectin-1 and nectin-2 belong to a subgroup of the immunoglobulin (Ig) superfamily, based on structural and sequence similarities. They share a similar structure which consists of an ectodomain region containing three immunoglobulim (Ig)-like domains, a single transmembrane region, and a cytoplasmic region. The three Ig-like domains consist of an N-terminal variable (V)-like domain and two constant (C)-like domains (Cocchi *et al.*, 1998). The ectodomain region has the most efficient viral entry activity, independent of the transmembrane region or cytoplasmic tail. The gD-binding region of both nectin-1 and nectin-2 is localized to the V-like domain (Martinez & Spear, 2001). CD155 is a single-pass transmembrane glycoprotein belonging to the immunoglobulin (Ig) superfamily of proteins, commonly known as Poliovirus Receptor (PVR) due to its involvement in the cellular poliovirus infection in primates. CD155 functions in the establishment of intercellular adherens junctions between epithelial cells. The extracellular portion of CD155 is composed of three Ig-like domains: an outermost V-like domain, followed by 2 C-like domains (Lange *et al.*, 2001). The homology between CD155 and nectin-1 is high, and their binding sites on gD may overlap (Fan *et al.*, 2014).

1.1.1.4. Pathogenesis of PrV infection

PrV is the causative agent of Aujeszky's disease. Most mammals, except higher primates, and some avian species are susceptible to PrV infection. The infection occurs naturally in swine species, but is lethal to susceptible non-swine species

(Kocan, 1990). In swine, the severity of the disease depends on strain, age and immunological status of the infected animal. Clinical symptoms range from fatal affliction of the central nervous system in young animals to mild respiratory problems including coughing, sneezing and pneumonia in older pigs. In pregnant sows, infection can cause reproductive failure, such as stillbirth, abortion and mummified fetuses (Kocan, 1990; Nauwynck *et al.*, 2007; Pomeranz *et al.*, 2005).

The common portal of entry of PrV is the respiratory mucosa (Nauwynck *et al.*, 2007). The replication kinetics and characteristics of PrV in the respiratory mucosa can be determined by different factors, such as virus strain, inoculation route, virus load in the inoculum, animal age and genetic and immunological status. In naïve pigs, PrV primarily targets the epithelial cells of the nasal mucosa. Within 24 h it subverts the basement membrane and afterwards infects all sorts of cells including fibrocytes, endothelial cells, and mononuclear cells in the lamina propria (Glorieux *et al.*, 2009; Kritas *et al.*, 1994). Replication in lower parts of the respiratory tract is restricted, except when the virus is administered via aerosol or intratracheal inoculation (Baskerville, 1971; Miry C., 1989). A similar “plaque-wise” spread is also found in tonsils and lungs (Nauwynck, 1997). Lung macrophages have also been identified as target cells (Iglesias *et al.*, 1989). Between 2 and 5 days post inoculation, the virus spreads over the whole mucosa and further into the submucosa. Virus replication induces an enormous influx of phagocytes which inverse attack the infected regions. The resulting destruction causes respiratory signs, such as sneezing, coughing, nasal discharge and dyspnea. The virus becomes neutralized and inactivated from 6-7 days, and is completely eliminated in the nasal cavity from 13 days post inoculation.

1.1.2. Swine influenza virus

1.1.2.1. Classification of influenza virus

Influenza viruses are enveloped, single stranded RNA viruses of the family Orthomyxoviridae. All members contain a segmented, negative-sense, single-stranded RNA genome. The influenza virus types are distinguished by differences in the antigenic properties of the internal nucleoprotein and matrix 1 (M1) proteins, the

number of gene segments, host range and morphological characteristics of the virion. Influenza A viruses are further classified into subtypes based on the antigenicity of their hemagglutinin (HA) and neuraminidase (NA) molecules. Up to date, 18 HA (H1-H18) and 10 NA subtypes (N1-N10) are identified (Tong *et al.*, 2013).

Type A influenza infects a wide variety of animals: pigs, horses, seals, whales, and many different kinds of birds. Type B influenza is confined to the human population, though one isolate of type B infection has been reported in harbor seals (Osterhaus *et al.*, 2000). Influenza C viruses infect both humans and pigs, but do not infect birds. Due to its limited host range and lack of genetic diversity, this influenza virus infection does not cause pandemics (Kida, 1992) (Table 1).

Table 1. Differences of influenza virus subtypes

Differences among Influenza A, B and C viruses			
	Influenza A	Influenza B	Influenza C
Genetics	8 gene segments	8 gene segments	7 gene segments
Structure	10 viral proteins M2 unique	11 viral proteins NB unique	9 viral proteins HEF unique
Host range	Human, swine, equine, avian, marine mammals	Human	Human, swine
Clinical features	Mild to severe disease, large pandemic, significant mortality	Mild to severe disease, no pandemic	Mild disease

HEF: hemagglutination, esterase and fusion activity; NB: membrane protein

1.1.2.2. Virion structure

The virion has spherical or filamentous forms with a diameter ranging between 80 and 120 nm (Harris *et al.*, 2006). The virion consists of three major components: an outer

envelope, the matrix and 8 internal ribonucleoproteins (RNPs) (Fig. 2). The envelope is a lipid bilayer derived from the host cell membrane during virus assembly. It consists of spike glycoproteins HA, NA and the ion-channel M2. HA is a homotrimer composed of three identical subunits, and each HA subunit consists of two disulfide-linked polypeptides. The HA is synthesized as a precursor protein (HA0) which is subsequently cleaved into HA1 and HA2 polypeptides, linked by disulfide bonds. Activation of HA0 cleavage can occur either extracellular by trypsin-like proteases after the virus has been released from the cell or intracellular by furin-like proteases in the trans-Golgi network (Bottcher-Friebertshauser *et al.*, 2010; Zhirnov *et al.*, 2002). Antigenic sites and sites for binding to cellular receptors are located in the globular head of the molecule. The viral NA is an enzyme that catalyzes the removal of terminal N-acetyl neuraminic acid (sialic acid, SA) from glycoproteins or proteoglycans. The NA spike has a mushroom-like shape. Electron micrographs of isolated neuraminidase "heads" are tetramers (Wrigley *et al.*, 1973) and the stalk of the neuraminidase varies in length (Els *et al.*, 1985; Mitnaul *et al.*, 1996). As in HA, the antigenic sites and the enzyme active site are located in the mushroom-shaped head. The M2 protein is an integral membrane protein which is also present in a minor percentage on the viral envelope. Influenza type B virus does not possess the M2 ion channel (Ruigrok, 1998).

Interior to the envelope is the matrix, also called M1 protein, associated with both the envelope and the RNPs. This protein forms frame structure to the virion and is important for virus assembly. The central core of the virion consists of eight nucleocapsid segments. Each nucleocapsid is composed of an RNA segment intimately associated with the viral nucleoprotein (NP), and three polymerase proteins PB1, PB2, and PA bound to one end. More recently, the novel influenza A virus protein PA-X was discovered. PA-X is a fusion protein that incorporates the N-terminal domain of PA (191 amino acids) with a short C-terminal domain (61 amino acids) encoded by an overlapping ORF ('X') in segment 3 that is accessed by +1 ribosomal frameshifting (Jagger *et al.*, 2012). Lastly, NS1 and NS2 (or nuclear

export protein NEP) which were once considered to be non-structural proteins, are present within virions. NS1 helps the viruses escape the anti-viral immune response of the host (Das *et al.*, 2008; Min & Krug, 2006). NS2 mediates the nuclear export of virion RNAs by acting as an adaptor between viral ribonucleoprotein complexes and the nuclear export machinery of the cell (O'Neill *et al.*, 1998). Two non-structural proteins have been identified: PB1-F2 and PB1-N40. The PB1-F2, which is not expressed by all influenza A viruses, may promote apoptosis of monocytes and other immune cells (Chen *et al.*, 2001; Conenello *et al.*, 2007).

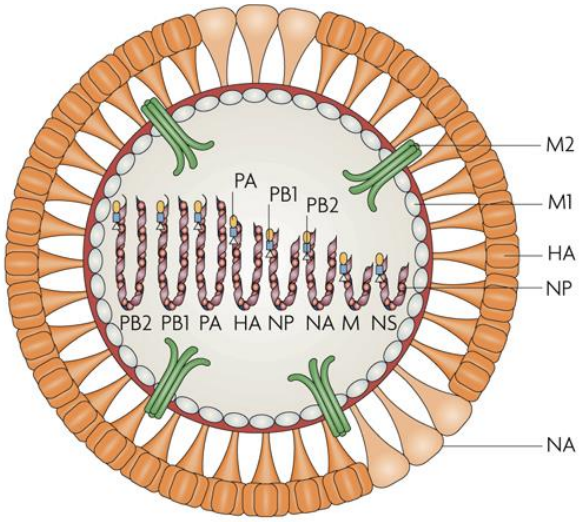

Figure 2. Schematic structure of an influenza A virion. Three viral surface proteins: haemagglutinin (HA), neuraminidase (NA) and M2, comprise the envelope. The matrix protein M1 associates inside the viral membrane. Eight negative-stranded RNA segments are packaged into the particle as ribonucleoproteins in complex with nucleocapsid protein (NP) and the viral polymerases PA, PB1 and PB2. Adapted from (Subbarao & Joseph, 2007).

1.1.2.3. HA as determinant of receptor binding specificity

The influenza viruses attach via the HA protein to sialylated glycan receptors to infect host cells. HA is a homotrimeric type I transmembrane protein with an ectodomain composed of a globular head and a stem region. Each HA subunit is composed of two disulfide bond-linked chains, HA1 and HA2, which are formed by proteolytic cleavage of the HA0 precursor. The binding activity of influenza viruses for different SA-Gal linkage types is mainly determined by the receptor binding site (RBS) which is located in the globular head of HA1. The amino acid residues making up this RBS

are in general located at similar amino acid positions, regardless the virus subtype.

Receptor binding specificity is primarily distinguished by recognition of the terminal sialic acid and its linkage to the vicinal galactose of carbohydrates. Influenza viruses were first described in 1941 to be able to agglutinate and elute from red blood cells (Hirst, 1941). This ability was subsequently found to be sialic acid dependent by the treatment of the red blood cells with *Vibrio cholerae* neuraminidase (VCNA) (Gottschalk, 1957). Later on, by using red blood cells and cells expressing only a certain type of SA, the HA of human and animal influenza viruses are described to have different receptor specificity (Rogers & Paulson, 1983). Apart from hemagglutination assay with resialylated cells, receptor binding specificity of influenza viruses has also been studied by a solid-phase virus binding assay with sialo-glycoconjugates (Gambaryan & Matrosovich, 1992), a thin layer chromatography (TLC) virus overlay assay with sialo-glycoconjugates (Muthing & Unland, 1994), and by glycoarray analysis with synthetic and natural glycans (Stevens *et al.*, 2006a; Stevens *et al.*, 2006b). Overall, the HA of human influenza viruses attach to sialic acids that are α2,6 linked to galactose (Gambaryan *et al.*, 1997; Matrosovich *et al.*, 2000); pig influenza viruses either attach to both α2,3-SA and α2,6-SA, or exclusively to α2,6-SA (Rogers & Paulson, 1983), while avian influenza viruses have a preference for sialic acids that are linked to the galactose in an α2,3 linkage (Nobusawa *et al.*, 1991; Rogers & Paulson, 1983). These gross differences in receptor binding properties are important determinants of virus host range and cell and tissue tropism. Furthermore, the development of printed covalent glycan arrays by the Consortium for Functional Glycomics allows a clear differentiation of what sugar structures bind to a given lectin (Blixt *et al.*, 2004). Binding assays which allow the investigation of hundreds of different sialylated glycan structures, have demonstrated that influenza virus receptor specificity also involves structural modifications of the sialic acid and overall glycan (Gambaryan *et al.*, 2005; Stevens *et al.*, 2006b).

1.1.2.4. Influenza virus receptors

Sialic acids (SA) are derivatives of neuraminic acid. Neuraminic acid is a negatively

charged nine-carbon sugar that contains a pyranose ring with a carboxylic group, an amino group and a glycerol tail. The N-acetyl derivative of neuraminic acid is shown in Figure 3. N-acetylneuraminic acid (Neu5Ac) and N-glycolylneuraminic acid (Neu5Gc) are the most prevalently terminal SAs found in mammals (Varki & Varki, 2007). The latter are abundantly present in pig, horse, mouse and a number of bird species, but humans and some avian species like chicken or other poultry, do not contain Neu5Gc or only minor quantities (Chou *et al.*, 1998; Muchmore *et al.*, 1998; Schauer, 2009; Walther *et al.*, 2013).

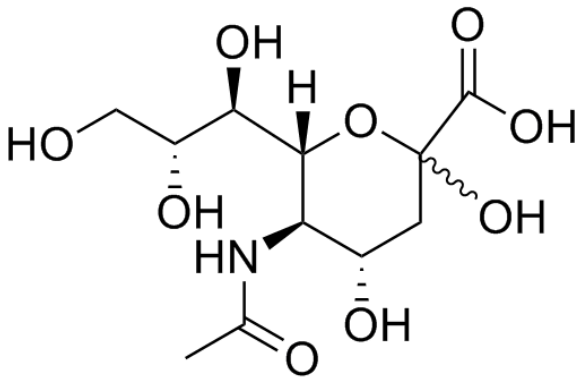

Figure 3. Chemical structure of N-acetylneuraminic acid

Lectin histochemistry is the most common method to determine the receptor distribution pattern in tissue sections. Plant derived lectins, such as *Sambucus nigra* agglutinin (SNA) and *Maackia amurensis* agglutinin (MAA), specifically recognize and bind α2,6-SA and α2,3-SA, respectively. There are two different isotypes of MAA: MAA-1 (also known as MAL or MAM) and MAA-2 (also known as MAH). MAA-1 binds primarily to SAα2,3Galβ1-4GlcNAc that is found in N-glycans and O-glycans. MAA-2 preferentially binds to SAα2,3Galβ1-3GalNAc in O-glycans. An alternative method to study sialic acid receptors is determination of the pattern of viral attachment (PVA) by virus histochemistry (van Riel *et al.*, 2007; van Riel *et al.*, 2010). Besides sialic acids, the overall glycan structures, including the number of glycan branches, fucosylation, and the presence of N-acetyllactosamine repeats, can influence influenza virus receptor binding. This encouraged further elucidation of the glycome of the respiratory tissue of different influenza virus host species. A method

using high-performance liquid chromatography (HPLC) coupled with matrix-assisted laser desorption/ionization time-of-flight (MALDI-TOF-MS) has been developed to determine the precise N-glycan structures and quantitative analysis of those N-glycans. N-glycans derived from tissues of interest were enzymatically released, fluorescent labeled, separated according to charge, size and hydrophobicity, and structurally identified by a two-dimensional (size and hydrophobicity) HPLC mapping technique and MALDI-TOF mass spectrometry before and after exo-glycosidase digestion (Walther *et al.*, 2013).

Table 2. Sialic acid expression in different tissues of different species

		SA expression in tissues determined by lectin histochemistry							
		Nasal mucosa	Nasopharynx	Trachea	Bronchi	Bronchiole	Alveolar cells	Intestine	Colon
Human	α2,3	+→+++	+→+++	+→+++	+→+++	+++	+++	ND	ND
	α2,6	+++	+++	+→+++	+→+++	+→++	+	ND	ND
Swine	α2,3	-→++	-→++	-→++	-→++	-→++	+→ +++	ND	ND
	α2,6	+++	+++	++→ +++	++→ +++	+++	+→ +++	ND	ND
Chicken	α2,3	++	++	+	+++	+++	+++	+++	++
	α2,6	+	+	+	++	++	++	+	+

ND: not determined

The expression pattern of α2,6-SA and α2,3-SA variants differs between animal species and different tissues and cell types within one species. An overview of the receptor distribution in different species and tissues is shown in Table 2. In humans, α2,6-SAs are expressed more abundantly in the upper respiratory tract compared to the lower respiratory tract, and α2,3-SAs are widely expressed in the respiratory tract of humans. Both α2,6-SAs and α2,3-SAs were found in ciliated epithelium, goblet cells and submucous glands in the bronchus as well as pneumocytes of the alveoli

(Nicholls *et al.*, 2007). Pigs, though considered to be a "mixing vessel" of human and avian influenza viruses, possess similar sialic acid distribution to the human tissues (C., 1990; Ito *et al.*, 1998; Nelli *et al.*, 2010; Van Poucke *et al.*, 2010). The α2,6-SAs were expressed dominantly along the porcine upper respiratory lining. There was a progressively increased expression in α2,3-SA from the bronchi down to the alveoli. The α2,3-SA receptors were more dominantly expressed in the epithelial lining of the lower respiratory tract (bronchioles and alveoli) (Nelli *et al.*, 2010). Avian species have α2,3-SA and α2,6-SA in both the respiratory and intestinal tract, although there are differences in the abundance of these receptors between different species (Costa *et al.*, 2012; Franca *et al.*, 2013; Kimble *et al.*, 2010). Both α-2,3 and α-2,6 receptors were present in the respiratory and intestinal tracts of the chicken, common quail, red-legged partridge, turkey, and golden pheasant. In ostriches, the expression of the receptor was basically restricted to α-2,3 in both the respiratory and intestinal tracts.

1.1.2.5. Structure, function and role of neuraminidase

The receptor-destroying activity of influenza virus was first observed by Hirst (Hirst, 1941) and the substrate was identified by Gottschalk as N-acetylneuraminic acid, one of the sialic acids, thus designating the enzyme as neuraminidase (sialidase) (Gottschalk, 1957). Later on, neuraminidase "heads" released by pronase from a number of strains of H2N2 and H3N2 influenza virus were crystallized (Laver, 1978). Fig. 4A shows the three-dimensional (3D) structure of influenza A neuraminidase. The NA is a tetramer of 4 identical polypeptides partially stabilized by metal ions bound on the symmetry axis. Each polypeptide contains about 470 amino acids arranged in four domains, an N-terminal cytoplasmic sequence, followed by a membrane-anchoring transmembrane domain and a hypervariable stalk, connecting to a globular "head" domain that houses the enzyme active site (Fig. 4B). Sequences of neuraminidase from influenza A and B strains can differ by as much as 75%. Nevertheless, some residues scattered along the neuraminidase polypeptide are totally conserved among all strains. The structure of the NA globular head domain is remarkably conserved across subtypes. Additionally, it is recently reported that an

eight amino acid fragment in the NA active site is 100% conserved in all influenza A virus subtypes as well as in the NAs of influenza B strains (Doyle *et al.*, 2013a; Doyle *et al.*, 2013b). This amino acid sequence, "ILRTQESEC", is located between residues 222 and 230 (N2 numbering) in the enzymatic active site. When the linear neuraminidase polypeptide folded into its three-dimensional structure, these conserved residues all came together and clustered on the rim and walls of the pocket. These pockets were identified as the catalytic sites by soaking substrate (sialic acid) into neuraminidase crystals and solving the structure of the complex (Varghese *et al.*, 1983). There are 40–50 NA spikes per virion and these occur in clusters amidst 300–400 hemagglutinin (HA) spikes on an average sized virion of diameter 120 nm. The highly conserved structure of NA active site makes it an ideal target for structure-based drug design.

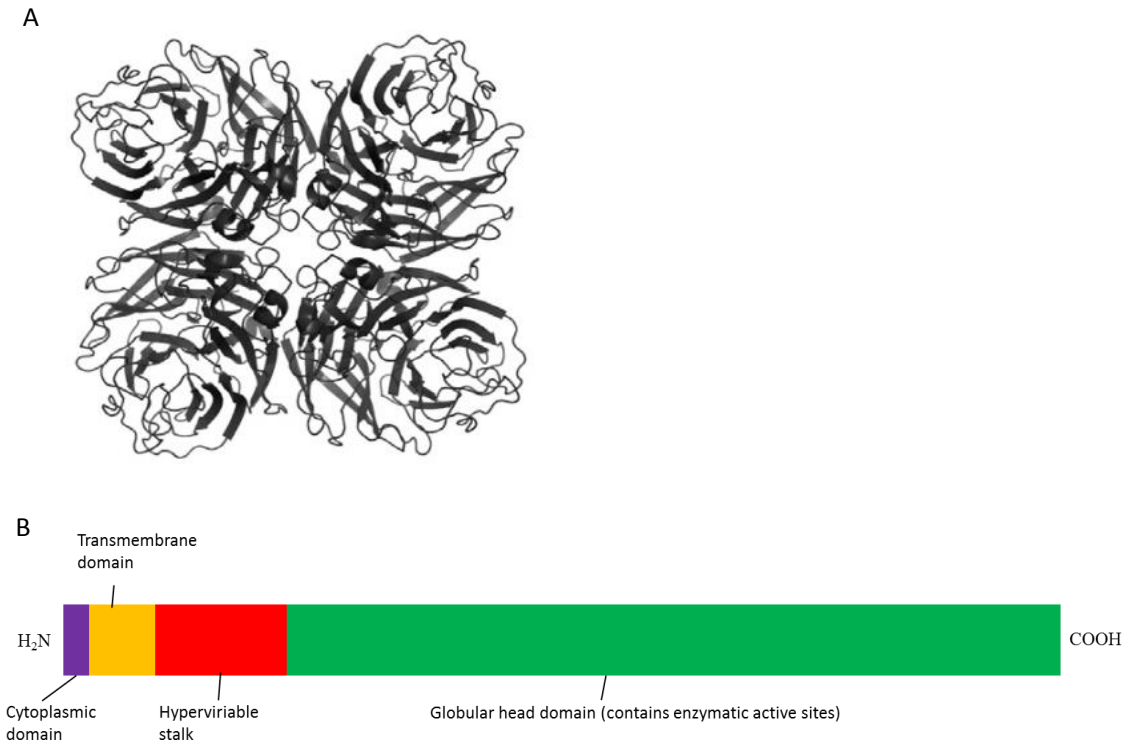

Figure 4. The structure of influenza A Virus NA is highly conserved. (A) 3D crystal structure of the globular head domain of the NA from A/Brevig Mission/1/1918 (H1N1) (PDB ID: 3B7E), shown as a tetramer. (B) Schematic of the NA protein showing the cytoplasmic, transmembrane, hypervariable stalk, and globular head domains, using amino acid residue numbering from the NA of A/Brevig Mission/1/1918 (H1N1). Adapted from (Wohlbold *et al*, 2014).

Substrate specificity assays showed that all influenza viruses had similar specificities for α2,3-linked sialic acid. Avian and early N2 human viruses showed marginal activities for α2,6-linked sialic acid. The swine and human viruses cleave α2,6-linked sialic acid more efficiently than the avian viruses, but the activity does not exceed the one that cleaves α2,3-linked sialic acid (Kobasa *et al.*, 1999). NA is needed for the successful detachment of newly formed progeny virus particles from host cells (Wagner *et al.*, 2000). Secondly, NA may promote virus entry into target cells during the initial stage of infection (Ohuchi *et al.*, 2006). Moreover, the enzymatic activity of NA is considered to facilitate influenza virus infection by penetrating respiratory tract mucus and cleaving decoy receptors from the glycocalyx of epithelial cells (Cohen *et al.*, 2013).

1.1.2.6. Pathogenesis of SIV infection

Up to 50% of the acute outbreaks of respiratory disease in pigs on commercial farms are caused by SIV or by a combination of SIV with bacteria (Loeffen *et al.*, 1999). SIV infection is generally limited to the epithelial cells of the respiratory tract, especially the nasal mucosa, tonsils, trachea and lungs. The infection in the bronchi, bronchioles and alveoli is the most severe, and the virus load can reach up to 10^8 mean tissue culture infectious dose ($TCID_{50}$) per gram (Heinen *et al.*, 2000; Van Reeth *et al.*, 1999). The virus is shed via nasal secretions and transmitted through nasal virus shedding, pig-to-pig contact and aerosol formation (Van Gucht *et al.*, 2006). The disease spreads rapidly in a herd, whereas the virus can be cleared within 1 week after infection (Van Reeth, 2007).

All three virus subtypes (H1N1, H3N2, H1N2) can cause swine influenza, with no distinguishable differences in virulence between subtypes or strains. Morbidity is high but mortality is low. Only when immunological naïve pigs are infected, the animals display typical symptoms characterized as fever, anorexia, lethargy, nasal and ocular discharge, coughing, sneezing and dyspnea. This clinical appearance can be observed following both a natural infection and an experimental intratracheal inoculation with a high virus dose. The animals recover within 1 week after onset of the disease

(Kitikoon *et al.*, 2006; Van Reeth, 2007). However, subclinical influenza virus infections occur frequently and pigs can be infected with one or more influenza virus subtypes without showing clinical signs (Maes *et al.*, 2000; Olsen, 2006).

1.2. Airway mucus and its contribution to innate immunity

Epithelial surfaces including the respiratory, gastrointestinal and urogenital tracts in contact with the outer environment are protected by mucus layers. Although possessing common properties such as heterogeneous in the composition and viscoelastic, the airway mucus may have co-evolved with its host and obtained unique functions to exclude the host-specific pathogens.

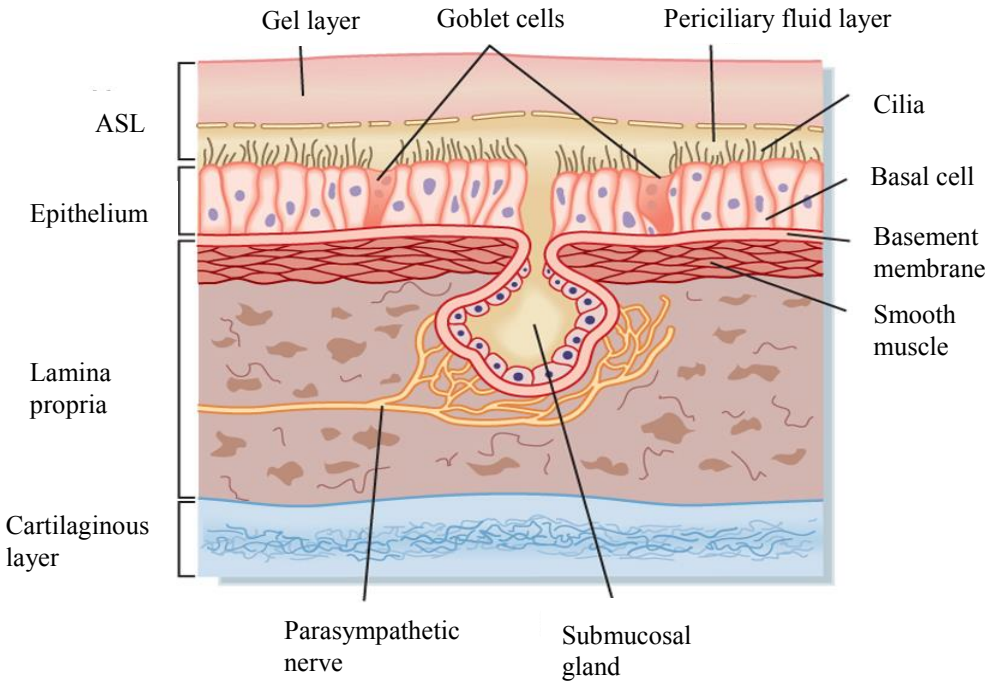

Figure 5. Schematic structure of respiratory mucosa. The apical epithelium is lined by a thin layer of airway surface liquid produced by goblet cells and submucosal gland mucous cells. The cilia of the epithelial cells reside in the periciliary fluid layer with the mucus on top. Interspersed between the ciliated epithelial cells are surface secretory (goblet) cells and submucosal glands. Adapted from (Bruce M. Koeppen).

1.2.1. Airway mucus and its thickness

Airway mucus is heterogeneous, viscoelastic biogel that lines the respiratory tract. The latter consists of the mucus (gel) layer, the periciliary fluid or sol layer,

epithelium, basement membrane and lamina propria from the lumen (Fig. 5). Together with the underlying periciliary fluid, the mucus layer forms the airway surface liquid (ASL). Mucus is the secretory production of the goblet cells as well as the submucosal glands, which are located between the spiral bands of smooth muscle and the cartilage plates. The gel layer contains a high concentration of oligomerized glycoproteins, and is therefore highly viscous and elastic. The periciliary fluid contains mainly non-oligomerized glycoproteins, thus it possesses lower viscosity and elasticity (Van der Schans, 2007).

The thickness of the mucus varies strongly and is dependent on the species, location in the respiratory tract, methods of measurement and the presence of a pathologic condition. It is believed that the periciliary fluid layer has a depth equal to the length of the cilia, 5-10 μm (Derichs *et al.*, 2011; Widdicombe *et al.*, 1997). However, the mucus gel thickness is controversial. Due to technical limitation, differentiating gel and sol phases is practically impossible. Therefore, the thickness of gel and sol phases, which together forms the airway surface liquid, is normally taken together in one measurement. As summarized in Table 3, there is remarkable variability in the thickness of the airway surface liquid depending on species, locations and methods of measurement. Generally, the airway surface liquid in large airways is thicker than the one in small airways; the mucus under pathological conditions is thicker than that in healthy individuals; it is not correlated with the size of animals. For instance, the thickness of the airway surface liquid in healthy humans varies between 10 and 30 μm in the trachea and between 2 and 5 μm in the bronchi, while in cystic fibrosis patients, the mucus layer is much thicker, ranging between 10-55 μm (Button *et al.*, 2008; Johnson, 2011). The airway surface liquid of the rapidly frozen bovine trachea was as thin as 20 μm measured by low temperature scanning electron microscopy (Wu *et al.*, 1998), whereas, the airway surface liquid of guinea pig trachea was more than 100 μm thick after creating a small window in the trachea and scanning through the ASL with an electrode (Rahmoune & Shephard, 1995).

1.2.2. Mucociliary beating and mucus transport

Mucociliary clearance is a critical host defense mechanism of the airways, which is an outcome of cilia beating in the mucus layer. Mucus traps inhaled particles and is transported by ciliated cells towards the pharynx where it gets swallowed. Upon arrival in the stomach, the pathogens become degraded by the low pH and enzymes. Effective mucociliary clearance requires both appropriate mucus production and coordinated ciliary beating. The mucus flow rate is influenced by the thickness of the periciliary fluid layer, frequency of the ciliary beating, airflow, inflammations and the viscoelasticity of the mucus.

Table 3. Thickness of airway surface liquid in the trachea of different species

Species	Methods	Thickness (μm)	Reference(s)
Sheep	Light microscopy	33±5	(Seybold *et al.*, 1990)
Guinea pig	Microelectrode manipulation	87±51	(Rahmoune & Shephard, 1995)
Bovine	Rapid freezing/electron microscopy	23±6	(Wu *et al.*, 1998)
Mouse	Confocal fluorescence microscopy	45±5	(Jayaraman *et al.*, 2001)
Human	Confocal fluorescence microscopy	55±5	(Jayaraman *et al.*, 2001)

The thickness of the periciliary layer provides the critical distance that allows optimal ciliary contact with the mucus layer above. Under normal conditions, the cilia beat while completely immersed in periciliary fluid, with only the tips of the cilia coming in contact with the mucus blanket. If the serous fluid is too deep or too shallow, the mucociliary clearance rate will decrease (King *et al.*, 1993).

Airway mucus rheology also plays an important role in maintaining the mucociliary

clearance. The elasticity of mucus is important for clearance by cilia because it efficiently transmits energy, with little energy loss. An increased viscosity of the mucus results in energy loss, but is necessary for mucus to be displaced and either expectorated or swallowed. The ratio of viscosity to elasticity is an important determinant of mucociliary clearance. Increasing viscosity at constant elasticity can cause a decreased mucociliary clearance rate. A balance between these factors must be maintained for optimal mucociliary clearance (King, 1998).

Another key determinant of the rate of mucociliary clearance is the ciliary beating amplitude and frequency that determine maximal velocity at the tips of the cilia, which is important for the maximal forward velocity of the mucous layer. The beating of groups of neighboring cilia is coordinated into “metachronal waves” as a result of a similarity in viscous forces experienced by the cilia at a given location. In principle, the faster the cilia beat, the higher the mucociliary clearance rate and the longer cilia are, the faster they clear mucus because they can generate greater forward velocities. The density or spacing between cilia probably also affect the mucociliary clearance rate because the greater the distance between the cilia, the more energy will be dissipated in the mucus, reducing the net forward velocity (King, 2005).

Infections can impair the mucociliary clearance. It is recently reported that pneumococci infections cause severe lesions in the F-actin cytoskeleton that affect both the architecture and the mechanical stability of the ciliated respiratory epithelium. The disintegration of the epithelium together with weakened mechanical stability consequently causes turbulence in the mucus flow, resulting in a hampered mucociliary clearance (Fliegauf *et al.*, 2013).

Due to the mucocilary clearance, the mucus is renewed rapidly. In the healthy maxillary sinus, the mucus layer is renewed as fast as every 20 to 30 min. The nasal mucus is cleansed and replaced within 10 min, and lower respiratory mucus is transported up and out of the lungs at rates of ~100 μm/s, clearing the lungs within minutes to hours in humans (Cone, 2009). This rapid turnover adds to the protective features of the mucosa.

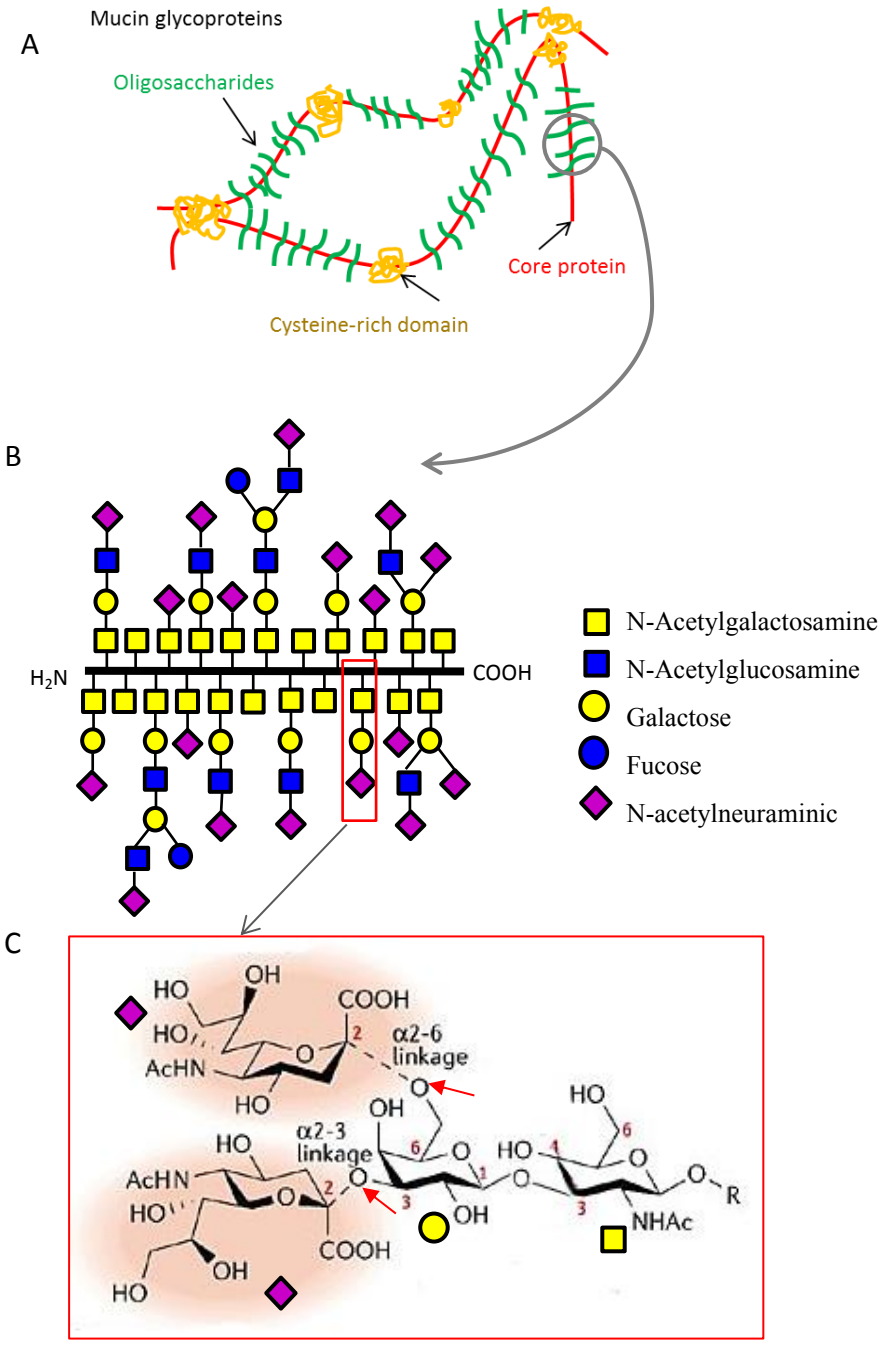

Figure 6. Schematic structure of mucin glycoproteins. (A) Polymeric mucins are exceedingly large molecules (up to 50 MDa in the molecular weight), consisting of up to 20 monomers. A mucin monomer has several glycosylated domains which are separated by non-glycosylated domains (yellow) containing approximately 10 cysteines out of 110 amino acids. Glycans (green) are O-linked via N-acetylgalactosamine (GalNAc) to the hydroxyl groups of serine or threonine residues of the mucin backbone (red). (B) A side chain oligosaccharide consists of 1 to 20 sugar monomers, which starts with GalNAc and mostly terminates with N-acetylneuraminic acids. (C) Chemical structure of a mucin side chain oligosaccharide marked in B. The terminal N-acetylneuraminic acid is α2,3- or α2,6-linked to Galactose (Gal). The linkages (red arrows) are the target sites of neuraminidase.

1.2.3. Composition of mucus

a) Mucins

Heavily o-glycosylated glycoproteins, known as mucins, are the major component of mucus. Mucin content usually ranges between 2 and 5% by weight in healthy individuals for gastrointestinal, cervical, ocular, nasal, and lung mucus despite significant differences in glycosylation (Lai *et al.*, 2009; Thornton *et al.*, 2008). A mucin monomer has several 'PTS' (proline, threonine and serine) domains which are highly glycosylated with glycans covalently linked via N-acetylgalactosamine (GalNAc) to the hydroxyl groups of serine or threonine residues of the mucin backbone. The sugar chains, containing 1 to 20 sugar monomers, are mostly terminated with N-acetylneuramic acids (Rose & Voynow, 2006; Thornton *et al.*, 2008) (Fig. 6A and B). The N-acetylneuraminic acids are attached to either galactose or N-acetylglucosamine units via α2,3- or α2,6-linkages, which can be catalyzed by neuraminidase (Fig. 6C).

Seven mucin-encoding genes (Muc1, Muc2, Muc4, Muc5ac, Muc5b, Muc6 and Muc13) have been identified in the porcine respiratory tract, of which Muc1, Muc4 and Muc13 encode membrane associated mucins (Kim *et al.*, 2012a; Kim *et al.*, 2012b) and the rest express the secreted, gel-forming mucins. Membrane bound mucins consist of a large, heavily O-glycosylated extracelluar domain at the N-terminal, a single and short transmembrane domain and a C-terminal cytoplasmic domain (Constantinou *et al.*, 2011). The extracelluar domain is often cleaved by proteolysis that allows it to be shed from the cell. Transmembrane mucins play important biological roles in cell signaling, through extracellular domain-mediated ligand binding or by interacting with receptors for growth and differentiation factors. Four secreted mucins are expressed in the pig airways: MUC2, MUC5AC, MUC5B and MUC6 (Kim *et al.*, 2012a; Kim *et al.*, 2012b). In general, the genes and corresponding proteins of secreted mucins are much larger than those of cell-associated mucins. Polymeric mucins isolated from airway secretions share a common macromolecular organization. These polymers consisting of between 2 and 20 subunits, are polydisperse in mass (2-50 MDa) and length (0.5-10 μm) and have a

random-coil conformation in solution. Secreted mucins contain characteristic cysteine rich domains (also referred to as disulfide rich domain), which are involved in mucin oligomerization, a property essential for their mucus gel-forming ability (Cone, 2009). In the normal respiratory tract, the secreted mucins, MUC5AC and MUC5B, provide the major framework of the airways mucus gel and are determinants of mucus rheological properties. The two major sources of airway mucus are epithelial goblet cells that produce predominantly MUC5AC, and mucous cells of the submucosal glands that secrete MUC5B (Rose & Voynow, 2006; Thornton *et al.*, 2008).

b) Lipids

The airway surface liquid contains neutral lipids, phospholipids and glycolipids. These lipids are located mainly in the surfactant layer between the periciliary fluid and the mucus gel layer (Kim *et al.*, 1997; Nadziejko *et al.*, 1993). These lipid molecules are associated with mucins prior to exocytosis, probably within the secretory granules. Several reports (Baseman *et al.*, 1980; Bhaskar *et al.*, 1986; Jacquot *et al.*, 1992; Jozwiak *et al.*, 1984) have demonstrated that phospholipids, glycosphingolipids, glycerides and sterols were associated to mucins isolated from supernatants of animal and human tracheal explants or airway epithelial cell cultures. The amount of lipids ranges from 5-15% of the dry material.

c) Antimicrobial agents

The respiratory tract mucosa plays an important role in innate immunity by constituting a physical barrier to microorganisms as well as by producing an array of defense effector molecules. In addition to their protective actions against invading microorganisms and the destructive effects of microbial and host proteinases on the epithelium, these defense effector molecules may regulate innate and adaptive immunity. The best studied antiviral molecules present in the airway secretions include defensins, secretory leukocyte protease inhibitor, lactoferrin, collectin and so on (Lillehoj & Kim, 2002; Tjabringa *et al.*, 2005).

Defensins are small (3 to 5 kDa in size) antimicrobial and antiviral proteins secreted

by neutrophils and epithelial cells. They have been extensively demonstrated to protect the skin and mucosal membranes of the respiratory, genitourinary and gastrointestinal tracts against microbial infections. Mammalian defensins can be classified into three subfamilies (α, β and θ-defensins) based on the arrangement of the canonical six cysteine motif and the disulfide bridges that stabilize the β sheet structure (Ganz, 2003; White *et al.*, 1995). The α-defensins are produced by neutrophils, Paneth cells in the crypts of the small intestine and by epithelial cells of the female genital tract (Fang *et al.*, 2003; Lundy *et al.*, 2004; Muller *et al.*, 2002). β-Defensins are secreted by epithelial cells, and they are expressed at high levels the respiratory tract (Harimurti *et al.*, 2011; Hiratsuka *et al.*, 1998; Yanagi *et al.*, 2005). Up till now, only β-defensins have been identified in pigs (Sang *et al.*, 2006; Veldhuizen *et al.*, 2008). Defensins have a dual role in antiviral activity. One aspect of antiviral activity involves direct interaction with viral envelopes, and the other involves indirect antiviral activity through interactions with potential target cells. These defensin-cell interactions are complex and possibly mediated by interacting with cell-surface glycoproteins and/or interfering with cell-signaling pathways that are required for viral replication.

Secretory leukocyte protease inhibitor is an abundant antimicrobial protein of the airway secretions and as such is thought to play an important role in protecting the hosts from microbes. The antimicrobial activity of the secretory leukocyte protease inhibitor has been shown to reside in the N-terminal domain of the protein (Doumas *et al.*, 2005; Reviglio *et al.*, 2007) and may be mediated via the cationic charge of secretory leukocyte protease inhibitor, which would allow it to disruptively interact with the microbial cell membrane. In addition, secretory leukocyte protease inhibitor can inhibit human immunodeficiency virus (HIV) replication in monocytes and it has recently been shown that secretory leukocyte protease inhibitor binds the annexin II protein on the surface of macrophages, an important cellular cofactor supporting HIV infections (Ma *et al.*, 2004; Wahl *et al.*, 1997).

Lactoferrin, a member of the transferrin family, is one of the most abundant

antimicrobial proteins secreted into the airway lumen (Dubin *et al.*, 2004). It is also present in milk, saliva, tears, seminal fluid, endocervix and vaginal secretions (Baker & Baker, 2004; Dubin *et al.*, 2004; Kutta *et al.*, 2008). Lactoferrin is an important host defense effector against pathogenic microorganisms and has also been shown to be capable of inhibiting replication of a wide range of viruses. Lactoferrin either directly binds to virus particles, as described for HCV (Iwasa *et al.*, 2002), polio- and rotavirus (Superti *et al.*, 1997; Superti *et al.*, 2001), HSV (Fujihara & Hayashi, 1995; Jenssen *et al.*, 2008) and HIV (Berkhout *et al.*, 2002), or binds to the viral cellular receptor or co-receptors, thereby preventing the virus entry or replication. For instance, lactoferrin has been reported to bind HSPGs which tend to be used as primary receptor by many viruses.

Surfactant protein D (SP-D) is a member of the collectin family of the mammalian C-type lectins present in the lining fluid of the respiratory tract (Grubor *et al.*, 2006). There is increasing evidence that collectins are involved in innate host defense against various bacterial, fungal, and viral pathogens. Collectins form multimeric structures resembling C1q (the first component of the complement cascade), and consist of collagenous N-terminal domains and globular C-terminal, carbohydrate binding domains (Crouch *et al.*, 2005; Lim *et al.*, 1994). SP-D is produced primarily by alveolar type II cells in the alveolar level of the lung, and by tracheobronchial glands and nonciliated bronchiolar cells in the proximal lung (Schmiedl *et al.*, 2009). SP-D binds to alveolar macrophages and increases macrophage association with gram-negative bacteria (Pikaar *et al.*, 1995). In addition, SP-D forms a part of the defense against influenza virus (IAV) infection. It is recently shown that recombinant porcine SP-D has antiviral activities against a broad range of IAV strains mainly by preventing the virions from binding to their target cells *in vitro* (Hillaire *et al.*, 2011), as well as by reducing viral replication and spread *ex vivo* (Hillaire *et al.*, 2014).

1.2.4. Mucus barrier to infection

Airway mucus plays a crucial role in protecting the respiratory mucosa from diverse pathogens, noxious particles and inhaled gases. Some of this protection is

physical-mucus forms a highly glycosylated, crosslinked network that inhibits or delays via its viscosity the migration of pathogens. Some protection is chemical-mucins may bind to the traversing pathogens, thereby inhibiting their invasion. Moreover, mucus presents a vast array of antigenically active oligosaccharides that serve as recognition sites for surface receptors of bacteria and viruses. However, pathogens may have developed unique strategies to overcome the mucus barrier. As different types of mucus share similar mucin content and viscoelastic properties, they may exert resembling mechanisms to affect different pathogens including viruses, bacteria and parasites. Thus, interactions of bacteria and parasites, besides viruses, with the corresponding types of mucus they may contact, will be reviewed and discussed in this part.

1.2.4.1. Viruses and mucus

Most viruses initiate their infection at the mucosal surface of the respiratory tract, gastrointestinal tract, eye and/or cervical vagina which are coated by mucus. The interactions between virus and mucus have not been well demonstrated. Further, information about how respiratory viruses interact with the airway mucus is still lacking. Up till now, only a few data converning the virus interaction with human cervicovaginal mucus or porcine gastric mucins are available. It is reported that two capsid virus-like particles, human papillomavirus (55 nm) and Norwalk virus (38 nm) (Olmsted *et al.*, 2001), diffused rapidly in human cervicovaginal mucus. In contrast, large, enveloped viruses such as herpes simplex virus (HSV) (Lai *et al.*, 2010), and HIV (Shukair *et al.*, 2013) were highly trapped in the cervicovaginal mucus. It is hypothesized that the small capsid viruses could drill their way through the mucus because of the neutral charge of viral capsids and probably also due to their size. On the other hand, another research group analyzed the mobility of human papillomavirus in reconstituted porcine gastric mucin solution, and found that the virus was severely hindered. They further discovered that the gastric mucin solution was able to protect an underlying cell layer from infection by human papillomavirus, Merkel cell polyomavirus, and a strain of influenza A virus (Lieleg *et al.*, 2012). Due to the lack

of information, in-depth investigations will be needed in order to unravel mechanisms behind virus diffusion or immobilization in mucus.

Mucins display many kinds of side chain glycans that are found on the cell surface. For instance, sialic acids, which are used by influenza viruses, reoviruses, adenoviruses, enteroviruses, and coronaviruses for binding, are present both at the epithelial surface and on mucins. Whereas, little information exists on whether and how viruses cope with the mucin carbohydrates to avoid attaching to the decoy receptors, and how this affects their pathogenicity.

1.2.4.2. Bacteria and mucus

The mucus layer and its components form part of the innate defense against pathogens, various kind of bacteria have evolved remarkable strategies to circumvent (or even subvert for their own advantage) this barrier.

First, mucins may serve as a primary target for bacteria to colonize. Mucin glycoproteins polymerize, forming a framework to which certain microbial populations can adhere. The best studied example of mucus-targeting bacterial adhesins is the mucus-binding protein, MUB, produced by *Lactobacillus reuteri* (Mackenzie *et al.*, 2010). The MUB protein contains repeated functional domains, referred to as Mub domains, which are responsible for the protein's adhesive properties. In addition, various carbohydrate moieties have been identified as receptors for *Pseudomonas aeruginosa* adhesion (Hazlett *et al.*, 1993; Prince, 1992).

Secondly, bacterial pathogens typically breach the mucus layer by employing mucus degradative enzymes, which destabilize the mucus as well as removing mucin decoy carbohydrates for bacterial adhesins. Mucinases (mucin degrading enzymes), sialidases, N-acetyl neuraminate lyases, glycosulfatases, and sialate o-acetylesterases are some of the mucinolytic enzymes produced by a broad spectrum of bacterial pathogens (Corfield *et al.*, 1992; Haider *et al.*, 1993; Homer *et al.*, 1994). For example, *Vibrio cholerae* expresses haemagglutinin/protease (Hap) which has mucinolytic activity (Silva *et al.*, 2003). The Hap mucinase was shown to detach the *Vibrios* from adhering to a mixed form of mucins consisting of MUC2, MUC3 and

MUC5AC serected by cultured HT29-18N2 cells (Benitez *et al.*, 1997).

Last but not least, chemotaxis and flagellar motility facilitates the pathogens to colonize and penetrate the mucus barrier. Flagellation is a shared characteristic of the majority of successful mucosal pathogens that are highly motile, such as *Campylobacter jejuni* and *Helicobacter pylori*. Motility, along with the corkscrew morphology of these bacteria, allows them to drill their way through the mucus layer to reach the epithelium. Indeed, *Helicobacter pylori* that have dysfunctional flagella show a clearly reduced ability to infect (Ottemann & Lowenthal, 2002). The elevation pH, which triggers the transition from gel to sol of gastric mucin has been shown to aid *Helicobacter pylori* to swim through the mucus (Celli *et al.*, 2009).

1.2.4.3. Parasites and mucus

The heavily glycosylated mucins polymerize via disulphide bond formation, giving rise to the viscosity of mucus. Protozoan parasites interact with mucus, especially the major constituent mucins, in various ways:

(1) The secreted mucins are likely to function as inhibitors for adhesins of parasites, as the mucins display many of the oligosaccharides that are found on the cell surface. Purified rat and human colonic mucins inhibit *Entamoeba histolytica in vitro* adherence to and lysis of colonic epithelial cells by binding to the amoebic galactose lectin (Chadee *et al.*, 1987). Galactose and N-acetyl-D-galactosamine residues of mucins specifically and competitively inhibited amoebic binding to target cells via its heavy subunit Gal-lectin (Gottke *et al.*, 1998). This may be due to the fact that the mucin preparations contain high amounts of saccharides typical of the O-linked carbohydrate side chains, such as N-acetyl-glucosamine, galactose, N-acetyl-galactosamine, fucose and sialic acid, which could bind to the surface lectin of *Entamoeba histolytica*.

(2) Some parasites have been evolved to utilize the mucin glycans as for adhesion. *Tritrichomonas foetus,* and *Entamoeba histolytica* express a sialic acid-specific lectin which facilitate their adherence to host cells, as well as host mucins (Chadee *et al.*, 1987; Hicks *et al.*, 2000). Lectin-mediated binding to mucus is one of the initial steps

in colonization.

(3) Some parasites are able to degrade mucins to facilitate their passage through mucus barrier to reach the mucosal epithelium. Digestion of the mucus barrier by parasite enzymes such as glycosidases and sialidases would then allow adherence to the underlying epithelium. For instance, secreted *E. histolytica* cysteine proteinases degraded human colonic mucins, by depolymerizing the mucin polymeric network. The depolymerized mucins were then less effective in inhibiting amoebic adherence to target cells, probably due to loss of its viscous properties (Moncada *et al.*, 2003; 2005).

(4) Mucins derivatives may be utilized by parasites as metabolic fuel. Carbohydrates derived from host epithelial cells, red blood cells, as well as on bacteria are the major energy source for parasites in the distal colon (Hicks *et al.*, 2000). Glycan degradation of mucins is also likely to provide an important source of energy for the parasites. Specific concentrations of galactose-terminated glycoproteins, such as asialofetuin and mucin, can substitute for serum supplementation in culture medium and trigger the differentiation of the trophozoite to the cyst form (Coppi & Eichinger, 1999).

1.3. References

Baker, H. M. & Baker, E. N. (2004). Lactoferrin and iron: structural and dynamic aspects of binding and release. *Biometals* **17**, 209-216.

Baseman, J. B., Hayes, N. S., Goldman, W. E. & Collier, A. M. (1980). Mucus and surfactant synthesis and secretion by cultured hamster respiratory cells. *Environ Health Perspect* **35**, 139-146.

Baskerville, A. (1971). The histopathology of pneumonia produced by aerosol infection of pigs with a strain of Aujeszky's disease virus. *Res Vet Sci* **12**, 590-592.

Ben-Porat T., K. A. S. (1985). *Molecular biology of pseudorabies virus*: Plenum press.

Benitez, J. A., Spelbrink, R. G., Silva, A., Phillips, T. E., Stanley, C. M., Boesman-Finkelstein, M. & Finkelstein, R. A. (1997). Adherence of Vibrio cholerae to cultured differentiated human intestinal cells: an in vitro colonization model. *Infect Immun* **65**, 3474-3477.

Berkhout, B., van Wamel, J. L., Beljaars, L., Meijer, D. K., Visser, S. & Floris, R. (2002). Characterization of the anti-HIV effects of native lactoferrin and other milk proteins and protein-derived peptides. *Antiviral Res* **55**, 341-355.

Bhaskar, K. R., O'Sullivan, D. D., Opaskar-Hincman, H., Reid, L. M. & Coles, S. J. (1986). Density gradient analysis of secretions produced in vitro by human and canine airway mucosa: identification of lipids and proteoglycans in such secretions. *Exp Lung Res* **10**, 401-422.

Blixt, O., Head, S., Mondala, T., Scanlan, C., Huflejt, M. E., Alvarez, R., Bryan, M. C., Fazio, F., Calarese, D., Stevens, J., Razi, N., Stevens, D. J., Skehel, J. J., van Die, I., Burton, D. R., Wilson, I. A., Cummings, R., Bovin, N., Wong, C. H. & Paulson, J. C. (2004). Printed covalent glycan array for ligand profiling of diverse glycan binding proteins. *Proc Natl Acad Sci U S A* **101**, 17033-17038.

Bottcher-Friebertshauser, E., Freuer, C., Sielaff, F., Schmidt, S., Eickmann, M., Uhlendorff, J., Steinmetzer, T., Klenk, H. D. & Garten, W. (2010). Cleavage of influenza virus hemagglutinin by airway proteases TMPRSS2 and HAT differs in subcellular localization and susceptibility to protease inhibitors. *J Virol* **84**, 5605-5614.

Bruce M. Koeppen, B. A. S. http://blp6.atw.hu/BLP6/HTML/C0259780323045827.htm.

Button, B., Boucher, R. C. & University of North Carolina Virtual Lung, G. (2008). Role of mechanical stress in regulating airway surface hydration and mucus clearance rates. *Respir Physiol Neurobiol* **163**, 189-201.

C., S. (1990). Pigs as 'mixing vessels' for the creation of new pandemic influenza A viruses. *Med Princ Pract* **2**, 7.

Campadelli-Fiume, G., Cocchi, F., Menotti, L. & Lopez, M. (2000). The novel receptors that mediate the entry of herpes simplex viruses and animal alphaherpesviruses into cells. *Reviews in Medical Virology* **10**, 305-319.

Celli, J. P., Turner, B. S., Afdhal, N. H., Keates, S., Ghiran, I., Kelly, C. P., Ewoldt, R. H., McKinley, G. H., So, P., Erramilli, S. & Bansil, R. (2009). Helicobacter pylori moves through mucus by reducing mucin viscoelasticity. *Proc Natl Acad Sci U S A* **106**, 14321-14326.

Chadee, K., Petri, W. A., Jr., Innes, D. J. & Ravdin, J. I. (1987). Rat and human colonic mucins bind to and inhibit adherence lectin of Entamoeba histolytica. *J Clin Invest* **80**, 1245-1254.

Chen, W. S., Calvo, P. A., Malide, D., Gibbs, J., Schubert, U., Bacik, I., Basta, S., O'Neill, R., Schickli, J., Palese, P., Henklein, P., Bennink, J. R. & Yewdell, J. W. (2001). A novel influenza A virus mitochondrial protein that induces cell death. *Nature Medicine* **7**, 1306-1312.

Chou, H. H., Takematsu, H., Diaz, S., Iber, J., Nickerson, E., Wright, K. L., Muchmore, E. A., Nelson, D. L., Warren, S. T. & Varki, A. (1998). A mutation in human CMP-sialic acid hydroxylase occurred after the Homo-Pan divergence. *Proc Natl Acad Sci U S A* **95**, 11751-11756.

Cocchi, F., Lopez, M., Menotti, L., Aoubala, M., Dubreuil, P. & Campadelli-Fiume, G. (1998). The V domain of herpesvirus Ig-like receptor (HIgR) contains a major functional region in herpes simplex virus-1 entry into cells and interacts physically with the viral glycoprotein D. *Proc Natl Acad Sci U S A* **95**, 15700-15705.

Cohen, M., Zhang, X. Q., Senaati, H. P., Chen, H. W., Varki, N. M., Schooley, R. T. & Gagneux, P. (2013). Influenza A penetrates host mucus by cleaving sialic acids with neuraminidase. *Virol J* **10**, 321.

Cohrs, R. & Gilden, D. (2011). Alphaherpesvirus latency. *J Neurovirol* **17**, 509-511.

Cone, R. A. (2009). Barrier properties of mucus. *Adv Drug Deliv Rev* **61**, 75-85.

Conenello, G. M., Zamarin, D., Perrone, L. A., Tumpey, T. & Palese, P. (2007). A single mutation in the PB1-F2 of H5N1 (HK/97) and 1918 influenza A viruses contributes to increased virulence. *PLoS Pathog* **3**, 1414-1421.

Constantinou, P. E., Danysh, B. P., Dharmaraj, N. & Carson, D. D. (2011). Transmembrane mucins as novel therapeutic targets. *Expert Rev Endocrinol Metab* **6**, 835-848.

Coppi, A. & Eichinger, D. (1999). Regulation of Entamoeba invadens encystation and gene expression with galactose and N-acetylglucosamine. *Mol Biochem Parasitol* **102**, 67-77.

Corfield, A. P., Wagner, S. A., Clamp, J. R., Kriaris, M. S. & Hoskins, L. C. (1992). Mucin degradation in the human colon: production of sialidase, sialate O-acetylesterase, N-acetylneuraminate lyase, arylesterase, and glycosulfatase activities by strains of fecal bacteria. *Infect Immun* **60**, 3971-3978.

Costa, T., Chaves, A. J., Valle, R., Darji, A., van Riel, D., Kuiken, T., Majo, N. & Ramis, A. (2012). Distribution patterns of influenza virus receptors and viral attachment patterns in the respiratory and intestinal tracts of seven avian species. *Vet Res* **43**, 28.

Crouch, E., Tu, Y., Briner, D., McDonald, B., Smith, K., Holmskov, U. & Hartshorn, K. (2005). Ligand specificity of human surfactant protein D: expression of a mutant trimeric collectin that shows enhanced interactions with influenza A virus. *J Biol Chem* **280**, 17046-17056.

Daikoku, T. (2000). [The functions of alpha herpesvirus gene products]. *Nihon Rinsho* **58**, 787-793.

Das, K., Ma, L. C., Xiao, R., Radvansky, B., Aramini, J., Zhao, L., Marklund, J., Kuo, R. L., Twu, K. Y., Arnold, E., Krug, R. M. & Montelione, G. T. (2008). Structural basis for suppression of a host antiviral response by influenza A virus. *Proc Natl Acad Sci U S A* **105**, 13093-13098.

Derichs, N., Jin, B. J., Song, Y., Finkbeiner, W. E. & Verkman, A. S. (2011). Hyperviscous airway periciliary and mucous liquid layers in cystic fibrosis measured by confocal fluorescence photobleaching. *FASEB J* **25**, 2325-2332.

Doumas, S., Kolokotronis, A. & Stefanopoulos, P. (2005). Anti-inflammatory and antimicrobial roles of secretory leukocyte protease inhibitor. *Infect Immun* **73**, 1271-1274.

Doyle, T. M., Hashem, A. M., Li, C., Van Domselaar, G., Larocque, L., Wang, J., Smith, D., Cyr, T., Farnsworth, A., He, R., Hurt, A. C., Brown, E. G. & Li, X. (2013a). Universal anti-neuraminidase antibody inhibiting all influenza A subtypes. *Antiviral Res* **100**, 567-574.

Doyle, T. M., Li, C., Bucher, D. J., Hashem, A. M., Van Domselaar, G., Wang, J., Farnsworth, A., She, Y. M., Cyr, T., He, R., Brown, E. G., Hurt, A. C. & Li, X. (2013b). A monoclonal antibody targeting a highly conserved epitope in influenza B neuraminidase provides protection against drug resistant strains. *Biochem Biophys Res Commun* **441**, 226-229.

Dubin, R. F., Robinson, S. K. & Widdicombe, J. H. (2004). Secretion of lactoferrin and lysozyme by cultures of human airway epithelium. *Am J Physiol Lung Cell Mol Physiol* **286**, L750-755.

Els, M. C., Air, G. M., Murti, K. G., Webster, R. G. & Laver, W. G. (1985). An 18-amino acid deletion in an influenza neuraminidase. *Virology* **142**, 241-247.

Enquist, L. W. http://molbio.princeton.edu/labs/enquist/research/pseudorabies-virus-prv-1?start=5

Fan, Q., Longnecker, R. & Connolly, S. A. (2014). Substitution of herpes simplex virus 1 entry glycoproteins with those of saimiriine herpesvirus 1 reveals a gD-gH/gL functional interaction and a region within the gD profusion domain that is critical for fusion. *J Virol* **88**, 6470-6482.

Fang, X. M., Shu, Q., Chen, Q. X., Book, M., Sahl, H. G., Hoeft, A. & Stuber, F. (2003). Differential expression of alpha- and beta-defensins in human peripheral blood. *Eur J Clin Invest* **33**, 82-87.

Fliegauf, M., Sonnen, A. F., Kremer, B. & Henneke, P. (2013). Mucociliary clearance defects in a murine in vitro model of pneumococcal airway infection. *PLoS One* **8**, e59925.

Franca, M., Stallknecht, D. E. & Howerth, E. W. (2013). Expression and distribution of sialic acid

influenza virus receptors in wild birds. *Avian Pathol* **42**, 60-71.

Fujihara, T. & Hayashi, K. (1995). Lactoferrin inhibits herpes simplex virus type-1 (HSV-1) infection to mouse cornea. *Arch Virol* **140**, 1469-1472.

Gambaryan, A., Yamnikova, S., Lvov, D., Tuzikov, A., Chinarev, A., Pazynina, G., Webster, R., Matrosovich, M. & Bovin, N. (2005). Receptor specificity of influenza viruses from birds and mammals: new data on involvement of the inner fragments of the carbohydrate chain. *Virology* **334**, 276-283.

Gambaryan, A. S. & Matrosovich, M. N. (1992). A solid-phase enzyme-linked assay for influenza virus receptor-binding activity. *J Virol Methods* **39**, 111-123.

Gambaryan, A. S., Tuzikov, A. B., Piskarev, V. E., Yamnikova, S. S., Lvov, D. K., Robertson, J. S., Bovin, N. V. & Matrosovich, M. N. (1997). Specification of receptor-binding phenotypes of influenza virus isolates from different hosts using synthetic sialylglycopolymers: non-egg-adapted human H1 and H3 influenza A and influenza B viruses share a common high binding affinity for 6'-sialyl(N-acetyllactosamine). *Virology* **232**, 345-350.

Ganz, T. (2003). Defensins: antimicrobial peptides of innate immunity. *Nat Rev Immunol* **3**, 710-720.

Geraghty, R. J., Krummenacher, C., Cohen, G. H., Eisenberg, R. J. & Spear, P. G. (1998). Entry of alphaherpesviruses mediated by poliovirus receptor-related protein 1 and poliovirus receptor. *Science* **280**, 1618-1620.

Glorieux, S., Favoreel, H. W., Meesen, G., de Vos, W., Van den Broeck, W. & Nauwynck, H. J. (2009). Different replication characteristics of historical pseudorabies virus strains in porcine respiratory nasal mucosa explants. *Vet Microbiol* **136**, 341-346.

Gottke, M. U., Keller, K., Belley, A., Garcia, R. M., Hollingsworth, M. A., Mack, D. R. & Chadee, K. (1998). Functional heterogeneity of colonic adenocarcinoma mucins for inhibition of Entamoeba histolytica adherence to target cells. *J Eukaryot Microbiol* **45**, 17S-23S.

Gottschalk, A. (1957). Neuraminidase: the specific enzyme of influenza virus and Vibrio cholerae. *Biochim Biophys Acta* **23**, 645-646.

Grubor, B., Meyerholz, D. K. & Ackermann, M. R. (2006). Collectins and cationic antimicrobial peptides of the respiratory epithelia. *Vet Pathol* **43**, 595-612.

Grunewald, K., Desai, P., Winkler, D. C., Heymann, J. B., Belnap, D. M., Baumeister, W. & Steven, A. C. (2003). Three-dimensional structure of herpes simplex virus from cryo-electron tomography. *Science* **302**, 1396-1398.

Guo, H., Shen, S., Wang, L. & Deng, H. (2010). Role of tegument proteins in herpesvirus assembly and egress. *Protein Cell* **1**, 987-998.

Haider, K., Hossain, A., Wanke, C., Qadri, F., Ali, S. & Nahar, S. (1993). Production of mucinase and neuraminidase and binding of Shigella to intestinal mucin. *J Diarrhoeal Dis Res* **11**, 88-92.

Harimurti, K., Djauzi, S., Witarto, A. B. & Dewiasty, E. (2011). Human beta-defensin 2 concentration of respiratory tract mucosa in elderly patients with pneumonia and its associated factors. *Acta Med Indones* **43**, 218-223.

Harris, A., Cardone, G., Winkler, D. C., Heymann, J. B., Brecher, M., White, J. M. & Steven, A. C. (2006). Influenza virus pleiomorphy characterized by cryoelectron tomography. *Proc Natl Acad Sci U S A* **103**, 19123-19127.

Hazlett, L. D., Masinick, S., Barrett, R. & Rosol, K. (1993). Evidence for asialo GM1 as a corneal glycolipid receptor for Pseudomonas aeruginosa adhesion. *Infect Immun* **61**, 5164-5173.

Heinen, P. P., van Nieuwstadt, A. P., Pol, J. M., de Boer-Luijtze, E. A., van Oirschot, J. T. & Bianchi, A. T. (2000). Systemic and mucosal isotype-specific antibody responses in pigs to experimental influenza virus infection. *Viral Immunol* **13**, 237-247.

Heldwein, E. E. & Krummenacher, C. (2008). Entry of herpesviruses into mammalian cells. *Cell Mol Life Sci* **65**, 1653-1668.

Hicks, S. J., Theodoropoulos, G., Carrington, S. D. & Corfield, A. P. (2000). The role of mucins in host-parasite interactions. Part I-protozoan parasites. *Parasitol Today* **16**, 476-481.

Hillaire, M. L., van Eijk, M., van Trierum, S. E., van Riel, D., Saelens, X., Romijn, R. A., Hemrika, W., Fouchier, R. A., Kuiken, T., Osterhaus, A. D., Haagsman, H. P. & Rimmelzwaan, G. F. (2011). Assessment of the antiviral properties of recombinant porcine SP-D against various influenza A viruses in vitro. *PLoS One* **6**, e25005.

Hillaire, M. L., van Eijk, M., Vogelzang-van Trierum, S. E., Fouchier, R. A., Osterhaus, A. D., Haagsman, H. P. & Rimmelzwaan, G. F. (2014). Recombinant porcine surfactant protein D inhibits influenza A virus replication ex vivo. *Virus Res* **181**, 22-26.

Hiratsuka, T., Nakazato, M., Date, Y., Ashitani, J., Minematsu, T., Chino, N. & Matsukura, S. (1998). Identification of human beta-defensin-2 in respiratory tract and plasma and its increase in bacterial pneumonia. *Biochem Biophys Res Commun* **249**, 943-947.

Hirst, G. K. (1941). The Agglutination of Red Cells by Allantoic Fluid of Chick Embryos Infected with Influenza Virus. *Science* **94**, 22-23.

Homa, F. L. & Brown, J. C. (1997). Capsid assembly and DNA packaging in herpes simplex virus. *Rev Med Virol* **7**, 107-122.

Homer, K. A., Whiley, R. A. & Beighton, D. (1994). Production of specific glycosidase activities by Streptococcus intermedius strain UNS35 grown in the presence of mucin. *J Med Microbiol* **41**, 184-190.

Iglesias, G., Pijoan, C. & Molitor, T. (1989). Interactions of Pseudorabies virus with swine alveolar macrophages I: virus replication. *Arch Virol* **104**, 107-115.

Ito, T., Couceiro, J. N., Kelm, S., Baum, L. G., Krauss, S., Castrucci, M. R., Donatelli, I., Kida, H., Paulson, J. C., Webster, R. G. & Kawaoka, Y. (1998). Molecular basis for the generation in pigs of influenza A viruses with pandemic potential. *J Virol* **72**, 7367-7373.

Iwasa, M., Kaito, M., Ikoma, J., Takeo, M., Imoto, I., Adachi, Y., Yamauchi, K., Koizumi, R. & Teraguchi, S. (2002). Lactoferrin inhibits hepatitis C virus viremia in chronic hepatitis C patients with high viral loads and HCV genotype 1b. *Am J Gastroenterol* **97**, 766-767.

Jacquot, J., Hayem, A. & Galabert, C. (1992). Functions of proteins and lipids in airway secretions. *Eur Respir J* **5**, 343-358.

Jagger, B. W., Wise, H. M., Kash, J. C., Walters, K. A., Wills, N. M., Xiao, Y. L., Dunfee, R. L., Schwartzman, L. M., Ozinsky, A., Bell, G. L., Dalton, R. M., Lo, A., Efstathiou, S., Atkins, J. F., Firth, A. E., Taubenberger, J. K. & Digard, P. (2012). An overlapping protein-coding region in influenza A virus segment 3 modulates the host response. *Science* **337**, 199-204.

Jayaraman, S., Song, Y., Vetrivel, L., Shankar, L. & Verkman, A. S. (2001). Noninvasive in vivo fluorescence measurement of airway-surface liquid depth, salt concentration, and pH. *J Clin Invest* **107**, 317-324.

Jenssen, H., Sandvik, K., Andersen, J. H., Hancock, R. E. & Gutteberg, T. J. (2008). Inhibition of HSV cell-to-cell spread by lactoferrin and lactoferricin. *Antiviral Res* **79**, 192-198.

Johnson, D. C. (2011). Airway mucus function and dysfunction. *N Engl J Med* **364**, 978; author reply

978.

Jozwiak, Z., Snyder, C. E., Murty, V. L., Slomiany, A., Slomiany, B. L. & Herp, A. (1984). Lipid composition of the secretion from human bronchial explant culture. *Biochim Biophys Acta* **802**, 282-286.

Karger, A., Saalmuller, A., Tufaro, F., Banfield, B. W. & Mettenleiter, T. C. (1995). Cell surface proteoglycans are not essential for infection by pseudorabies virus. *J Virol* **69**, 3482-3489.

Kida, H. (1992). [Host range of influenza virus]. *Tanpakushitsu Kakusan Koso* **37**, 2785-2791.

Kim, C. H., Oh, Y., Han, K., Seo, H. W., Kim, D., Kang, I., Park, C., Jang, K. Y., Kim, S. H. & Chae, C. (2012a). Expression of secreted mucins (MUC2, MUC5AC, MUC5B, and MUC6) and membrane-bound mucin (MUC4) in the lungs of pigs experimentally infected with Actinobacillus pleuropneumoniae. *Res Vet Sci* **92**, 486-491.

Kim, C. H., Oh, Y., Han, K., Seo, H. W., Kim, D., Park, C., Kang, I. & Chae, C. (2012b). Expression of secreted and membrane-bound mucins in the airways of piglets experimentally infected with Mycoplasma hyopneumoniae. *Vet J* **192**, 120-122.

Kim, K. C., McCracken, K., Lee, B. C., Shin, C. Y., Jo, M. J., Lee, C. J. & Ko, K. H. (1997). Airway goblet cell mucin: its structure and regulation of secretion. *Eur Respir J* **10**, 2644-2649.

Kimble, B., Nieto, G. R. & Perez, D. R. (2010). Characterization of influenza virus sialic acid receptors in minor poultry species. *Virol J* **7**, 365.

King, M. (1998). Experimental models for studying mucociliary clearance. *Eur Respir J* **11**, 222-228.

King, M. (2005). Mucus and its role in airway clearance and cytoprotection. In *Physiologic Basis of Respiratory Disease*, pp. 409-416. Edited by J. S. Qutayba Hamid, James Martin: PMPH-USA.

King, M., Agarwal, M. & Shukla, J. B. (1993). A planar model for mucociliary transport: effect of mucus viscoelasticity. *Biorheology* **30**, 49-61.

Kitikoon, P., Nilubol, D., Erickson, B. J., Janke, B. H., Hoover, T. C., Sornsen, S. A. & Thacker, E. L. (2006). The immune response and maternal antibody interference to a heterologous H1N1 swine influenza virus infection following vaccination. *Vet Immunol Immunopathol* **112**, 117-128.

Klupp, B. G., Hengartner, C. J., Mettenleiter, T. C. & Enquist, L. W. (2004). Complete, annotated sequence of the pseudorabies virus genome. *J Virol* **78**, 424-440.

Kobasa, D., Kodihalli, S., Luo, M., Castrucci, M. R., Donatelli, I., Suzuki, Y., Suzuki, T. & Kawaoka, Y. (1999). Amino acid residues contributing to the substrate specificity of the influenza A virus neuraminidase. *J Virol* **73**, 6743-6751.

Kocan, A. (1990). Review of wildlife disease status in game animals in North America, ADF. In *Pseudorabies*, pp. 43-44. Edited by R. Lind. Saskatchewan, Canada: Saskatchewan
Agriculture Development Fund.

Kritas, S. K., Pensaert, M. B. & Mettenleiter, T. C. (1994). Invasion and spread of single glycoprotein deleted mutants of Aujeszky's disease virus (ADV) in the trigeminal nervous pathway of pigs after intranasal inoculation. *Vet Microbiol* **40**, 323-334.

Kutta, H., Willer, A., Steven, P., Brauer, L., Tsokos, M. & Paulsen, F. (2008). Distribution of mucins and antimicrobial substances lysozyme and lactoferrin in the laryngeal subglottic region. *J Anat* **213**, 473-481.

Lai, S. K., Wang, Y. Y., Hida, K., Cone, R. & Hanes, J. (2010). Nanoparticles reveal that human

cervicovaginal mucus is riddled with pores larger than viruses. *Proc Natl Acad Sci U S A* **107**, 598-603.

Lai, S. K., Wang, Y. Y., Wirtz, D. & Hanes, J. (2009). Micro- and macrorheology of mucus. *Adv Drug Deliv Rev* **61**, 86-100.

Lange, R., Peng, X., Wimmer, E., Lipp, M. & Bernhardt, G. (2001). The poliovirus receptor CD155 mediates cell-to-matrix contacts by specifically binding to vitronectin. *Virology* **285**, 218-227.

Laver, W. G. (1978). Crystallization and peptide maps of neuraminidase "heads" from H2N2 and H3N2 influenza virus strains. *Virology* **86**, 78-87.

Lieleg, O., Lieleg, C., Bloom, J., Buck, C. B. & Ribbeck, K. (2012). Mucin Biopolymers As Broad-Spectrum Antiviral Agents. *Biomacromolecules* **13**, 1724-1732.

Lillehoj, E. R. & Kim, K. C. (2002). Airway mucus: its components and function. *Arch Pharm Res* **25**, 770-780.

Lim, B. L., Willis, A. C., Reid, K. B., Lu, J., Laursen, S. B., Jensenius, J. C. & Holmskov, U. (1994). Primary structure of bovine collectin-43 (CL-43). Comparison with conglutinin and lung surfactant protein-D. *J Biol Chem* **269**, 11820-11824.

Loeffen, W. L., Kamp, E. M., Stockhofe-Zurwieden, N., van Nieuwstadt, A. P., Bongers, J. H., Hunneman, W. A., Elbers, A. R., Baars, J., Nell, T. & van Zijderveld, F. G. (1999). Survey of infectious agents involved in acute respiratory disease in finishing pigs. *Vet Rec* **145**, 123-129.

Lundy, F. T., Orr, D. F., Gallagher, J. R., Maxwell, P., Shaw, C., Napier, S. S., Gerald Cowan, C., Lamey, P. J. & Marley, J. J. (2004). Identification and overexpression of human neutrophil alpha-defensins (human neutrophil peptides 1, 2 and 3) in squamous cell carcinomas of the human tongue. *Oral Oncol* **40**, 139-144.

Ma, G., Greenwell-Wild, T., Lei, K., Jin, W., Swisher, J., Hardegen, N., Wild, C. T. & Wahl, S. M. (2004). Secretory leukocyte protease inhibitor binds to annexin II, a cofactor for macrophage HIV-1 infection. *J Exp Med* **200**, 1337-1346.

Mackenzie, D. A., Jeffers, F., Parker, M. L., Vibert-Vallet, A., Bongaerts, R. J., Roos, S., Walter, J. & Juge, N. (2010). Strain-specific diversity of mucus-binding proteins in the adhesion and aggregation properties of Lactobacillus reuteri. *Microbiology* **156**, 3368-3378.

Maes, D., Deluyker, H., Verdonck, M., Castryck, F., Miry, C., Vrijens, B. & de Kruif, A. (2000). Herd factors associated with the seroprevalences of four major respiratory pathogens in slaughter pigs from farrow-to-finish pig herds. *Vet Res* **31**, 313-327.

Martinez, W. M. & Spear, P. G. (2001). Structural features of nectin-2 (HveB) required for herpes simplex virus entry. *J Virol* **75**, 11185-11195.

Matrosovich, M., Tuzikov, A., Bovin, N., Gambaryan, A., Klimov, A., Castrucci, M. R., Donatelli, I. & Kawaoka, Y. (2000). Early alterations of the receptor-binding properties of H1, H2, and H3 avian influenza virus hemagglutinins after their introduction into mammals. *J Virol* **74**, 8502-8512.

McGeoch, D. J. (1987). The genome of herpes simplex virus: structure, replication and evolution. *J Cell Sci Suppl* **7**, 67-94.

Mettenleiter, T. C. (2000). Aujeszky's disease (pseudorabies) virus: the virus and molecular pathogenesis--state of the art, June 1999. *Vet Res* **31**, 99-115.

Mettenleiter, T. C. (2002). Herpesvirus assembly and egress. *J Virol* **76**, 1537-1547.

Mettenleiter, T. C., Zsak, L., Zuckermann, F., Sugg, N., Kern, H. & Ben-Porat, T. (1990).

Interaction of glycoprotein gIII with a cellular heparinlike substance mediates adsorption of pseudorabies virus. *J Virol* **64**, 278-286.

Min, J. Y. & Krug, R. M. (2006). The primary function of RNA binding by the influenza A virus NS1 protein in infected cells: Inhibiting the 2'-5' oligo (A) synthetase/RNase L pathway. *Proc Natl Acad Sci U S A* **103**, 7100-7105.

Miry C., P. M. (1989). Aujeszky's disease replication in tonsils and respiratory tract of non-immune and immune pigs. In *Vaccination and control of Aujeszky's disease*, pp. 163-167. Edited by v. O. J.T.

Mitnaul, L. J., Castrucci, M. R., Murti, K. G. & Kawaoka, Y. (1996). The cytoplasmic tail of influenza A virus neuraminidase (NA) affects NA incorporation into virions, virion morphology, and virulence in mice but is not essential for virus replication. *J Virol* **70**, 873-879.

Moncada, D., Keller, K. & Chadee, K. (2003). Entamoeba histolytica cysteine proteinases disrupt the polymeric structure of colonic mucin and alter its protective function. *Infect Immun* **71**, 838-844.

Moncada, D., Keller, K. & Chadee, K. (2005). Entamoeba histolytica-secreted products degrade colonic mucin oligosaccharides. *Infect Immun* **73**, 3790-3793.

Montgomery, R. I., Warner, M. S., Lum, B. J. & Spear, P. G. (1996). Herpes simplex virus-1 entry into cells mediated by a novel member of the TNF/NGF receptor family. *Cell* **87**, 427-436.

Muchmore, E. A., Diaz, S. & Varki, A. (1998). A structural difference between the cell surfaces of humans and the great apes. *Am J Phys Anthropol* **107**, 187-198.

Muller, C. A., Markovic-Lipkovski, J., Klatt, T., Gamper, J., Schwarz, G., Beck, H., Deeg, M., Kalbacher, H., Widmann, S., Wessels, J. T., Becker, V., Muller, G. A. & Flad, T. (2002). Human alpha-defensins HNPs-1, -2, and -3 in renal cell carcinoma: influences on tumor cell proliferation. *Am J Pathol* **160**, 1311-1324.

Muthing, J. & Unland, F. (1994). A comparative assessment of TLC overlay technique and microwell adsorption assay in the examination of influenza A and Sendai virus specificities towards oligosaccharides and sialic acid linkages of gangliosides. *Glycoconj J* **11**, 486-492.

Nadziejko, C. E., Slomiany, B. L. & Slomiany, A. (1993). Most of the lipid in purulent sputum is bound to mucus glycoprotein. *Exp Lung Res* **19**, 671-684.

Nauwynck, H., Glorieux, S., Favoreel, H. & Pensaert, M. (2007). Cell biological and molecular characteristics of pseudorabies virus infections in cell cultures and in pigs with emphasis on the respiratory tract. *Vet Res* **38**, 229-241.

Nauwynck, H. J. (1997). Functional aspects of Aujeszky's disease (pseudorabies) viral proteins with relation to invasion, virulence and immunogenicity. *Vet Microbiol* **55**, 3-11.

Nelli, R. K., Kuchipudi, S. V., White, G. A., Perez, B. B., Dunham, S. P. & Chang, K. C. (2010). Comparative distribution of human and avian type sialic acid influenza receptors in the pig. *BMC Vet Res* **6**, 4.

Newcomb, W. W., Homa, F. L., Thomsen, D. R., Trus, B. L., Cheng, N., Steven, A., Booy, F. & Brown, J. C. (1999). Assembly of the herpes simplex virus procapsid from purified components and identification of small complexes containing the major capsid and scaffolding proteins. *J Virol* **73**, 4239-4250.

Newcomb, W. W., Trus, B. L., Booy, F. P., Steven, A. C., Wall, J. S. & Brown, J. C. (1993). Structure of the herpes simplex virus capsid. Molecular composition of the pentons and the

triplexes. *J Mol Biol* **232**, 499-511.

Nicholls, J. M., Bourne, A. J., Chen, H., Guan, Y. & Peiris, J. S. (2007). Sialic acid receptor detection in the human respiratory tract: evidence for widespread distribution of potential binding sites for human and avian influenza viruses. *Respir Res* **8**, 73.

Nixdorf, R., Schmidt, J., Karger, A. & Mettenleiter, T. C. (1999). Infection of Chinese hamster ovary cells by pseudorabies virus. *J Virol* **73**, 8019-8026.

Nobusawa, E., Aoyama, T., Kato, H., Suzuki, Y., Tateno, Y. & Nakajima, K. (1991). Comparison of complete amino acid sequences and receptor-binding properties among 13 serotypes of hemagglutinins of influenza A viruses. *Virology* **182**, 475-485.

O'Neill, R. E., Talon, J. & Palese, P. (1998). The influenza virus NEP (NS2 protein) mediates the nuclear export of viral ribonucleoproteins. *EMBO J* **17**, 288-296.

Ohuchi, M., Asaoka, N., Sakai, T. & Ohuchi, R. (2006). Roles of neuraminidase in the initial stage of influenza virus infection. *Microbes Infect* **8**, 1287-1293.

Olmsted, S. S., Padgett, J. L., Yudin, A. I., Whaley, K. J., Moench, T. R. & Cone, R. A. (2001). Diffusion of macromolecules and virus-like particles in human cervical mucus. *Biophys J* **81**, 1930-1937.

Olsen, C. W. (2006). Swine Influenza. In *Disease of Swine*, pp. 469-482. Edited by Z. J. J. Straw B.E., D'Allaire S., Taylor D.J. Ames, Iowa, USA: Iowa State University Press.

Osterhaus, A. D., Rimmelzwaan, G. F., Martina, B. E., Bestebroer, T. M. & Fouchier, R. A. (2000). Influenza B virus in seals. *Science* **288**, 1051-1053.

Ottemann, K. M. & Lowenthal, A. C. (2002). Helicobacter pylori uses motility for initial colonization and to attain robust infection. *Infect Immun* **70**, 1984-1990.

Pikaar, J. C., Voorhout, W. F., van Golde, L. M., Verhoef, J., Van Strijp, J. A. & van Iwaarden, J. F. (1995). Opsonic activities of surfactant proteins A and D in phagocytosis of gram-negative bacteria by alveolar macrophages. *J Infect Dis* **172**, 481-489.

Pomeranz, L. E., Reynolds, A. E. & Hengartner, C. J. (2005). Molecular biology of pseudorabies virus: impact on neurovirology and veterinary medicine. *Microbiol Mol Biol Rev* **69**, 462-500.

Prince, A. (1992). Adhesins and receptors of Pseudomonas aeruginosa associated with infection of the respiratory tract. *Microb Pathog* **13**, 251-260.

Rahmoune, H. & Shephard, K. L. (1995). State of airway surface liquid on guinea pig trachea. *J Appl Physiol (1985)* **78**, 2020-2024.

Reviglio, V. E., Sambuelli, R. H., Olmedo, A., Falco, M., Echenique, J., O'Brien, T. P. & Kuo, I. C. (2007). Secretory leukocyte protease inhibitor is an inducible antimicrobial peptide expressed in Staphylococcus aureus endophthalmitis. *Mediators Inflamm* **2007**, 93857.

Rogers, G. N. & Paulson, J. C. (1983). Receptor determinants of human and animal influenza virus isolates: differences in receptor specificity of the H3 hemagglutinin based on species of origin. *Virology* **127**, 361-373.

Roizman, B. a. P., P. E. (2001). *Family Herpesviridae: A Brief Introduction*. Philadelphia: Lippincott Williams & Wilkins.

Rose, M. C. & Voynow, J. A. (2006). Respiratory tract mucin genes and mucin glycoproteins in health and disease. *Physiol Rev* **86**, 245-278.

Ruigrok, R. W. H. (1998). Structure of Influenza A, B and C Viruses. In *Textbook of Influenza*, pp. 29-42. Edited by W. R. G. Nicholson K.G., Hay A.J. Malden, MA, USA: Blackwell Science Ltd.

Sang, Y., Patil, A. A., Zhang, G., Ross, C. R. & Blecha, F. (2006). Bioinformatic and expression analysis of novel porcine beta-defensins. *Mamm Genome* **17**, 332-339.

Schauer, R. (2009). Sialic acids as regulators of molecular and cellular interactions. *Curr Opin Struct Biol* **19**, 507-514.

Schmiedl, A., Luhrmann, A., Pabst, R. & Koslowski, R. (2009). Increased surfactant protein a and d expression in acute ovalbumin-induced allergic airway inflammation in brown norway rats. *Int Arch Allergy Immunol* **148**, 118-126.

Seybold, Z. V., Mariassy, A. T., Stroh, D., Kim, C. S., Gazeroglu, H. & Wanner, A. (1990). Mucociliary interaction in vitro: effects of physiological and inflammatory stimuli. *J Appl Physiol (1985)* **68**, 1421-1426.

Shukair, S. A., Allen, S. A., Cianci, G. C., Stieh, D. J., Anderson, M. R., Baig, S. M., Gioia, C. J., Spongberg, E. J., Kauffman, S. M., McRaven, M. D., Lakougna, H. Y., Hammond, C., Kiser, P. F. & Hope, T. J. (2013). Human cervicovaginal mucus contains an activity that hinders HIV-1 movement. *Mucosal Immunol* **6**, 427-434.

Shukla, D., Liu, J., Blaiklock, P., Shworak, N. W., Bai, X., Esko, J. D., Cohen, G. H., Eisenberg, R. J., Rosenberg, R. D. & Spear, P. G. (1999). A novel role for 3-O-sulfated heparan sulfate in herpes simplex virus 1 entry. *Cell* **99**, 13-22.

Shukla, D. & Spear, P. G. (2001). Herpesviruses and heparan sulfate: an intimate relationship in aid of viral entry. *J Clin Invest* **108**, 503-510.

Silva, A. J., Pham, K. & Benitez, J. A. (2003). Haemagglutinin/protease expression and mucin gel penetration in El Tor biotype Vibrio cholerae. *Microbiology* **149**, 1883-1891.

Spear, P. G., Eisenberg, R. J. & Cohen, G. H. (2000). Three classes of cell surface receptors for alphaherpesvirus entry. *Virology* **275**, 1-8.

Spear, P. G. & Longnecker, R. (2003). Herpesvirus entry: an update. *J Virol* **77**, 10179-10185.

Stevens, J., Blixt, O., Glaser, L., Taubenberger, J. K., Palese, P., Paulson, J. C. & Wilson, I. A. (2006a). Glycan microarray analysis of the hemagglutinins from modern and pandemic influenza viruses reveals different receptor specificities. *J Mol Biol* **355**, 1143-1155.

Stevens, J., Blixt, O., Paulson, J. C. & Wilson, I. A. (2006b). Glycan microarray technologies: tools to survey host specificity of influenza viruses. *Nat Rev Microbiol* **4**, 857-864.

Subbarao, K. & Joseph, T. (2007). Scientific barriers to developing vaccines against avian influenza viruses. *Nat Rev Immunol* **7**, 267-278.

Superti, F., Ammendolia, M. G., Valenti, P. & Seganti, L. (1997). Antirotaviral activity of milk proteins: lactoferrin prevents rotavirus infection in the enterocyte-like cell line HT-29. *Med Microbiol Immunol* **186**, 83-91.

Superti, F., Siciliano, R., Rega, B., Giansanti, F., Valenti, P. & Antonini, G. (2001). Involvement of bovine lactoferrin metal saturation, sialic acid and protein fragments in the inhibition of rotavirus infection. *Biochim Biophys Acta* **1528**, 107-115.

Thornton, D. J., Rousseau, K. & McGuckin, M. A. (2008). Structure and function of the polymeric mucins in airways mucus. *Annu Rev Physiol* **70**, 459-486.

Tjabringa, G. S., Vos, J. B., Olthuis, D., Ninaber, D. K., Rabe, K. F., Schalkwijk, J., Hiemstra, P. S. & Zeeuwen, P. L. (2005). Host defense effector molecules in mucosal secretions. *FEMS Immunol Med Microbiol* **45**, 151-158.

Tong, S., Zhu, X., Li, Y., Shi, M., Zhang, J., Bourgeois, M., Yang, H., Chen, X., Recuenco, S., Gomez, J., Chen, L. M., Johnson, A., Tao, Y., Dreyfus, C., Yu, W., McBride, R., Carney, P.

J., Gilbert, A. T., Chang, J., Guo, Z., Davis, C. T., Paulson, J. C., Stevens, J., Rupprecht, C. E., Holmes, E. C., Wilson, I. A. & Donis, R. O. (2013). New world bats harbor diverse influenza A viruses. *PLoS Pathog* **9**, e1003657.

Van Gucht, S., Atanasova, K., Barbe, F., Cox, E., Pensaert, M. & Van Reeth, K. (2006). Effect of porcine respiratory coronavirus infection on lipopolysaccharide recognition proteins and haptoglobin levels in the lungs. *Microbes Infect* **8**, 1492-1501.

Van Poucke, S. G., Nicholls, J. M., Nauwynck, H. J. & Van Reeth, K. (2010). Replication of avian, human and swine influenza viruses in porcine respiratory explants and association with sialic acid distribution. *Virol J* **7**, 38.

Van Reeth, K. (2007). Avian and swine influenza viruses: our current understanding of the zoonotic risk. *Vet Res* **38**, 243-260.

Van Reeth, K., Labarque, G., Nauwynck, H. & Pensaert, M. (1999). Differential production of proinflammatory cytokines in the pig lung during different respiratory virus infections: correlations with pathogenicity. *Res Vet Sci* **67**, 47-52.

van Riel, D., Munster, V. J., de Wit, E., Rimmelzwaan, G. F., Fouchier, R. A., Osterhaus, A. D. & Kuiken, T. (2007). Human and avian influenza viruses target different cells in the lower respiratory tract of humans and other mammals. *Am J Pathol* **171**, 1215-1223.

van Riel, D., Rimmelzwaan, G. F., van Amerongen, G., Osterhaus, A. D. & Kuiken, T. (2010). Highly pathogenic avian influenza virus H7N7 isolated from a fatal human case causes respiratory disease in cats but does not spread systemically. *Am J Pathol* **177**, 2185-2190.

Varghese, J. N., Laver, W. G. & Colman, P. M. (1983). Structure of the influenza virus glycoprotein antigen neuraminidase at 2.9 A resolution. *Nature* **303**, 35-40.

Varki, N. M. & Varki, A. (2007). Diversity in cell surface sialic acid presentations: implications for biology and disease. *Lab Invest* **87**, 851-857.

Veldhuizen, E. J., Rijnders, M., Claassen, E. A., van Dijk, A. & Haagsman, H. P. (2008). Porcine beta-defensin 2 displays broad antimicrobial activity against pathogenic intestinal bacteria. *Mol Immunol* **45**, 386-394.

Wagner, R., Wolff, T., Herwig, A., Pleschka, S. & Klenk, H. D. (2000). Interdependence of hemagglutinin glycosylation and neuraminidase as regulators of influenza virus growth: a study by reverse genetics. *J Virol* **74**, 6316-6323.

Wahl, S. M., McNeely, T. B., Janoff, E. N., Shugars, D., Worley, P., Tucker, C. & Orenstein, J. M. (1997). Secretory leukocyte protease inhibitor (SLPI) in mucosal fluids inhibits HIV-I. *Oral Dis* **3 Suppl 1**, S64-69.

Walther, T., Karamanska, R., Chan, R. W., Chan, M. C., Jia, N., Air, G., Hopton, C., Wong, M. P., Dell, A., Malik Peiris, J. S., Haslam, S. M. & Nicholls, J. M. (2013). Glycomic analysis of human respiratory tract tissues and correlation with influenza virus infection. *PLoS Pathog* **9**, e1003223.

Warner, M. S., Geraghty, R. J., Martinez, W. M., Montgomery, R. I., Whitbeck, J. C., Xu, R., Eisenberg, R. J., Cohen, G. H. & Spear, P. G. (1998). A cell surface protein with herpesvirus entry activity (HveB) confers susceptibility to infection by mutants of herpes simplex virus type 1, herpes simplex virus type 2, and pseudorabies virus. *Virology* **246**, 179-189.

White, S. H., Wimley, W. C. & Selsted, M. E. (1995). Structure, function, and membrane integration of defensins. *Curr Opin Struct Biol* **5**, 521-527.

Widdicombe, J. H., Bastacky, S. J., Wu, D. X. & Lee, C. Y. (1997). Regulation of depth and composition of airway surface liquid. *Eur Respir J* **10**, 2892-2897.

Wrigley, N. G., Skehel, J. J., Charlwood, P. A. & Brand, C. M. (1973). The size and shape of influenza virus neuraminidase. *Virology* **51**, 525-529.

Wu, D. X., Lee, C. Y., Uyekubo, S. N., Choi, H. K., Bastacky, S. J. & Widdicombe, J. H. (1998). Regulation of the depth of surface liquid in bovine trachea. *Am J Physiol* **274**, L388-395.

Yanagi, S., Ashitani, J., Ishimoto, H., Date, Y., Mukae, H., Chino, N. & Nakazato, M. (2005). Isolation of human beta-defensin-4 in lung tissue and its increase in lower respiratory tract infection. *Respir Res* **6**, 130.

Zhirnov, O. P., Ikizler, M. R. & Wright, P. F. (2002). Cleavage of influenza a virus hemagglutinin in human respiratory epithelium is cell associated and sensitive to exogenous antiproteases. *J Virol* **76**, 8682-8689.

Chapter 2

2. Aims

The mucosa of the respiratory tract is a common site for entry of many viruses. Concerning mucosal invasion, an explant model has been developed in our laboratory and it is demonstrated that alphaherpesviruses and influenza viruses behave differently in the respiratory mucosa. Pseudorabies virus (PrV), the causative agent of Aujeszky's disease, easily invades the mucosa and submucosa for subsequent spread throughout the body. On the other hand, swine influenza virus (SIV), replicates almost exclusively in the epithelial cells in the respiratory tract. However, these explant models do not take into account the principle role of mucus which covers the mucosa and serves as the first barrier of host defense. Little is known about how respiratory viruses interact with the respiratory mucus. Unraveling the mechanism behind the penetration of viruses across the mucosal barriers has potentially significant implications for the development of novel antiviral strategies. The general goal of this doctoral research was to get a better understanding of the virus-respiratory mucus interaction.

We first aimed to set up a virus tracking model using PrV, porcine respiratory mucus and single particle tracking, and to analyze the mobility of PrV particles in mucus (**Chapter 3.1**). Secondly, to determine if mucins are responsible for the inhibitory effects of mucus on virus migration, the distribution of two major types of mucins was examined, and the effect of mucin on PrV entry into target epithelial cells was studied *ex vivo* and *in vitro* (**Chapter 3.2**). Thirdly, as cold temperature is often associated with a higher incidence of respiratory viral infections, the effect of low temperature on the ability of PRV to overcome the mucus barrier was examined (**Chapter 3.3**).

Despite the inhibitory activity of the respiratory mucus, the influenza virus is ultimately able to reach the susceptible epithelial cells. It has long been assumed that neuraminidase promotes the influenza virus access to target cells in the airway by mucus degradation. However, this concept is scarcely supported by experimental data. In the second part of this thesis, the mobility of swine influenza virus particles in mucus was examined by using single particle tracking and a virus in-capsule-mucus

penetration system. In addition, the role of neuraminidase in this virus-mucus interaction was studied by the use of a neuraminidase inhibitor and the addition of exogenous neuraminidase (**Chapter 4**).

Chapter 3

3. Interactions of pseudorabies virus with porcine respiratory mucus

Chapter 3.1

3.1 Immobilization of pseudorabies virus in porcine tracheal respiratory mucus revealed by single particle tracking

Xiaoyun Yang, Katrien Forier, Lennert Steukers, Sandra Van Vlierberghe, Peter Dubruel, Kevin Braeckmans, Sarah Glorieux, Hans J. Nauwynck

PLoS ONE 7(12): e51054. doi:10.1371/journal.pone.0051054 (2012)

3.1.1. Abstract

Pseudorabies virus (PrV) initially replicates in the porcine upper respiratory tract. It easily invades the mucosae and submucosae for subsequent spread throughout the body via blood vessels and nervous system. In this context, PrV developed ingenious processes to overcome different barriers such as epithelial cells and the basement membrane. Another important but often overlooked barrier is the substantial mucus layer which coats the mucosae. However, little is known about how PrV particles interact with porcine respiratory mucus. We therefore measured the barrier properties of porcine tracheal respiratory mucus, and investigated the mobility of nanoparticles including PrV in this mucus. We developed an *in vitro* model utilizing single particle tracking microscopy. Firstly, the mucus pore size was evaluated with polyethylene glycol coupled (PEGylated) nanoparticles and atomic force microscope. Secondly, the mobility of PrV in porcine tracheal respiratory mucus was examined and compared with that of negative, positive and PEGylated nanoparticles. The pore size of porcine tracheal respiratory mucus ranged from 80 to 1500 nm, with an average diameter of 455±240 nm. PrV (zeta potential: -31.8±1.5 mV) experienced a severe obstruction in porcine tracheal respiratory mucus, diffusing 59-fold more slowly than in water. Similarly, the highly negatively (-49.8±0.6 mV) and positively (36.7±1.1 mV) charged nanoparticles were significantly trapped. In contrast, the nearly neutral, hydrophilic PEGylated nanoparticles (-9.6±0.8 mV) diffused rapidly, with the majority of particles moving 50-fold faster than PrV. The mobility of the particles measured was found to be related but not correlated to their surface charge. Furthermore, PEGylated PrV (-13.8±0.9 mV) was observed to diffuse 13-fold faster than native PrV. These findings clearly show that the mobility of PrV was significantly hindered in porcine tracheal respiratory mucus, and that the obstruction of PrV was due to complex mucoadhesive interactions including charge interactions rather than size exclusion.

3.1.2. Introduction

Herpesviruses are double-stranded DNA viruses with the potential to cause severe diseases in different species. Many members of the subfamily *Alphaherpesvirinae* initially replicate in the epithelial cells of the respiratory and/or genital mucosae (Murphy *et al.*, 2003; Steukers *et al.*, 2011). An important member is pseudorabies virus (PrV), the prototype veterinary alphaherpesvirus. PrV causes respiratory tract problems, nervous system disorders and abortions in pigs. After local replication in the epithelial cells, these viruses gain access to the connective tissue and find their way to blood vessels and nerve endings for spread throughout the host (Gibson *et al.*, 1992; Maeda *et al.*, 1998; Nauwynck *et al.*, 2007; Nauwynck, 1997). Different important barriers of the host try to hamper PrV invasion. Recently, it has been shown that in order to invade, different alphaherpesviruses including PrV use proper processes to pass an important barrier underneath the epithelium, the basement membrane (Glorieux *et al.*, 2009; Steukers *et al.*, 2011; Vandekerckhove *et al.*, 2010). Importantly, prior to epithelial cell entry, a mucus layer that coats the epithelium and serves as the first line of defense, has to be overcome by the virus (Wittmann *et al.*, 1980).

Mucus is a viscoelastic and adhesive gel that coats the non-keratinized epithelial surface of different mucosae. The thickness of the mucus layer varies among different types and species, ranging from several to more than 100 microns for the trachea of different animals (Sims & Horne, 1997; Varum *et al.*, 2012; Verkman *et al.*, 2003). Next to serving as a lubricant and assisting the adsorption of nutrients, the mucus layer acts as the body's first barrier against microbial infections. The major component and property determinant are heavily glycosylated glycoproteins, known as mucins. The assembly of these mucins in fiber structures creates an entangled mucus meshwork (Lai *et al.*, 2009c; Thornton *et al.*, 2008). The mesh (pore) size sets a threshold beyond which particle diffusion is hindered: particles with diameters larger than this mesh size are rejected while smaller, minimally interactive particles should pass through the mucus. However, in addition to this size filtering mechanism,

mucus seems to use more sophisticated strategies to interact with the traversing particles, especially diverse viruses that attempt to invade the body through the mucosae. Olmsted et al. (Olmsted *et al.*, 2001) reported that two capsid virus-like particles, human papillomavirus (diameter 55 nm) and Norwalk virus (38 nm), diffused rapidly in human cervicovaginal mucus, because of the neutral charge of viral capsids and probably also due to the size. It is hypothesized that small particles expose less hydrophobic patches, and are therefore limited in making polyvalent bonds with the hydrophobic domains distributed along the mucin fibers. However, Hida and colleagues described an even smaller capsid virus, adeno-associated virus serotype 5 (20 nm), to be highly trapped in human cystic fibrosis sputum of which the pore size ranged from 60 to 300 nm (Hida *et al.*, 2011). To date, the motion of different viruses ranging from large enveloped viruses, such as herpes simplex virus (Lai *et al.*, 2010) and human immunodeficiency virus (HIV) (Lai *et al.*, 2009a), to small non-enveloped viruses, such as adenovirus (Hida *et al.*, 2011), human papillomavirus and adeno-associated virus, have been investigated in mucus. However, these studies were limited to human cervicovaginal mucus and human cystic fibrosis sputum because none of the other types of mucus were readily available. Particularly, the interaction of aerosol respiratory viruses with healthy respiratory mucus has never been studied. Unraveling the mechanism behind the penetration of viruses across the mucosal barriers has potentially significant implications for the development of novel antiviral strategies. To achieve a better understanding in this matter, an *in vitro* model resembling the *in vivo* situation is needed. As PrV is commonly used as a good model for human alphaherpesviruses, it is highly interesting to investigate how PrV interacts with porcine respiratory mucus. Therefore, the main objectives of this study were to fully characterize the protective properties of porcine respiratory mucus, and to better understand the interactions between PrV and the mucus through which it invades in an attempt to unravel the mechanism of how PrV penetrates through porcine respiratory mucus.

In order to measure the microstructure of porcine respiratory mucus, atomic force

microscopy (AFM), a high-resolution imaging technique, was used to visualize the surface of the mucus samples and to measure the pore size formed by the mucus elements. It enables to measure the forces acting between a sample and a fine tip, which is attached to the free end of a cantilever and brought very close to the surface. Attractive or repulsive forces resulting from interactions between the tip and the surface can lead to a deflection of the cantilever according to Hooke's law (Gadegaard, 2006; Ramachandran *et al.*, 2011). As such, a three-dimensional image of the sample surface can be obtained and the pore size can be measured with the line profiling feature of the AFM software. Additionally, the effective pore size of porcine tracheal respiratory mucus was further evaluated by analyzing the motion of polyethylene glycol (PEG) coupled, non-adhesive nanoparticles in function of particle size. Based on the theory that particle transport in heterogeneous environments is regulated by the local properties of the material, non-adhesive particles smaller than the effective mesh spacing (pore size) of the network are capable of diffusion because they tend to experience the lower viscosity of the interstitial space (Lai *et al.*, 2009b; Lai *et al.*, 2009c).

In this study, we have developed a model to study the virus-mucus interactions and demonstrated the mucoadhesive influence of porcine respiratory mucus on the mobility of PrV. We have implied single particle tracking (SPT) microscopy, which uses high speed video microscopy to track the diffusion of hundreds of particles simultaneously and analyzes the motion of particles. Particle trajectories are used to calculate time-averaged mean squared displacements (*MSD*) and to determine time-dependent diffusion coefficients, which are subsequently used to characterize individual particle transport modes (Suh *et al.*, 2005). Utilizing the technique, we analyzed the microstructure of the porcine tracheal respiratory mucus, and detected the mobility of PrV and different charge modified nanoparticles in the mucus.

3.1.3. Materials and methods

3.1.3.1. Mucus sampling and preparation

Tracheal respiratory mucus was collected from porcine tracheas within 3 h after slaughter. Porcine tracheas were obtained with the permission of and collected from a local slaughterhouse (G. Van Landschoot & Zonen N.V., Adegem, Belgium) and stored on ice prior to mucus collection. The trachea was isolated and cut open longitudinally. Mucus was gently scraped with a spoon, collected with a syringe (1 ml, without needle), and stored at -70 °C until use.

3.1.3.2. Atomic force microscopy

Porcine tracheal respiratory mucus (100 µl) was evenly coated on glass (1 cm^2) and was air-dried at room temperature, according to the protocol adapted from Broughton-Head et al. (Broughton-Head *et al.*, 2007). Atomic force microscopy (AFM) images were obtained in ambient conditions in air using a multimode scanning probe microscope (Digital Instruments, Santa Barbara, CA, USA) equipped with a Nanoscope IIIa controller. 5 µm × 5 µm scans were recorded in tapping mode using a silicon cantilever (OTESPA, Veeco, CA, USA). Pore diameters were obtained using the line profiling feature of the AFM software (NanoScope software version 4.43r8, Veeco Instruments, USA).

3.1.3.3. Preparation and characterization of nanoparticles

Negatively charged, yellow-green fluorescent carboxylate-modified FluoSpheres® of different diameters, 100 nm, 200 nm and 500 nm, were purchased from Invitrogen (Merelbeke, Belgium). According to the protocol of Symens *et al.* (Symens *et al.*, 2011), positively charged nanoparticles were obtained as a result of amide formation between the carboxylate groups of the carboxylate modified FluoSpheres® and the primary amine group of N, N-dimethylethylenediamine. PEGylated nanoparticles were prepared by covalent modification of the surface carboxylate groups of carboxylate modified FluoSpheres® with methoxy-polyethylene glycol-amine (mPEGa, 2 kD, Creative PEGWorks, Winston Salem, USA.) as previously described (Forier *et al.*, 2013). Particle size (diameter) and surface charge (zeta potential) were determined by dynamic light scattering and laser Doppler anemometry, respectively,

using the Zetaziser Nano-ZS (Malvern, Worcestershire, UK).

3.1.3.4. PEGylation of PrV

The recombinant PrV Becker strain expressing green fluorescent protein fused to the VP26 capsid protein was a kind gift of Dr. Greg Smith (Northwestern University, Chicago, IL, USA). The PrV stock ($10^{8.0}$ $TCID_{50}$/ml) was concentrated by ultracentrifugation at 80 000 g for 90 min at 4°C in a Type 35 rotor (Beckman, Fullerton, CA, USA). The pellet was resuspended in phosphate buffered saline (PBS: 137 mM NaCl, 10 mM Na_2HPO_4, 2.7 mM KCl, 2 mM KH_2PO_4, pH 7.4), loaded upon a 30% sucrose cushion and followed by ultracentrifugation at 100 000 g for 3 h at 4°C in an SW41Ti rotor (Beckman, Fullerton, CA, USA). The virus pellet was resuspended in PBS to give an approximate concentration of 10^{10} $TCID_{50}$/ml. Methoxy-polyethylene glycol activated by succinimidyl succinate (mPEG-NHS, 2 kD) (NANCOS, Huissen, Netherlands) was added to the virus suspension, giving a final concentration of 20 mg/ml. The coupling reaction was performed for 2 h at 25°C. Afterwards, unreacted mPEG-NHS and the byproducts were removed by buffer exchange over a centrifugal filter (50 K membrane, Millipore). The size and zeta (ζ) potential of the PEGylated PrV were measured with the Zetaziser Nano-ZS (Malvern) and the PEGylated PrV was preserved at 4°C until use.

3.1.3.5. Real-time single particle tracking

The trajectories of fluorescent particles in porcine tracheal respiratory mucus were recorded by a fast and sensitive electron-multiplying charge-coupled device (EMCCD) camera (Cascade II: 512; Roper Scientific, Tucson, AZ, USA) mounted on an inverted epifluorescence microscope (Nikon TE2000E, Nikon Belux, Brussels, Belgium) equipped with a 100× oil-immersion objective (Plan Apochromat, Nikon). Tracking experiments were performed in press-to-seal™ silicone isolators (20 mm diameter, 0.5 mm deep, Invitrogen, Merelbeke, Belgium). Three microliters of virus suspension (10^{10} particles/ml) or nanoparticles (approximately 10^{10} particles/ml) were mixed with 100 µl of porcine tracheal respiratory mucus by gentle stirring to avoid perturbation.

The movies were captured with the NIS Elements AR software (Nikon) at a temporal resolution of 46.2 ms for 5 s. The illumination time was 10 ms per frame. Trajectories of n ≥ 500 particles were analyzed for each experiment and at least three independent experiments were performed for each condition. Movies were analyzed with the Image Processing Software (IPS, in-house developed software) to extract x, y positional data over time. The time-averaged mean squared displacements (*MSD*) and apparent diffusion coefficient (D_a) were calculated as a function of the time scale (t) for each particle.

3.1.3.6. Data analysis

Analysis of the movies was performed with custom made image processing software (Braeckmans *et al.*, 2010). Individual particles were identified in each frame of a movie and their centroids were calculated. The trajectories of the particles were determined by a nearest neighbor algorithm. For each trajectory, the mean squared displacement (*MSD*) was calculated for the available time lags t (i.e. multiples of the time Δt between the images). The *MSD* versus t plots were analyzed by a weighted fit of the anomalous diffusion model (Qian *et al.*, 1991; Saxton & Jacobson, 1997): $MSD = \Gamma t^{\alpha}$, with the transport coefficient Γ and the anomalous exponent α as free fitting parameters. The value of α is a measure for the mode of diffusion: for free diffusion $\alpha = 1$ (Γ becomes equal to 4 times the diffusion coefficient), while $\alpha < 1$ indicates hindered diffusion. The deviation of α from 1 is thus a measure for the anomaly of the diffusion. By analyzing the trajectories according to this anomalous diffusion model, distributions of the corresponding α-values can be obtained. Besides this, the apparent diffusion coefficient D_a corresponding to the first time lag Δt was calculated according to the classical expression: $D_a = MSD/4\Delta t$ (Saxton & Jacobson, 1997).

Note that in the case of free diffusion, D_a reduces to the diffusion coefficient. Distributions of the apparent diffusion coefficient can be obtained by analyzing the trajectories of the particles. These distributions are further refined with a maximum entropy method (MEM) (Braeckmans *et al.*, 2010). The MEM analysis improves the precision of the distributions, and removes features that are not statistically warranted

by the data.

3.1.4. Results

3.1.4.1. Microstructure of porcine tracheal respiratory mucus

The porous nature of porcine tracheal respiratory mucus was visualized using Tapping Mode AFM. The color intensity shows the vertical profile of the sample surface, with light regions representing the highest points and the dark points representing the depressions and pores (Fig. 1A). Pore diameters were measured with the line profiling feature of the AFM software. Distribution of the pore diameters (n=500) obtained from three independent experiments illustrated that the pore size of the porcine tracheal respiratory mucus was highly various, ranging between 80 and 1500 nm. The average pore size was 455±240 nm in diameter, with 85% of the pores being larger than the diameter of PrV particles (Fig. 1B). To further evaluate the effective mesh spacing of porcine tracheal respiratory mucus, translocations of 100, 200, and 500 nm PEGylated muco-inert nanoparticles, were tracked and transport rates were analyzed. The *MSD* of the nanoparticles was fitted to the equation $MSD = \Gamma\Delta t^{\alpha}$ to obtain α, an indicator of the extent of particle impediment. After PEGylation, the nanoparticles were slightly enlarged in diameter due to the coverage with PEG. The nearly neutral surface charge suggested that the PEGylation of the particles was complete (Table 1). As demonstrated in Fig. 1C, most of 100 nm and 200 nm PEGylated nanoparticles diffused freely through mucus, whereas, part of the 500 nm PEGylated nanoparticles were subdiffusive. This partially hindered motion is also apparent from the bimodality of the distribution of diffusion coefficient for the 500 nm nanoparticles (Fig. 1D).

Table 1. Surface charge and size of the PEGylated nanoparticles

Size	ζ potential (mV)	Diameter (nm)
100 nm*	-8.7±0.5	124.6±0.5
200 nm*	-9.6±0.8	232.6±2.4
500 nm*	-9.3±0.9	538.0±7.5

*Provided by the manufacture

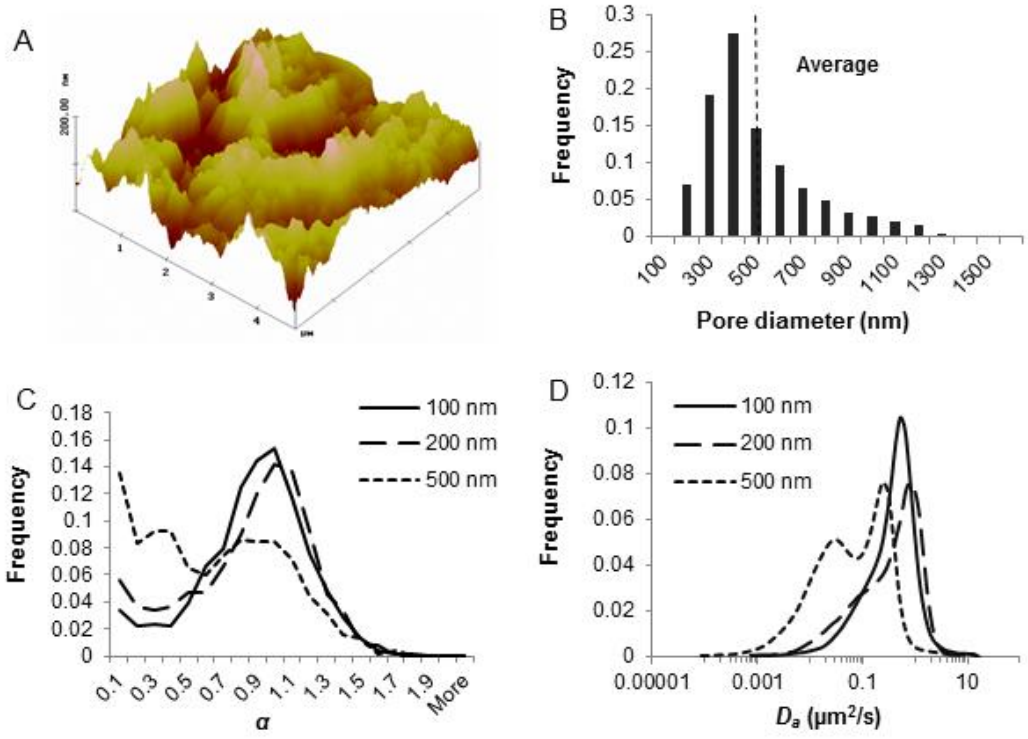

Figure 1. Evaluation of the microstructure of porcine tracheal respiratory mucus. (A) AFM visualization (5 μm × 5 μm) of porcine tracheal respiratory mucus. (B) Pore size distribution of the porcine tracheal respiratory mucus as measured by AFM. Pore diameters were analyzed by the line profiling of the 3-D images. Three scans were performed for each sample, and three independent samples were measured. The dashed line indicates the average of pore diameters (n=500). (C) Transport modes of 100, 200 and 500 nm PEGylated nanoparticles indicated by α value. More than 2000 trajectories from 3 independent experiments were tested to obtain α. (D) Distributions of the apparent diffusion coefficient of PEGylated nanoparticles. Trajectories of 10 steps were analyzed for each of the 2000 diffusion coefficients. Distributions were refined with MEM.

3.1.4.2. PrV was highly obstructed in porcine tracheal respiratory mucus

The motion of PrV (245.7±11.5 nm) in porcine tracheal respiratory mucus or in water was investigated and compared with those of 200 nm PEGylated nanoparticles. PrV was greatly slowed down in mucus with respect to the PEGylated particles. At the time scale of 1 s, the ensemble mean squared displacement <*MSD*> of the PEGylated nanoparticles was 160-fold higher than that of PrV (Fig. 2A). Trajectories of 10 steps have been analyzed, from which a distribution of the apparent diffusion coefficients was obtained (Fig. 2B). This clearly demonstrates that PrV experienced a severe obstruction in porcine tracheal respiratory mucus, with the majority of virus particles diffusing 50-fold slower than PEGylated nanoparticles. Similarly, an average α value of 0.17 was observed for PrV compared to 0.86 for the 200 nm PEGylated nanoparticles. PEGylated nanoparticles thus freely diffused through the porcine tracheal respiratory mucus whereas PrV was significantly immobilized.

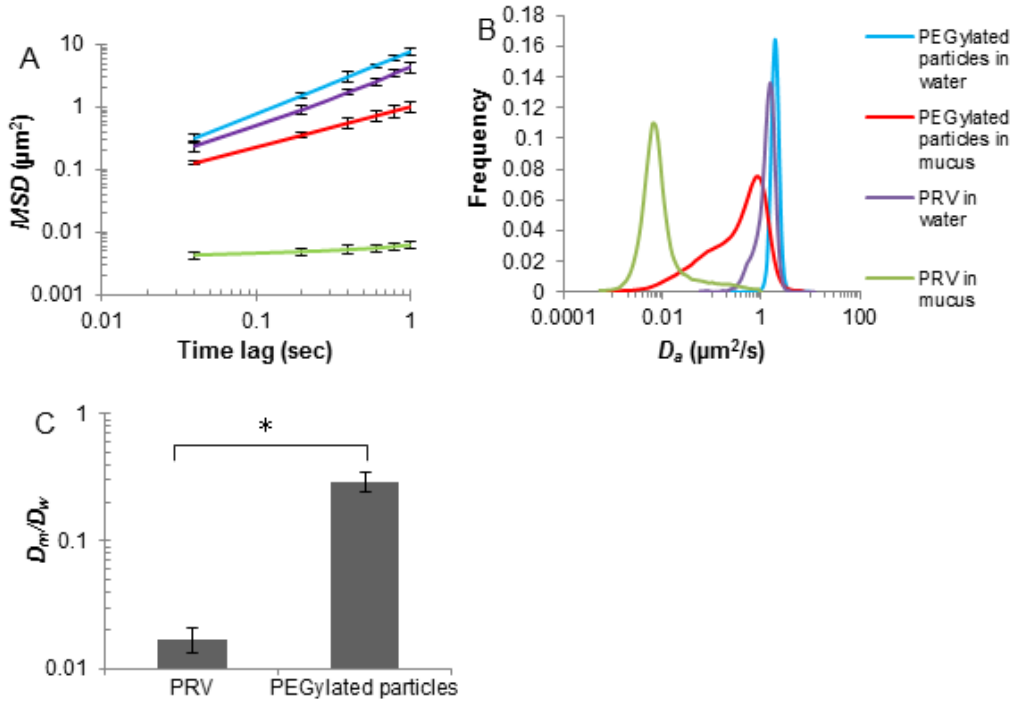

Figure 2. Transport rates of PrV and 200 nm PEGylated nanoparticles in porcine tracheal respiratory mucus or in water. (A) Averaged ensemble mean squared displacements <*MSD*> of PrV and 200 nm PEGylated nanoparticles with respect to time scale. Error bars indicate standard errors of the mean. (B) Distributions of the apparent diffusion coefficient of PrV and 200 nm PEGylated nanoparticles. Trajectories of 10 steps were analyzed for each of the 2000 diffusion coefficients.

Distributions were refined with MEM. (C) Ratios of the average diffusion coefficients in mucus (D_m) to those in water (D_w). Three independent experiments were performed for each condition. Error bars indicate the standard deviation. The asterisk (*) indicates statistical significance ($P < 0.005$).

3.1.4.3. Particle surface charge and particle mobility

To determine the relationship between surface charge and particle mobility, the diffusion of strongly negatively and positively charged nanoparticles, the nearly neutral, hydrophilic PEGylated nanoparticles (200 nm) and PrV were measured in mucus. Indicated by the representative trajectories (Fig. 3B), the diffusive motion of the strongly charged nanoparticles and PrV was highly obstructed. In contrast, PEGylated nanoparticles were allowed to diffuse rapidly. PEGylated nanoparticles diffused 30-fold faster than PrV in mucus and more than 15 and 17-fold faster than the positive and negative nanoparticles, respectively (Fig. 3C). These data suggest that the surface charge was involved in the interactions between particles and the mucus environments, which further affected the particle mobility. However, PrV clearly diffused more slowly than the higher negatively charged nanoparticles implying that other types of interactions may also play a role in this case.

3.1.4.4. PrV mobility was increased by PEGylation

The PEGylated PrV was less adhesive to porcine tracheal respiratory mucus than the native PrV. After PEGylation, the diameter of PEGylated PrV was slightly greater than the uncoated virus. ζ potential analysis revealed that the surface charge was altered from -31.8±1.5 mV to -13.8±0.9 mV after PEGylation. The transport rate of PEGylated PrV was 11-fold higher than PrV (Table 2). Taken together, the mobility of PrV in porcine tracheal respiratory mucus was increased by coating uncharged, hydrophilic PEG onto its surface.

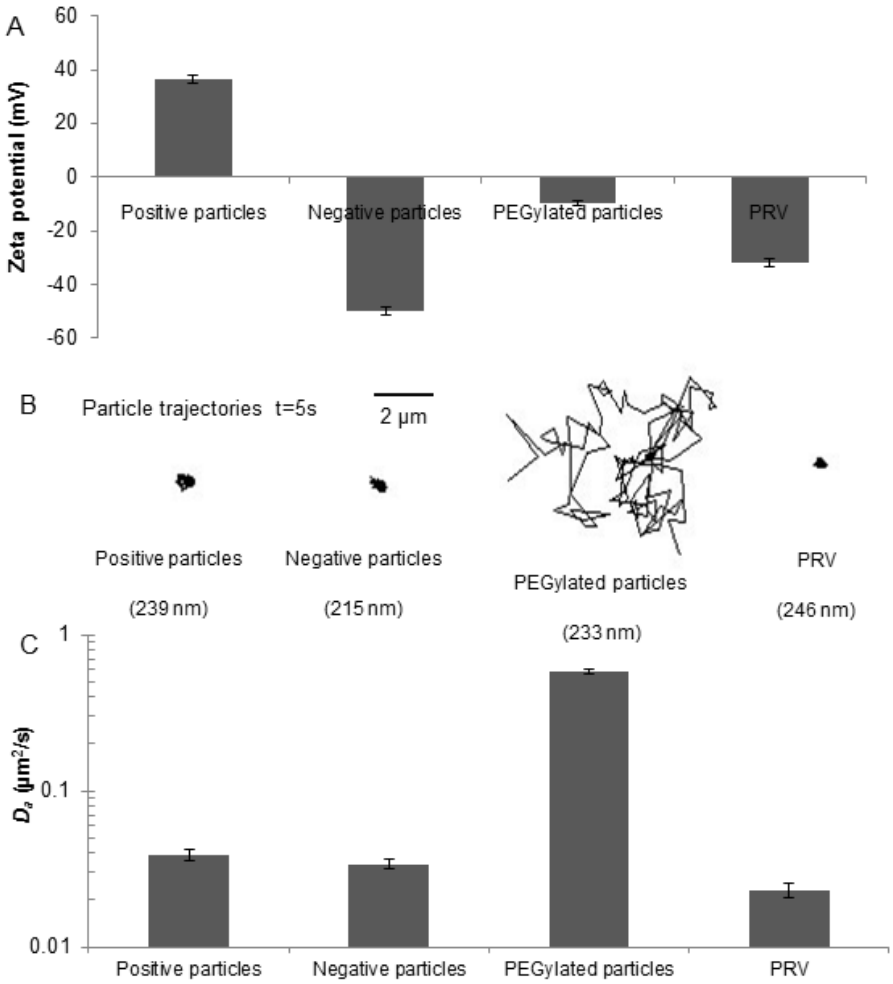

Figure 3. Particle surface charge and particle mobility. (A) ζ potentials for the particles measured with laser Doppler anemometry. (B) Representative trajectories of PrV and 200 nm nanoparticles with different surface charge modifications. The diffusions of negatively and positively charged nanoparticles and PrV were significantly suppressed; the PEGylated nanoparticles diffused rapidly. (C) Diffusion coefficient of the PrV and modified nanoparticles. Apparent diffusion coefficients D_a were determined by particle tracking for ensembles of 2000 particles for each condition. Error bars indicate the standard error of the mean.

Table 2. Diffusion comparison of PrV and PEGylated PrV

Particles	α	Diameter (nm)	ζ potential (mV)	D_a (μm^2/s)	D_m/D_w
PrV	0.167	245.7±11.5	-31.8±1.5	0.023±0.061	0.017±0.004
PEGylated PrV	0.591	269.4±16.3	-13.8±0.9	0.289±0.779	0.212±0.182

3.1.5. Discussion

PrV, often used as a representative for alphaherpesviruses, initially infects the porcine upper respiratory tract. In order to unravel the invasion of PrV through the mucus layer, we have set up an *in vitro* model of porcine tracheal respiratory mucus and analyzed the mobility of PrV through it.

In the first part, AFM was used to visualize and measure the pore diameter in porcine tracheal respiratory mucus. AFM has several advantages over electron microscopy. Firstly, analysis of the cantilever deflections enables the calculation of all three dimensions of the currently analyzed feature of the specimen, e.g. width, length and height. As a result, three-dimensional images are generated (Xie *et al.*, 2009). Secondly, samples viewed by AFM do not require special treatments such as fixation and metal coating that would irreversibly change or damage the samples. Thirdly, when imaging a dried sample deposited on a glass surface instead of a hydrated sample, the mucus polymers are immobilized, and the resolution is improved (Broughton-Head *et al.*, 2007; Manzenreiter *et al.*, 2012). Using this technique, we demonstrated that the mesh size of porcine tracheal respiratory mucus was highly heterogeneous, ranging from 80 nm to 1500 nm. Furthermore, PEGylated nanoparticles are minimally interactive with mucus and therefore are an ideal approach to probe the mucus microscopic structure. The dense PEG shielding is able to provide nanoparticles with highly hydrophilic surface properties, resulting in less hydrophobic patches subjected to mucoadhesion as well as less capability of ionic bonding due to the nearly uncharged surface (PEG is nonionic at physiological pH values). The hindered motion of the 500 nm PEGylated nanoparticles suggested that these particles were probably obstructed by the mesh. This also fits the pore size estimation by AFM. Unlike mucus, the range of the pore size of the collagen-laminin network in the basement membrane is much smaller, approximately 50-100 nm (Abrams *et al.*, 2000; LeBleu *et al.*, 2007; Steukers *et al.*, 2012). Only small particles are able to diffuse across such pores. Passage of microorganisms through this barrier often involves regulatory protease breakdown of the collagen-laminin network. Thus

the basement membrane clearly warrants a potent physical barrier against pathogenic invasion and passage of microorganisms. As the mucus pore size is tremendously heterogeneous, and most of the pores are larger than the diameter of viruses, it would be risky if the mucus exclusively relies on a size exclusion mechanism to repel the potentially invading viruses. Instead, alternative filtering mechanisms may be employed.

In the second part, we analyzed the mobility of negative, positive and PEGylated nanoparticles in porcine tracheal respiratory mucus and compared this to the motion characteristics of PrV. Mucin content, governed by mucin secretion rates as well as the degree of mucus hydration, is a major determinant of mucus rheology. Small differences in the concentrations of mucins may be sufficient to cause significant changes in the mucus viscoelasticity (King, 1980; Lai *et al.*, 2009c). Therefore, to retain the rheological properties of mucus, a small volume of PrV or nanoparticle suspension was mixed with porcine tracheal respiratory mucus. At the time scale of 1 s, PrV (-31.8±1.5 mV, 245.7±11.5 nm) experienced a significant obstruction in porcine tracheal respiratory mucus, with approximately 96% of the population exhibiting subdiffusive transport. The slightly smaller PEGylated nanoparticles (9.6±0.8 mV, 232.6±2.4 nm) exhibited a 160-fold higher <*MSD*> than PrV at the time scale of 1 s (Fig. 2A). Our results indicate that the immobility of PrV in porcine tracheal respiratory mucus cannot be explained by a size filtering mechanism. Instead, a complex interplay of mucoadhesive interactions is proposed to fully explain this issue. Therefore, the mobility of positively charged and negatively charged nanoparticles, nearly neutral PEGylated nanoparticles and PrV was measured. The strongly charged nanoparticles and PrV were significantly trapped in porcine tracheal respiratory mucus, whereas relatively neutral PEGylated nanoparticles were diffusive, implying the role of electrostatic forces in the interactions between mucus and particles. Similarly, Lieleg et al. (Lieleg *et al.*, 2009) analyzed the diffusions of amine-, carboxyl-terminated and PEGylated particles (1 μm) in extracellular matrix (ECM) purified from the Engelbreth-Holm-Swarm sarcoma of mice, and found that

the diffusion of charged particles was extremely suppressed compared to the neutral PEG modified particles, indicating particle mobility was related to the surface charge. Moreover, it is reported that the higher the surface potential of amine-terminated particles, the stronger the particle mobility was suppressed in porcine gastric mucin, and that a high salt concentration could increase the mobility of amine-terminated particles by shielding the surface of particles with counter ions (Lieleg *et al.*, 2010). Our findings suggest that charged particles interacted with the mucin polymers via electrostatic forces, and these interactions may reduce particle mobility. Furthermore, the non-glycosylated protein regions may provide a sufficiently hydrophobic region for adequate particle-mucin interactions (Fig. 4). This is supported by an investigation of the translocation of modified polystyrene microspheres in gastrointestinal mucin, in which the least hydrophobic amidine-terminated microspheres were found to have the highest diffusion among the microspheres (Yang *et al.*, 2012). In addition, the envelope of PrV and hydrophobic domains on its glycoproteins may be subjected to the hydrophobic cysteine-rich domains along mucin fibers, forming multiple low-affinity bonds. Although their low-affinity bonds have short half-lives and are easily broken by thermal energy (Cone, 2009), a great number of such bonds can keep virus particles attached to mucin fibers and entrap them. Lastly, hydrogen bonding appears to play a crucial role in mucoadhesion and disruption of hydrogen bonds can substantially reduce the adhesive strength of a mucoadhesive system. Previous studies showed that the addition of hydrogen bond breaking agents, such as urea and potassium thiocyanate (KCNS), to porcine gastric homogenized mucus resulted in a reduction in the elastic (G') and viscous (G") values (Mortazavi, 1995) and that amylose gel strength could be significantly reduced by the addition of urea (McGrane *et al.*, 2004). Interestingly, mucins contain a high density of negatively charged glycoproteins that present both strong proton acceptor and donor functionalities which mediate hydrogen bonding (Khutoryanskiy, 2011). We thus hypothesize that sialic acid and sulphate residues on the oligosaccharide chains of the mucin glycoproteins (Fig. 4) are likely to form hydrogen bonds with the glycoproteins of entrapped PrV

particles. Therefore, investigating the influence of sialic acid and sulphate residues of porcine respiratory mucins on the mobility of PrV could help to further unravel the interplay between PrV particles and the mucus barrier.

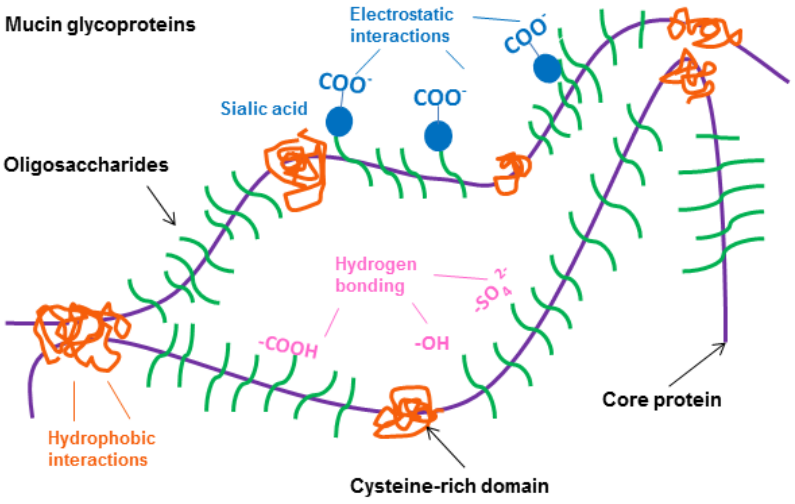

Figure 4. Schematic structure of mucin glycoproteins and their potential mucoadhesive elements

In the third part, we modified the surface of PrV particles by PEGylation and measured the mobility of the resulting virus particles. Lysine, one of the most prevalent amino acids in proteins, is known as an ideal target for PEGylation. The NHS esters of mPEG-NHS react with the primary amine groups of lysine to form stable amide bonds. Lysine mediated PEGylation of adenoviruses (Croyle *et al.*, 2000) and vesicular stomatitis virus G pseudotyped lentivirus vectors (Croyle *et al.*, 2004) have been described to sufficiently shield the viral surface and to protect the viruses from immune responses. In our study, attachment of mPEG-NHS to the PrV surface significantly increased the mobility of the PEGylated PrV. After PEGylation, the virus still possessed a net surface charge of -13.8±0.9 mV (Table 2), thus implying that besides highly reduced charge-charge interactions, other important interactions may be abolished. The coverage of the surface of virus/nanoparticles with uncharged, hydrophilic PEG did not only neutralize the charges which mediates electrostatic interactions, but also shielded the hydrophobicity and capability of hydrogen bonding. Hence, PEGylation could turn the “active” PrV into more “inert” particles.

Alternatively, PrV may bind directly to specific components of the respiratory mucus. It is known for PrV that heparan sulfate acts as a cellular receptor for viral attachment and subsequent entry (Trybala *et al.*, 1998; Trybala *et al.*, 1996). In addition to the cell surface heparan sulfate, secretory heparan sulfate may be present as one of the major proteoglycans in the airway secretions (Emery *et al.*, 1995; Hampson *et al.*, 1984). These heparan sulfates in different forms might function as a "captor" for PrV. We thus conducted experiments using polyclonal antibodies (hyperimmune serum) to determine if the entrapment of PrV in the porcine tracheal respiratory mucus could be mediated by binding to heparan sulfate (data not shown). Although it is not known if the PrV glycoprotein C (gC) was fully blocked, we assume this glycoprotein, responsible for heparan sulfate binding, to be blocked by the polyclonal antibodies. However, the transport rate of the neutralized PrV was nearly the same as that of the natural virus, implying that other interactions rather than specific PrV-receptor binding may play a determinant role in such virus-mucus interactions. Furthermore, to determine if mucins may bind PrV, we performed immunofluorescent stainings using MUC5AC antibodies that recognize the protein backbone of the mucin glycoproteins and PrV gC monoclonal antibodies (data not shown). Attachment of PrV to the mucin network was observed, but no colocalization was seen, suggesting that the virus did not bind to the protein backbones of the mucins. Therefore, it would be interesting to investigate if the sugar side chains of mucins can be a target.

Our findings have clearly shown that porcine tracheal respiratory mucus is able to act as a barrier against PrV infection. This might explain in part the pathogenesis of PrV, as no signs of viral replication are found in the trachea *in vivo*. Next to that, our laboratory used *in vitro* models of respiratory mucosae of different parts of the respiratory tract to study the invasion of different viruses through mucosal surfaces. When applying PrV on porcine tracheal mucosae, we found that PrV was able to strongly replicate in the epithelium and even to breach the basement membrane to infiltrate the host (Steukers *et al.*, unpublished data). As these tissues were washed several times before inoculation with a virus, little mucus remained as a coating on

the surface. These latter findings put strength to our hypothesis that porcine tracheal respiratory mucus might be responsible for protection against PrV infection in the proximal trachea. It would therefore be highly interesting to analyze the barrier properties of porcine nasal respiratory mucus against PrV and compare this to the results presented in this study. A comparison can also be made with another alphaherpesvirus in bovine. Similar as for PrV, bovine herpesvirus 1 (BoHV-1) replicates in the upper respiratory tract. However, this is not limited to nasal mucosae as BoHV-1 strongly replicates in the proximal trachea as well. This is confirmed by a study performed in our lab by using bovine respiratory mucosal explant models which show that different upper respiratory tissues are susceptible to BoHV-1 infections (Steukers *et al.*, 2011). Extrapolation of our hypothesis for PrV to BoHV-1, suggests that bovine tracheal respiratory mucus might not have similar protective characteristics as the porcine counterpart and that this might be a matter of virus-host co-evolution. Further investigation on this matter might provide us some crucial information on the invasion capacities of different alphaherpesviruses through the mucus barrier. Additionally, an important aspect of mucus is that the gel phase mucus is a discontinuous layer. This is due to the fact that the mucus does not flow evenly but preferentially concentrates along troughs or grooves (Agarwal *et al.*, 1994). The thickness of rat tracheal mucus observed with light- and transmission electron microscopy ranged between 0.1 and 50 μm (Sims & Horne, 1997), indicating there were thin or even "bare" regions that may be more susceptible to viral insult. This might also explain why certain regions are more susceptible to PrV infection in the explant model. To fully illustrate this issue, further investigation will be needed.

In the present study, we've setup an *in vitro* virus tracking model using single particle tracking, porcine respiratory tracheal mucus and PrV to analyze viral particle diffusion in mucus. It is noteworthy that the mucus used in this study was one time frozen and thawed. Storing mucus at -70 ^{o}C did not alter its mocoadhesive properties, based on the fact that the movement of both PrV and 200 nm PEGylated nanoparticles in thawed mucus were identical to the respective diffusion in fresh mucus (data not

shown). Therefore, this virus tracking model is highly reproducible and may be applicable to the study of a broad range of viruses with different kinds of mucus they may interact.

In summary, we've found by using the particle tracking model that PrV was significantly trapped in porcine tracheal respiratory mucus, due to complex mucoadhesive interactions. Mucoadhesion may play a significant role in the host defense. This model may be a useful tool in revealing the invasion mechanisms of alphaherpesviruses and in providing some novel insights into the strategies of mucosal immunity.

3.1.6. Acknowledgements

The authors would like to express their gratitude to Zeger Vandenabeele and Bart Ellebaut for their help in preparing all the trachea samples. Special thanks to Dr. Greg Smith for providing GFP-labeled PrV Becker strain and Dr. Dries Vercauteren and Ing. Hendrik Deschout for the help in the data analysis.

3.1.7. References

Abrams, G. A., Schaus, S. S., Goodman, S. L., Nealey, P. F. & Murphy, C. J. (2000). Nanoscale topography of the corneal epithelial basement membrane and Descemet's membrane of the human. *Cornea* **19**, 57-64.

Agarwal, M., King, M. & Shukla, A. B. (1994). Mucous Gel Transport in a Simulated Cough Machine - Effects of Longitudinal Grooves Representing Spacings between Arrays of Cilia. *Biorheology* **31**, 11-19.

Braeckmans, K., Vercauteren, D., Demeester, J. & De Smedt, S. C. (2010). Single particle tracking. In: Diaspro A, editor. Nanoscopy multidimensional optical fluorescence microscopy. *Sci-Tech News* **64**, 92-92.

Broughton-Head, V. J., Smith, J. R., Shur, J. & Shute, J. K. (2007). Actin limits enhancement of nanoparticle diffusion through cystic fibrosis sputum by mucolytics. *Pulm Pharmacol Ther* **20**, 708-717.

Cone, R. A. (2009). Barrier properties of mucus. *Adv Drug Deliv Rev* **61**, 75-85.

Croyle, M. A., Callahan, S. M., Auricchio, A., Schumer, G., Linse, K. D., Wilson, J. M., Brunner, L. J. & Kobinger, G. P. (2004). PEGylation of a vesicular stomatitis virus G pseudotyped lentivirus vector prevents inactivation in serum. *Journal of Virology* **78**, 912-921.

Croyle, M. A., Yu, Q. C. & Wilson, J. M. (2000). Development of a rapid method for the PEGylation of adenoviruses with enhanced transduction and improved stability under harsh storage conditions. *Human Gene Therapy* **11**, 1713-1722.

Emery, N., Place, G. A., Dodd, S., Lhermitte, M., David, G., Lamblin, G., Perini, J. M., Page, A. M., Hall, R. L. & Roussel, P. (1995). Mucous and Serous Secretions of Human Bronchial Epithelial-Cells in Secondary Culture. *American Journal of Respiratory Cell and Molecular Biology* **12**, 130-141.

Forier, K., Messiaen, A. S., Raemdonck, K., Deschout, H., Rejman, J., De Baets, F., Nelis, H., De Smedt, S. C., Demeester, J., Coenye, T. & Braeckmans, K. (2013). Transport of nanoparticles in cystic fibrosis sputum and bacterial biofilms by single-particle tracking microscopy. *Nanomedicine (Lond)* **8**, 935-949.

Gadegaard, N. (2006). Atomic force microscopy in biology: technology and techniques. *Biotech Histochem* **81**, 87-97.

Gibson, J. S., Slater, J. D., Awan, A. R. & Field, H. J. (1992). Pathogenesis of equine herpesvirus-1 in specific pathogen-free foals: primary and secondary infections and reactivation. *Arch Virol* **123**, 351-366.

Glorieux, S., Favoreel, H. W., Meesen, G., de Vos, W., Van den Broeck, W. & Nauwynck, H. J. (2009). Different replication characteristics of historical pseudorabies virus strains in porcine respiratory nasal mucosa explants. *Vet Microbiol* **136**, 341-346.

Hampson, I. N., Kumar, S. & Gallagher, J. T. (1984). Heterogeneity of Cell-Associated and Secretory Heparan-Sulfate Proteoglycans Produced by Cultured Human Neuro-Blastoma Cells. *Biochimica Et Biophysica Acta* **801**, 306-313.

Hida, K., Lai, S. K., Suk, J. S., Won, S. Y., Boyle, M. P. & Hanes, J. (2011). Common gene therapy viral vectors do not efficiently penetrate sputum from cystic fibrosis patients. *PLoS One* **6**, e19919.

Khutoryanskiy, V. V. (2011). Advances in Mucoadhesion and Mucoadhesive Polymers. *Macromolecular Bioscience* **11**, 748-764.

King, M. (1980). Viscoelastic properties of airway mucus. *Fed Proc* **39**, 3080-3085.

Lai, S. K., Hida, K., Shukair, S., Wang, Y. Y., Figueiredo, A., Cone, R., Hope, T. J. & Hanes, J. (2009a). Human immunodeficiency virus type 1 is trapped by acidic but not by neutralized human cervicovaginal mucus. *J Virol* **83**, 11196-11200.

Lai, S. K., Wang, Y. Y., Cone, R., Wirtz, D. & Hanes, J. (2009b). Altering mucus rheology to "solidify" human mucus at the nanoscale. *PLoS One* **4**, e4294.

Lai, S. K., Wang, Y. Y., Hida, K., Cone, R. & Hanes, J. (2010). Nanoparticles reveal that human cervicovaginal mucus is riddled with pores larger than viruses. *Proc Natl Acad Sci U S A* **107**, 598-603.

Lai, S. K., Wang, Y. Y., Wirtz, D. & Hanes, J. (2009c). Micro- and macrorheology of mucus. *Adv Drug Deliv Rev* **61**, 86-100.

LeBleu, V. S., Macdonald, B. & Kalluri, R. (2007). Structure and function of basement membranes. *Exp Biol Med (Maywood)* **232**, 1121-1129.

Lieleg, O., Baumgartel, R. M. & Bausch, A. R. (2009). Selective filtering of particles by the extracellular matrix: an electrostatic bandpass. *Biophys J* **97**, 1569-1577.

Lieleg, O., Vladescu, I. & Ribbeck, K. (2010). Characterization of particle translocation through mucin hydrogels. *Biophys J* **98**, 1782-1789.

Maeda, K., Horimoto, T. & Mikami, T. (1998). Properties and functions of feline herpesvirus type 1 glycoproteins. *J Vet Med Sci* **60**, 881-888.

Manzenreiter, R., Kienberger, F., Marcos, V., Schilcher, K., Krautgartner, W. D., Obermayer, A.,

Huml, M., Stoiber, W., Hector, A., Griese, M., Hannig, M., Studnicka, M., Vitkov, L. & Hartl, D. (2012). Ultrastructural characterization of cystic fibrosis sputum using atomic force and scanning electron microscopy. *J Cyst Fibros* **11**, 84-92.

McGrane, S. J., Mainwaring, D. E., Cornell, H. J. & Rix, C. J. (2004). The role of hydrogen bonding in amylose gelation. *Starch-Starke* **56**, 122-131.

Mortazavi, S. A. (1995). An in-Vitro Assessment of Mucus Mucoadhesive Interactions. *International Journal of Pharmaceutics* **124**, 173-182.

Murphy, J. A., Duerst, R. J., Smith, T. J. & Morrison, L. A. (2003). Herpes simplex virus type 2 virion host shutoff protein regulates alpha/beta interferon but not adaptive immune responses during primary infection in vivo. *J Virol* **77**, 9337-9345.

Nauwynck, H., Glorieux, S., Favoreel, H. & Pensaert, M. (2007). Cell biological and molecular characteristics of pseudorabies virus infections in cell cultures and in pigs with emphasis on the respiratory tract. *Vet Res* **38**, 229-241.

Nauwynck, H. J. (1997). Functional aspects of Aujeszky's disease (pseudorabies) viral proteins with relation to invasion, virulence and immunogenicity. *Vet Microbiol* **55**, 3-11.

Olmsted, S. S., Padgett, J. L., Yudin, A. I., Whaley, K. J., Moench, T. R. & Cone, R. A. (2001). Diffusion of macromolecules and virus-like particles in human cervical mucus. *Biophys J* **81**, 1930-1937.

Qian, H., Sheetz, M. P. & Elson, E. L. (1991). Single particle tracking. Analysis of diffusion and flow in two-dimensional systems. *Biophys J* **60**, 910-921.

Ramachandran, S., Teran Arce, F. & Lal, R. (2011). Potential role of atomic force microscopy in systems biology. *Wiley Interdiscip Rev Syst Biol Med* **3**, 702-716.

Saxton, M. J. & Jacobson, K. (1997). Single-particle tracking: applications to membrane dynamics. *Annu Rev Biophys Biomol Struct* **26**, 373-399.

Sims, D. E. & Horne, M. M. (1997). Heterogeneity of the composition and thickness of tracheal mucus in rats. *Am J Physiol* **273**, L1036-1041.

Steukers, L., Glorieux, S., Vandekerckhove, A. P., Favoreel, H. W. & Nauwynck, H. J. (2012). Diverse microbial interactions with the basement membrane barrier. *Trends Microbiol* **20**, 147-155.

Steukers, L., Vandekerckhove, A. P., Van den Broeck, W., Glorieux, S. & Nauwynck, H. J. (2011). Comparative analysis of replication characteristics of BoHV-1 subtypes in bovine respiratory and genital mucosa explants: a phylogenetic enlightenment. *Vet Res* **42**, 33.

Suh, J., Dawson, M. & Hanes, J. (2005). Real-time multiple-particle tracking: applications to drug and gene delivery. *Adv Drug Deliv Rev* **57**, 63-78.

Symens, N., Walczak, R., Demeester, J., Mattaj, I., De Smedt, S. C. & Remaut, K. (2011). Nuclear inclusion of nontargeted and chromatin-targeted polystyrene beads and plasmid DNA containing nanoparticles. *Mol Pharm* **8**, 1757-1766.

Thornton, D. J., Rousseau, K. & McGuckin, M. A. (2008). Structure and function of the polymeric mucins in airways mucus. *Annu Rev Physiol* **70**, 459-486.

Trybala, E., Bergstrom, T., Spillmann, D., Svennerholm, B., Flynn, S. J. & Ryan, P. (1998). Interaction between pseudorabies virus and heparin/heparan sulfate - Pseudorabies virus mutants differ in their interaction with heparin/heparan sulfate when altered for specific glycoprotein C heparin-binding domain. *Journal of Biological Chemistry* **273**, 5047-5052.

Trybala, E., Bergstrom, T., Spillmann, D., Svennerholm, B., Olofsson, S., Flynn, S. J. & Ryan, P.

(1996). Mode of interaction between pseudorabies virus and heparan sulfate heparin. *Virology* **218**, 35-42.

Vandekerckhove, A. P., Glorieux, S., Gryspeerdt, A. C., Steukers, L., Duchateau, L., Osterrieder, N., Van de Walle, G. R. & Nauwynck, H. J. (2010). Replication kinetics of neurovirulent versus non-neurovirulent equine herpesvirus type 1 strains in equine nasal mucosal explants. *J Gen Virol* **91**, 2019-2028.

Varum, F. J., Veiga, F., Sousa, J. S. & Basit, A. W. (2012). Mucus thickness in the gastrointestinal tract of laboratory animals. *J Pharm Pharmacol* **64**, 218-227.

Verkman, A. S., Song, Y. & Thiagarajah, J. R. (2003). Role of airway surface liquid and submucosal glands in cystic fibrosis lung disease. *Am J Physiol Cell Physiol* **284**, C2-15.

Wittmann, G., Jakubik, J. & Ahl, R. (1980). Multiplication and distribution of Aujeszky's disease (pseudorabies) virus in vaccinated and non-vaccinated pigs after intranasal infection. *Arch Virol* **66**, 227-240.

Xie, H., Haliyo, D. S. & Regnier, S. (2009). A versatile atomic force microscope for three-dimensional nanomanipulation and nanoassembly. *Nanotechnology* **20**, 215301.

Yang, Y., Sunoqrot, S., Stowell, C., Ji, J., Lee, C. W., Kim, J. W., Khan, S. A. & Hong, S. (2012). Effect of size, surface charge, and hydrophobicity of poly(amidoamine) dendrimers on their skin penetration. *Biomacromolecules* **13**, 2154-2162.

Chapter 3.2

3.2 Distribution of MUC5AC and MUC5B in porcine respiratory tract and the inhibitory effect of MUC5AC on pseudorabies virus infection

Xiaoyun Yang, Yewei Li, Hans J. Nauwynck

Manuscript in preparation

3.2.1. Abstract

Porcine respiratory mucus has been shown to block pseudorabies virus (PrV) movement. However, the mechanism on how the mucus prevents the virus from infecting mucosal surfaces is not well understood. Defining the innate antiviral activity found in the airway mucus may be important in view of preventative therapy for viral infection. The purpose of this study was to investigate the location of two major types of mucins, MUC5AC and MUC5B, in the respiratory tract and to determine their anti-PrV activities. First, the expression of MUC5AC and MUC5B in the porcine respiratory mucosa tissues, including nasal mucosa, trachea, bronchus and lung, was examined. Secondly, the mucin type that would account for the inhibition of the virus was identified. Lastly, the effect of O-glycans on the inhibitory activity of mucus was studied by the use of O-glycosidase. We describe here that both MUC5AC and MUC5B were widely expressed in the whole respiratory tract. MUC5AC was mainly expressed in the goblet cells of apical epithelium and MUC5B expression was mainly located in the submucosal glands. Moreover, the presence of MUC5AC was inversely related to the attachment and infection of PrV to/in porcine tracheal explant, indicating that MUC5AC played a major role in blocking PrV spread through mucus to the target cells of the epithelium. O-glycosidase treatment enhanced the infection of PrV in MUC5AC-producing cells, suggesting that O-glycans may mediate the mucin inhibitory effect on virus penetration. In summary, MUC5AC was shown to be a dominant mucin type in the porcine respiratory tract, and may function as a major contributor via its O-glycans to the inhibitory effects of airway mucus against PrV infection.

3.2.2. Introduction

Viruses constitute a main class of pathogens that cause swine diseases. PrV is one of the most important viruses in respiratory problems in field situations, except for large parts of Europe and the US that have eradicated the virus. During infection, the first barrier PrV encounters is the mucus layer, a major constituent of the innate immune

system. Mucus is a biopolymeric hydrogel that lines all moist mucosa of human and animals. One important function of mucus is to provide a physical barrier that prevents microbial pathogens from reaching the underlying epithelial cells. The protective functions of the mucus layer have been demonstrated in a number of studies. We previously found by single particle tracking (SPT) (Yang *et al.*, 2012) that PrV is highly obstructed in porcine respiratory mucus determined. In line with this, native cervical mucus can trap various types of particles, including herpes simplex virus-1 (HSV-1) and human immunodeficiency virus-1 (HIV-1) (Lai *et al.*, 2010; Shukair *et al.*, 2013).

Mucins, as the major component of mucus, may be responsible for the mucus inhibitory features. Indeed, isolated human salivary mucins directly interact with HIV-1 (Bergey *et al.*, 1994; Habte *et al.*, 2006) and have also been suggested to reduce HSV-1 infectivity at the early stage of infection (adsorption and penetration) (Bergey *et al.*, 1993). In addition, purified gastric mucins have been described to inhibit the infectivity of various types of viruses, including human papillomavirus (HPV), Merkel cell polyomavirus (MCV), and influenza A virus (Lieleg *et al.*, 2012). Moreover, isolated gastrointestinal mucins inhibit rotaviruses (Yolken *et al.*, 1992) and noroviruses (Tian *et al.*, 2005) and human breast milk mucins can impede poxvirus infection (Habte *et al.*, 2007). Therefore, we hypothesize that PrV gets stuck in the mucus due to, at least to some extent, the interactions with mucins in the airway mucus.

MUC5AC and MUC5B are the major gel-forming mucins of the human airway mucus, with only trace amounts of MUC2 (Kirkham *et al.*, 2002). MUC5AC appears to be produced primarily by the goblet cells in the tracheobronchial surface epithelium, whereas MUC5B is secreted primarily by the submucosal glands (Kirkham *et al.*, 2002; Thornton *et al.*, 2008). One plausible hypothesis is that one mucin type is more involved in mucociliary capture and clearance of pathogens and the other type is more involved in transport and expectoration by coughing. Kim *et al*. also revealed that the major mucin types of the porcine lower respiratory tract were MUC5AC and MUC5B,

while a high amount of MUC2 was also found, which is in contrast with the human counterpart (Kim *et al.*, 2011; Kim *et al.*, 2012). Up till now, data on mucin distribution along the pig respiratory tract are lacking. Thus in the present study, we examined the expression of MUC5AC and MUC5B in porcine tracheal mucosa by immunofluorescence staining and compared their distributions in nose, trachea, bronchus and lungs.

O-glycosylation is a prominent feature of the mucin and is crucial to mucin structure and function. O-glycosylation is the chemical linkage formed between the sugar side chains and the hydroxyl group of serine or threonine residues of the mucin protein backbone (Cone, 2009; Thornton *et al.*, 2008). These O-linked carbohydrate side chains, which can account for 50-80% of the mucin mass, are involved in specific ligand–receptor interactions, and might bind various small molecules and proteins. Certain O-glycans act as specific binding sites for a variety of viruses, bacteria, and parasites, and as recognition targets for bacterial toxins (Linden *et al.*, 2008; Ricciuto *et al.*, 2008). On the other hand, mucins can be regulated in terms of their glycosylation. Infection and the associated inflammation can induce changes in the extensive glycosylation pattern of mucins and sulfation, hence influencing their chemical and physical properties and thereby protecting them from the action of bacterial glycosidases (Jentoft, 1990). Thus we hypothesized that O-glycan could play a role in hindering the virus in the respiratory mucus.

To investigate the interactions between PrV and porcine airway mucins in depth, we firstly examined the distribution of MUC5AC and MUC5B in the respiratory mucosa tissues. Secondly, the major mucin type that accounts for the resistance of mucus to PrV was identified. Lastly, the attribution of O-glycan to the inhibitory effect of mucin against PrV infection was studied.

3.2.3. Materials and methods

3.2.3.1. Tissues

Mucosa tissues were isolated from the nasal septum, nasal conchae, trachea, bronchus

and lungs of six to eight-week-old piglets. The tissues were embedded in methyl cellulose and were frozen at -70 °C until use.

3.2.3.2. Explants

Immediately after euthanasia of six to eight-week-old piglets, the tracheas were isolated and dissected. The tissues were cut into 8 mm × 8 mm pieces. The explants were cultured on gauzes in an air-liquid interface manner, in DMEM/Fμsupplemented with 100 U/ml penicillin (Continental Pharma), 0.1 mg/ml streptomycin (Certa) and 1 μg/ml gentamycin (Gibco) as previously described (Glorieux *et al.*, 2007).

3.2.3.3. Isolation and culture of primary trachea epithelial cells

Porcine trachea epithelial cells were isolated and cultured as previously described (Ferrari *et al.*, 2003). Briefly, the epithelium was stripped off the tracheal mucosa, and dissected into 1 cm^2 pieces. After incubation with collagenase I at 37 °C for 2 h, the dissociated cells were obtained, and cultured in DMEM/F12 supplemented with 10% fetal calf serum (FCS, Gibco), 100 μg/ml of streptomycin and 100 units/ml of penicillin (Invitrogen). The cells were used at the second or third passage.

3.2.3.4. Immunofluorescence staining of MUC5AC and MUC5B in respiratory tissues

Cryosections (10 μm) of nasal septum, nasal conchea, trachea, bronchus and the lung tissues were made, fixed in 4% paraformaldehyde (PF) for 20 min at 4 °C and permeabilized in 0.1% Triton X-100 for 10 min at room temperature. For the double immunofluorescence staining for MUC5AC and MUC5B, the sections were incubated with mouse anti-MUC5AC monoclonal IgG1 antibody (45M1, LifeSpan Biosciences, 1:100) and rabbit anti-MUC5B polyclonal antibody (H-300, Santa Cruz Biotechnology, 1:100) for 1 h at 37 °C. After two washings with PBS (10 min/each), the sections were incubated for 1 h with goat anti-mouse IgG polyclonal antibody labeled with FITC (Molecular Probes, 1:200) for MUC5AC visualization and goat anti-rabbit IgG polyclonal antibodies conjugated with Texas Red (Molecular Probes, 1:200) for MUC5B staining. During the last 10 minutes of incubation, Hoechst 33342

(Molecular Probes, 1:100) was added. The sections were then washed twice, mounted in glycerin-DABCO with coverslips.

3.2.3.5. Immunofluorescence staining of MUC5AC and/or PrV

For single immunofluorescence staining of MUC5AC, mouse anti-MUC5AC monoclonal IgG1 antibody (1:100) was used, followed by goat anti-mouse IgG polyclonal antibody labeled with FITC. To visualize PrV attachment or infection to/in explants, FITC conjugated swine polyclonal anti-PrV antibody was used. To determine if MUC5AC-producing cells were infected with PrV, double immunofluorescence staining was performed using mouse anti-MUC5AC monoclonal IgG1 antibody followed by Texas Red conjugated goat anti-mouse IgG polyclonal antibody for MUC5AC visualization, and FITC conjugated swine polyclonal anti-PrV antibodies for PrV staining.

3.2.3.6. MUC5AC and PrV attachment to/infection in pig tracheal explant

After 24 h adaptation at 37 °C, the apical surface of three tracheal explants was washed by pipetting up and down for 15 times, while other three tracheal explants were left unwashed. For both conditions, two explants were inoculated with PrV Becker, and at the same time the third explant was frozen. For inoculation, 20 µl of PrV (10^9 $TCID_{50}$/ml) was pipetted (drop by drop) on top of the apical surface of the mucosa explants. After 1 h incubation at 37 °C, the explants were submerged into 1 ml PBS and were pipetted up and down to remove the mucus-trapped or free viral particles. Afterwards, one explant was frozen in methyl cellulose (10%). The other was placed on the gauze again, and was cultured further for 24 h at 37 °C, followed by snap-freezing in methyl cellulose. For the detection of MUC5AC and PrV attachment to the mucosal surface, 10 sections (20 µm) were made with a trimming of 400 µm in between each section. To detect PrV plaques, 100 sections (20 µm) were continuously made with 1 mm trimming in between the first and second 50 sections. Three independent experiments were performed.

3.2.3.7. Effect of O-glycosidase on PrV infection in $MUC5AC^+$ trachea cells

To detect if O-glycan mediates the interaction between MUC5AC and PrV infection, the trachea epithelial cells were treated with different concentrations (0, 1, 5 and 25 mU/ml) of O-glycosidase from *Diplococcus pneumoniae* (Roche) in the presence of neuraminidase (50 mU/ml) from *Vibrio cholera* (Roche), at 37 ^{o}C for 2 h, followed by inoculation with PrV Becker at m.o.i. 1 for 1 h. Seven hours post inoculation, the cells were fixed with 4% PF for 10 min and permeabilized with 0.1% Triton X-100 for 10 min. Afterwards, double immunofluorescence staining was performed to detect single infected cells and MUC5AC-producing cells.

3.2.4. Results

3.2.4.1. Immunofluorescence location of MUC5AC and MUC5B in the respiratory tract

The whole respiratory tract was found to express large amounts of MUC5AC and MUC5B. MUC5AC was shown to be mainly produced in the epithelial mucus-secreting cells (Table 1, Fig. 1B), while MUC5B was mainly expressed in the submucosal glands (Table 1, Fig. 1C). In general, the upper respiratory tract has a higher mucin expression than the lower respiratory tract (Table 1). In the nasal conchae and septum mucosa, over 15% of the epithelial cells were positive for MUC5AC staining. In the submucosal glands of these tissues, about 5 to 15% of the nasal glands produced MUC5B, compared to less than 5% submucosal glands of the trachea and bronchus.

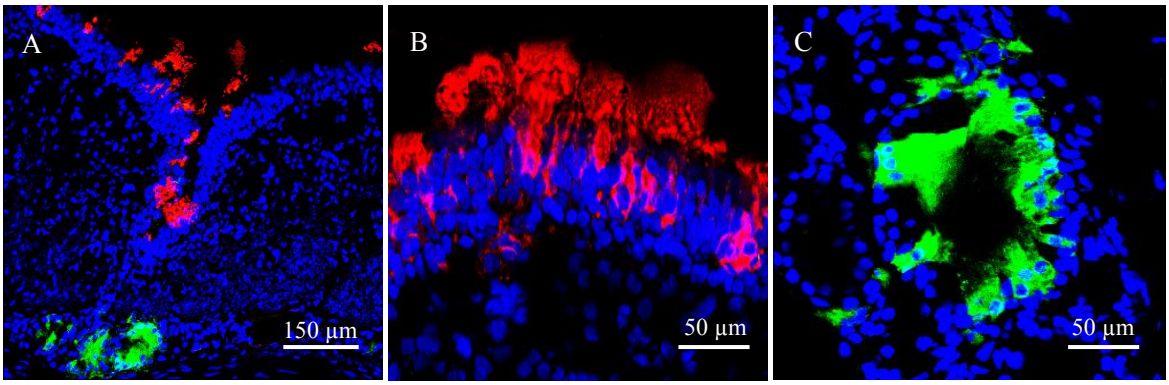

Tracheal mucosa Apical epithelium Submucosal gland

Figure 1. Double immunofluorescence of MUC5AC and MUC5B in porcine trachea tissues. Representative microscopy images of MUC5AC and MUC5B expression in the porcine trachea. MUC5AC (red) is expressed mainly in superficial epithelium, and MUC5B (green) is almost exclusively expressed in submucosal glands.

Table 1. Tissue location of MUC5AC and MUC5B in porcine respiratory tract

	Septum		Conchea		Trachea		Bronchi		Lung	
	Ep	SbG	Ep	SbG	Ep	SbG	Ep	SbG	Bronchiole Ep	Alveoli Ep
MUC5AC	+++	+/-	+++	+	++	+/-	++	+/-	+/-	-
MUC5B	-	++	-	+++	-	+	-	+	-	-

Ep: Epithelium; SbG: Submucosal gland
Positive cells/glands account for: + 0-5%; ++ 5-15%; +++ 15-30%; ++++ >30%

3.2.4.2. MUC5AC reduces PrV infection by blocking the access of virus to the mucosal epithelium

As shown by immunofluorescence staining, MUC5AC content was strongly reduced by washing. In the "unwashed" explants, the MUC5AC formed a continuous layer upon most of the mucosal surface (Fig. 2A), while it was only sparsely located after flushing (Fig. 2B). Ten regions, as indicated by the representative confocal micrographs (Fig. 2A and B), were randomly selected from 10 sections; the percentage of MUC5AC positive region to the region of interest (ROI, 300 µm × 300 µm) was calculated by ImageJ and 3 independent experiments were performed,

resulting in 30 measurements conducted. Totally, the MUC5AC presence on the mucosa epithelium was more than 2.5-fold reduced by flushing (Fig. 2C). Virus attaching to washed and unwashed explants was determined by immunofluorescence staining using FITC conjugated swine anti-PrV purified serum. For an image, PrV particles attached to the apical epithelium (20 μm thick and 100 μm long) were measured, and 10 images were examined. The total number of viral particles that attached to an epithelium surface of 2×10^4 μm^2 was calculated. At 1 h post inoculation, the number of PrV particles attached to apical epithelium of the unwashed explant, which was coated with mucus, was limited and sparsely located (Fig. 2D), whereas clearly more virions attached to the washed epithelium (Fig. 2E). Correspondingly, the number of PrV plaques formed in the washed explant was nearly 2-fold higher than that in the mock treated explant (Fig. 2I). Taken together, these findings indicate that MUC5AC indeed blocked the virions to get access to the target cells in the epithelium, resulting in significantly less virus infection in the explant.

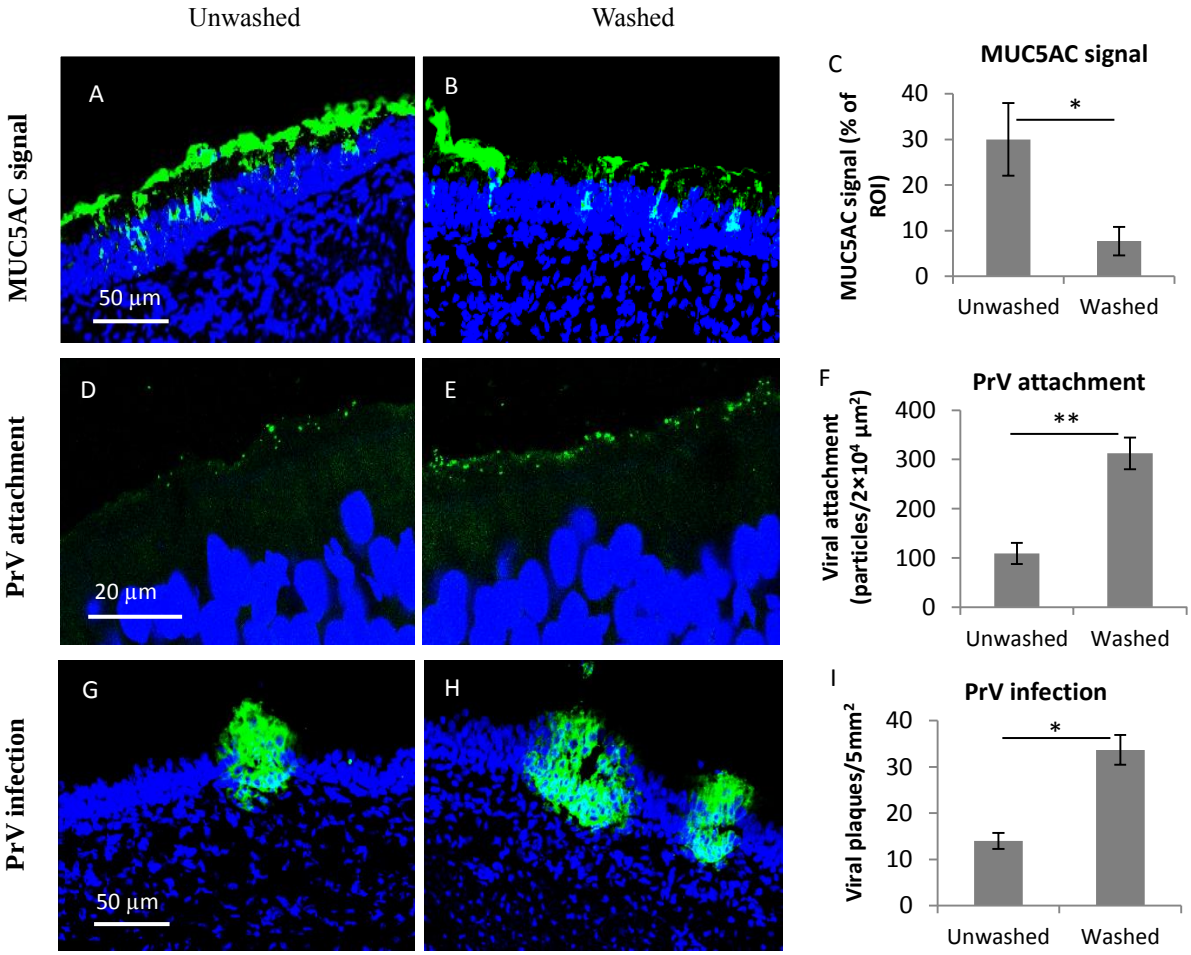

Figure 2. Correlation between PrV infection and MUC5AC content. MUC5AC presence (green) on unwashed (A) and washed (B) tracheal explants. Binding of PrV particles (green) to the unwashed (D) and washed (E) tracheal explants. (C) Quantification of MUC5AC presence in washed and unwashed tracheal explants. (F) PrV binding to washed and unwashed explants measured with imageJ. A representative confocal micrograph of the plaques (green) formed by PrV infection in the unwashed (G) and washed (H) tracheal explants. Average number of plaques measured from three independent experiments (I). Error bar indicates standard deviation. The asterisks (** and *) indicate statistical significance ($P<0.01$, and $P<0.05$, respectively, by Student's *t-test*).

3.2.4.3. O-glycans contribute to the resistance of MUC5AC-producing cells to PrV infection

O-glycosidase, also known as Endo-α-N-Acetylgalactosaminidase, catalyzes the removal of O-linked saccharides after the terminal sialic acids have been removed by neuraminidase from mucin glycoproteins. Treatment of the primary tracheal epithelial cells with O-glycosidase in the presence of neuraminidase is assumed to remove O-glycans from the secreted form of mucin 5AC as well as those that are still

associated with the cell membrane. Results show that in the mock control, approximately 10% of the primary cells were positive for MUC5AC (data not shown), and 16% of cells were infected with PrV. Cells infected with PrV were hardly positive for MUC5AC, with a ratio of 1 double positive cell out of 300 total cells counted, indicating that approximately 1 out of 30 $MUC5AC^{+}$ cells was infected. Treatment of the epithelial cells with O-glycosidase resulted in a dose-dependent increase in PrV infection in MUC5AC-producing cells. Specifically, at the concentration of 1 mU/ml, the O-glycosidase was shown to increase the infection of MUC5AC positive cells by 1.5-fold. At higher concentrations, the enzyme was able to enhance the infection of MUC5AC positive cells by several folds (Fig. 3). It should be noticed that infection was slightly increased while enhancing the concentration of O-glycosidase. These data suggest that O-glycan may mediate the inhibitory effect of MUC5AC with respect to blocking PrV entry into host cells.

3.2.5. Discussion

Mucus is a porous biopolymer matrix that coats all wet epithelia in the human body and serves as the first line of defense against many pathogenic bacteria and viruses. The identification of critical components of native mucus that provide antiviral activity might bear an enormous potential for the discovery of new antiviral substances. Native mucus can trap various types of viral particles, including PrV, swine influenza virus H1N1, HSV-1 and HIV-1 (Lai *et al.*, 2010; Lai *et al.*, 2009; Yang *et al.*, 2012; Yang *et al.*, 2014). This effect is often referred to as “mucoadhesion” and is based on binding interactions between the mucin biopolymers and the diffusing particles. The major gel-forming units of mucus are mucins, large glycoproteins with glycans covalently linked via N-acetylgalactosamine (GalNAc) to the hydroxyl groups of serine or threonine residues of the mucin backbone. These carbohydrates can make up 80% of the mucin mass (Cone, 2009; Lillehoj & Kim, 2002). It appears that mucins might play a major role in the phenomenon of mucoadhesion.

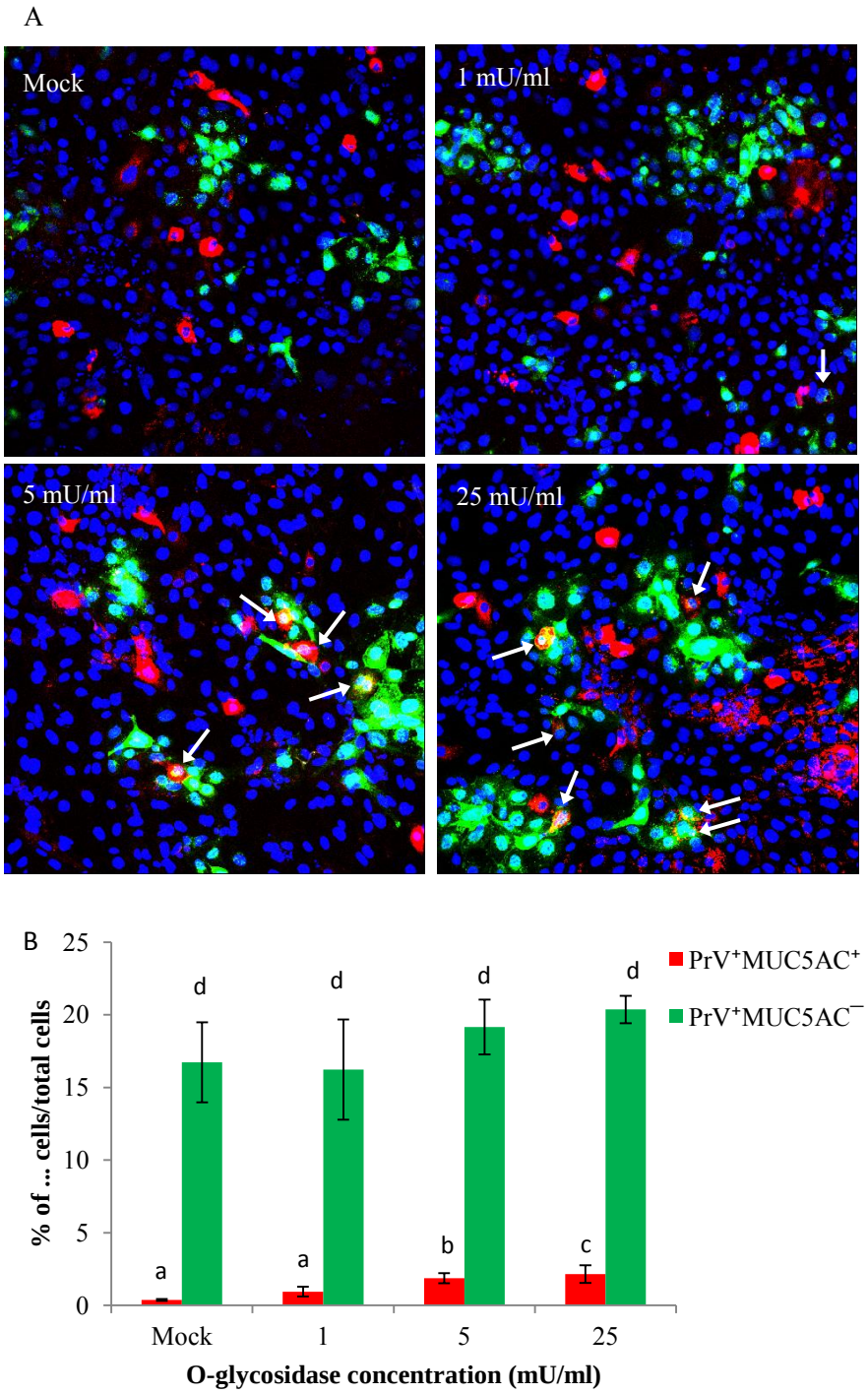

Figure 3. Effect of O-glycosidase on PrV infection in MUC5AC-producing cells. (A) Primary trachea cells were infected with PrV at m.o.i. 1, and cultured for 24 h. Double immunofluorescence staining was performed to visualize PrV infected cells (green) and MUC5AC-producing cells (red). Double positive cells are pointed by white arrows. (B) Percentages of PrV infected MUC5AC^{+} and PrV infected MUC5AC^{-} cells relative to the total trachea cells were determined. Error bar shows the standard deviation of three independent experiments. Significant differences are pointed out by the use of different letters (another letter means a statistical difference) ($P<0.05$).

Mucins form a heterogeneous family comprising monomeric mucins that may be secreted or tethered to cell surfaces and polymeric mucins that are secreted and form the scaffolding of mucus gels. Polymeric mucins, MUC2, MUC5AC, MUC5B, and MUC6, are normally expressed in the respiratory tract (Jeffery & Li, 1997; Lillehoj & Kim, 2002; Thornton *et al.*, 2008). The mucin genes that encode structurally related mucin glycoproteins are evolutionarily conserved among different species and expression locations (Fahy & Dickey, 2010; Young *et al.*, 2007). In the present study, MUC5AC and MUC5B were found to be widely expressed in the whole respiratory tract of the pig (Table 1). Although other types of mucins were not examined in this study, we assumed that MUC5AC and MUC5B are the major mucins found in the pig airway, due to the broad and strong expression. We found that MUC5AC was mainly expressed by the mucus-producing cells in the superficial epithelium, and MUC5B was almost exclusively expressed by the submucosal gland mucous cells (Fig 1). Hovenberg *et al.* reported that MUC5AC was the major mucin type of the healthy respiratory secretions in human (Hovenberg *et al.*, 1996). Furthermore, a recent study demonstrated that MUC5AC acts as a protective barrier against a specific influenza strain infection, by using a transgenic mouse model that overexpressed MUC5AC. The transgenic mice challenged with A/PR8/34 H1N1 influenza virus gave significantly less infection than the normal mice (Ehre *et al.*, 2012). Thus we next assessed the interactions between PrV and MUC5AC with tracheal explants and primary trachea epithelial cells. We found that, after 24 h adaptation at 37 ^{o}C, the explants were able to produce a continuous mucus layer consisting of MUC5AC (Fig. 2A), while the secreted MUC5B overlaying the apical epithelium was highly region-dependent (data not shown). Consistently, the unwashed explant which was covered with a mucus layer was more resistant to the PrV infection than the washed explant. The amount of MUC5AC on top of the pig tracheal explant indeed was inversely related to the number of virus reaching and attaching to the epithelium (Fig. 2). Moreover, MUC5AC-producing cells appeared largely resistant to PrV infection. Specifically, only 1 out of 30 MUC5AC positive cells was infected with PrV when the

primary epithelial cells were inoculated with PrV at m.o.i. 1. We assume that the MUC5AC positive cells, which comprised of approximately 10% the epithelial cells, may form an adherent mucin layer to prevent the virus from binding to the cells. Therefore, we suggest that MUC5AC may be a dominant type of pig airway mucins, and may contribute to the protection of the respiratory mucosa against PrV approach to epithelial cells. However, we have not performed immunofluorescence staining for other mucins such as MUC2, and contribution of other mucins to the inhibitory effects of the respiratory mucus cannot be excluded.

Although it is not demonstrated in this study, MUC5B may also be important for airway defense. It is reported by Roy *et al.* that mouse MUC5B is required for mucociliary clearance, for controlling infections in the airways and for maintaining immune homeostasis in mouse lungs. MUC5B deficiency caused materials to accumulate in upper and lower mouse airway (Roy *et al.*, 2014). In addition, a recent research suggests that the ratio of MUC5AC and MUC5B in the mucus gel can alter how the mucus is moved by cilia. The ratio of MUC5B to MUC5AC in the airway mucus of healthy individuals was 0.5, while in cystic fibrosis (CF) sputum the ratio increased to 2.4 (Henke *et al.*, 2004). Moreover, MUC5B mucin has been previously described as the major mucin of sputum in patients with chronic obstructive pulmonary disease (COPD) (Kirkham *et al.*, 2002). Therefore, MUC5B, produced in the submucosal gland, may contribute to virus clearance, especially in chronic infection. Taken together, our findings suggest that MUC5AC, owing to its production in the surface epithelium, is an acute-response mucin, whereas MUC5B, produced mainly in the glands, is involved in the response to more chronic insults.

In the last part, using O-glycosidase, we demonstrated that O-glycosylated glycans contributed to the effects of mucins. Mucins contain up to 80% O-linked oligosaccharides by weight, and these sugars have been shown to be important for mucin activity. O-glycosidase specifically catalyzes the removal of O-linked glycans from mucin glycoproteins. Treatment of primary epithelial cells with O-glycosidase rendered the MUC5AC-producing cells more susceptible to PrV infection (Fig. 3). As

PrV has been shown to directly bind to the mucus, we assume that the O-linked oligosaccharides of MUC5AC may function as decoy receptors for the virus in this case. This strategy is also utilized by colonic mucins to block parasite invasion. Some parasites recognize and bind with high-affinity to galactose (Gal) and N-acetylgalactosamine residues on colonic mucins or surface receptors of host cells. Belley *et al.* showed that Gal and GalNAc sugar residues of purified colonic mucins competitively inhibit amoeba binding to host epithelium. These authors further demonstrated that treatment of LS 174T cells with the O-linked glycosylation inhibitor benzyl-α-GalNAc rendered the monolayer susceptible to amoebic attack (Belley *et al.*, 1996). Furthermore, a recent study provides further evidence showing that O-glycans contribute to maintenance of barrier function on the apical surface by preventing clathrin-mediated endocytosis in human corneal keratinocytes (Guzman-Aranguez *et al.*, 2012). Together, these studies highlight a critical role for O-linked oligosaccharide residues of mucin in inhibiting pathogen invasion.

Given the wide range of viruses that are inhibited by different mucins, it is possible that mucins might be able to act as broad-spectrum antiviral agents. Thus it is crucial to regulate the synthesis and maintain the secretion of mucins. Factors, such as cytokines, environmental temperature and toxic gas, which can alter the mucin physiology, may be the targets of possible preventative therapy for viral infection (Davis & Dickey, 2008; Linden *et al.*, 2008). In addition to regulation of their synthesis and release, mucins are regulated in terms of their glycosylation (Tian & Ten Hagen, 2009). Terminal sugars, because of their hydrophobicity or charge, are thought to contribute to or determine the physical and/or biological properties of mucins. Thus alterations in terminal glycosylation of mucins, which may occur in disease states, have the potential to alter the physical properties of mucins and the rheological properties of mucus. Altering mucin carbohydrates may block mechanisms that pathogens use to subvert the mucin barrier. Such changes in mucin glycosylation need to be considered as a component of innate and adaptive immune responses to mucosal infection.

3.2.6. Acknowledgements

The authors would like to express their gratitude to Zeger Vandenabeele and Loes Loes Geypen for their help in preparing all the trachea samples. Special thanks to Lieve Sys for the help in the experiments and discussion.

3.2.7. References

Belley, A., Keller, K., Grove, J. & Chadee, K. (1996). Interaction of LS174T human colon cancer cell mucins with Entamoeba histolytica: an in vitro model for colonic disease. *Gastroenterology* **111**, 1484-1492.

Bergey, E. J., Cho, M. I., Blumberg, B. M., Hammarskjold, M. L., Rekosh, D., Epstein, L. G. & Levine, M. J. (1994). Interaction of HIV-1 and human salivary mucins. *J Acquir Immune Defic Syndr* **7**, 995-1002.

Bergey, E. J., Gu, M., Collins, A. R., Bradway, S. D. & Levine, M. J. (1993). Modulation of herpes simplex virus type 1 replication by human salivary secretions. *Oral Microbiol Immunol* **8**, 89-93.

Cone, R. A. (2009). Barrier properties of mucus. *Adv Drug Deliv Rev* **61**, 75-85.

Davis, C. W. & Dickey, B. F. (2008). Regulated airway goblet cell mucin secretion. *Annu Rev Physiol* **70**, 487-512.

Ehre, C., Worthington, E. N., Liesman, R. M., Grubb, B. R., Barbier, D., O'Neal, W. K., Sallenave, J. M., Pickles, R. J. & Boucher, R. C. (2012). Overexpressing mouse model demonstrates the protective role of Muc5ac in the lungs. *Proc Natl Acad Sci U S A* **109**, 16528-16533.

Fahy, J. V. & Dickey, B. F. (2010). Airway mucus function and dysfunction. *N Engl J Med* **363**, 2233-2247.

Ferrari, M., Scalvini, A., Losio, M. N., Corradi, A., Soncini, M., Bignotti, E., Milanesi, E., Ajmone-Marsan, P., Barlati, S., Bellotti, D. & Tonelli, M. (2003). Establishment and characterization of two new pig cell lines for use in virological diagnostic laboratories. *J Virol Methods* **107**, 205-212.

Glorieux, S., Van den Broeck, W., van der Meulen, K. M., Van Reeth, K., Favoreel, H. W. & Nauwynck, H. J. (2007). In vitro culture of porcine respiratory nasal mucosa explants for studying the interaction of porcine viruses with the respiratory tract. *J Virol Methods* **142**, 105-112.

Guzman-Aranguez, A., Woodward, A. M., Pintor, J. & Argueso, P. (2012). Targeted disruption of core 1 beta1,3-galactosyltransferase (C1galt1) induces apical endocytic trafficking in human corneal keratinocytes. *PLoS One* **7**, e36628.

Habte, H. H., Kotwal, G. J., Lotz, Z. E., Tyler, M. G., Abrahams, M., Rodriques, J., Kahn, D. & Mall, A. S. (2007). Antiviral activity of purified human breast milk mucin. *Neonatology* **92**, 96-104.

Habte, H. H., Mall, A. S., de Beer, C., Lotz, Z. E. & Kahn, D. (2006). The role of crude human saliva and purified salivary MUC5B and MUC7 mucins in the inhibition of Human Immunodeficiency Virus type 1 in an inhibition assay. *Virol J* **3**, 99.

Henke, M. O., Renner, A., Huber, R. M., Seeds, M. C. & Rubin, B. K. (2004). MUC5AC and

MUC5B Mucins Are Decreased in Cystic Fibrosis Airway Secretions. *Am J Respir Cell Mol Biol* **31**, 86-91.

Hovenberg, H. W., Davies, J. R., Herrmann, A., Linden, C. J. & Carlstedt, I. (1996). MUC5AC, but not MUC2, is a prominent mucin in respiratory secretions. *Glycoconj J* **13**, 839-847.

Jeffery, P. K. & Li, D. (1997). Airway mucosa: secretory cells, mucus and mucin genes. *European Respiratory Journal* **10**, 1655-1662.

Jentoft, N. (1990). Why are proteins O-glycosylated? *Trends Biochem Sci* **15**, 291-294.

Kim, C. H., Lee, K., Han, K., Oh, Y., Kim, D., Seo, H. W., Park, C., Ha, M. K., Kim, S. H., Cho, K. D., Lee, B. H. & Chae, C. (2011). Expression of mucins on the mucosal surface of lungs of 4-week-old pigs. *Vet Res Commun* **35**, 255-260.

Kim, C. H., Oh, Y., Han, K., Seo, H. W., Kim, D., Kang, I., Park, C., Jang, K. Y., Kim, S. H. & Chae, C. (2012). Expression of secreted mucins (MUC2, MUC5AC, MUC5B, and MUC6) and membrane-bound mucin (MUC4) in the lungs of pigs experimentally infected with Actinobacillus pleuropneumoniae. *Res Vet Sci* **92**, 486-491.

Kirkham, S., Sheehan, J. K., Knight, D., Richardson, P. S. & Thornton, D. J. (2002). Heterogeneity of airways mucus: variations in the amounts and glycoforms of the major oligomeric mucins MUC5AC and MUC5B. *Biochem J* **361**, 537-546.

Lai, S. K., Wang, Y. Y., Hida, K., Cone, R. & Hanes, J. (2010). Nanoparticles reveal that human cervicovaginal mucus is riddled with pores larger than viruses. *Proc Natl Acad Sci U S A* **107**, 598-603.

Lai, S. K., Wang, Y. Y., Wirtz, D. & Hanes, J. (2009). Micro- and macrorheology of mucus. *Adv Drug Deliv Rev* **61**, 86-100.

Lieleg, O., Lieleg, C., Bloom, J., Buck, C. B. & Ribbeck, K. (2012). Mucin Biopolymers As Broad-Spectrum Antiviral Agents. *Biomacromolecules* **13**, 1724-1732.

Lillehoj, E. R. & Kim, K. C. (2002). Airway mucus: its components and function. *Arch Pharm Res* **25**, 770-780.

Linden, S. K., Sutton, P., Karlsson, N. G., Korolik, V. & McGuckin, M. A. (2008). Mucins in the mucosal barrier to infection. *Mucosal Immunol* **1**, 183-197.

Ricciuto, J., Heimer, S. R., Gilmore, M. S. & Argueso, P. (2008). Cell surface O-glycans limit Staphylococcus aureus adherence to corneal epithelial cells. *Infect Immun* **76**, 5215-5220.

Roy, M. G., Livraghi-Butrico, A., Fletcher, A. A., McElwee, M. M., Evans, S. E., Boerner, R. M., Alexander, S. N., Bellinghausen, L. K., Song, A. S., Petrova, Y. M., Tuvim, M. J., Adachi, R., Romo, I., Bordt, A. S., Bowden, M. G., Sisson, J. H., Woodruff, P. G., Thornton, D. J., Rousseau, K., De la Garza, M. M., Moghaddam, S. J., Karmouty-Quintana, H., Blackburn, M. R., Drouin, S. M., Davis, C. W., Terrell, K. A., Grubb, B. R., O'Neal, W. K., Flores, S. C., Cota-Gomez, A., Lozupone, C. A., Donnelly, J. M., Watson, A. M., Hennessy, C. E., Keith, R. C., Yang, I. V., Barthel, L., Henson, P. M., Janssen, W. J., Schwartz, D. A., Boucher, R. C., Dickey, B. F. & Evans, C. M. (2014). Muc5b is required for airway defence. *Nature* **505**, 412-416.

Shukair, S. A., Allen, S. A., Cianci, G. C., Stieh, D. J., Anderson, M. R., Baig, S. M., Gioia, C. J., Spongberg, E. J., Kauffman, S. M., McRaven, M. D., Lakougna, H. Y., Hammond, C., Kiser, P. F. & Hope, T. J. (2013). Human cervicovaginal mucus contains an activity that hinders HIV-1 movement. *Mucosal Immunol* **6**, 427-434.

Thornton, D. J., Rousseau, K. & McGuckin, M. A. (2008). Structure and function of the polymeric

mucins in airways mucus. *Annu Rev Physiol* **70**, 459-486.

Tian, E. & Ten Hagen, K. G. (2009). Recent insights into the biological roles of mucin-type O-glycosylation. *Glycoconj J* **26**, 325-334.

Tian, P., Brandl, M. & Mandrell, R. (2005). Porcine gastric mucin binds to recombinant norovirus particles and competitively inhibits their binding to histo-blood group antigens and Caco-2 cells. *Lett Appl Microbiol* **41**, 315-320.

Yang, X., Forier, K., Steukers, L., Van Vlierberghe, S., Dubruel, P., Braeckmans, K., Glorieux, S. & Nauwynck, H. J. (2012). Immobilization of pseudorabies virus in porcine tracheal respiratory mucus revealed by single particle tracking. *PLoS One* **7**, e51054.

Yang, X., Steukers, L., Forier, K., Xiong, R., Braeckmans, K., Van Reeth, K. & Nauwynck, H. (2014). A beneficiary role for neuraminidase in influenza virus penetration through the respiratory mucus. *PLoS One* **9**, e110026.

Yolken, R. H., Peterson, J. A., Vonderfecht, S. L., Fouts, E. T., Midthun, K. & Newburg, D. S. (1992). Human milk mucin inhibits rotavirus replication and prevents experimental gastroenteritis. *J Clin Invest* **90**, 1984-1991.

Young, H. W., Williams, O. W., Chandra, D., Bellinghausen, L. K., Perez, G., Suarez, A., Tuvim, M. J., Roy, M. G., Alexander, S. N., Moghaddam, S. J., Adachi, R., Blackburn, M. R., Dickey, B. F. & Evans, C. M. (2007). Central role of Muc5ac expression in mucous metaplasia and its regulation by conserved 5' elements. *Am J Respir Cell Mol Biol* **37**, 273-290.

Chapter 3.3

3.3 Cold temperature helps pseudorabies virus to overcome the respiratory mucus: New insights into the association of exposure to cold with respiratory viral infection

Xiaoyun Yang, Tingting Cui, Hans J. Nauwynck

Manuscript in preparation

3.3.1. Abstract

Pseudorabies virus (PrV) uses the porcine upper respiratory tract as a primary portal for entry. During this process, the first barrier the virus encounters is the mucus layer, which lines the respiratory apical epithelium. PrV has been shown to be hindered in the porcine respiratory mucus in our previous studies. This finding fits with the fact that most PrV infections have a subclinical cause. Since most clinical outbreaks of PrV infection occur during winter season, the effect of low temperature on interactions of PrV with porcine respiratory mucus was investigated. First, the effect of temperature on the binding of PrV to porcine respiratory mucus was examined. Secondly, the virus penetration through the respiratory mucus was analyzed in the virus in-capsule-mucus penetration system at different temperatures. Furthermore, the effect of temperature on the ability of PrV to overcome the mucus barrier was studied in a well-established respiratory mucosa explant system (*ex vivo*) as well as in a culture system, where virus was first incubated with pig mucus or mucin solution (*in vitro*) and afterwards brought on top of the susceptible cells. The results showed that less virions were bound to the respiratory mucus at low temperature. In addition, the viral particles penetrated further with time in the mucus at 4 ^{o}C, which was not observed at 37 ^{o}C. The mucus almost did not prevent the virus from binding to the tracheal apical epithelium at 4 ^{o}C, but blocked 65% of the virions at 37 ^{o}C. Lastly, the percentage of PrV that overcame the mucus and caused infection in tracheal explants and swine testicular (ST) cells increased with decline of temperature. Taken together, these findings indicate that low temperature helps PrV to thwart the porcine respiratory mucus, which may shed new light on the interactions between exposure to cold, extent of virus replication during respiratory viral infections and severity of disease.

3.3.2. Introduction

Respiratory tract infections are the most common infections worldwide among humans and animals, and the cause of significant morbidity and a considerable

economic burden to health care. Seasonal outbreaks of respiratory tract viral infections are a common phenomenon, with peaks often being observed during winter time. Influenza outbreaks occur in human populations of the northern and southern hemispheres during their respective winters (Finkelman *et al.*, 2007; Hope-Simpson, 1981). Similarly, respiratory syncytial virus (RSV) infections in human show a clear seasonality with onset in late fall or early winter, a peak between mid December and early February, and season offset in late spring (Borchers *et al.*, 2013; Gilca *et al.*, 2006). Several animal respiratory viruses also cause outbreaks which peak in winter. Bovine respiratory syncytial virus (BRSV) is one of the major pathogens involved in the bovine respiratory disease complex (BRDC), detrimentally impacting production and animal welfare in the cattle industry all over the world (Edwards, 2010; Griffin, 1997; Snowder *et al.*, 2006). Outbreaks of respiratory disease in cattle associated with BRSV peak in autumn and winter (Valarcher & Taylor, 2007; Van der Poel *et al.*, 1993). Aujeszky's disease which is caused by PrV infection is a major contributor to winter porcine respiratory disease complex (PRDC) in growing pigs in regions where the virus is still circulating. Outbreaks of Aujeszky's disease were commonly seen during the winter time between 1980s and 1990s in Europe before the eradication campaign was performed (Christensen, 1995; Jestin *et al.*, 1990; Maes & Pensaert, 1984). In spite of the eradication of Aujeszky's disease in Denmark, a single outbreak was recorded in December 1988 and another severe epizootic took place during the winter and spring of 1989/90 (Christensen *et al.*, 1993). Later on, severe PrV outbreaks occurred in the winter of 2011/12 in several herds and the virus spread rapidly all over the area of northern China. Historically, swine influenza in the northern hemisphere is a disease that peaks in late fall and early winter months. European H1N1 swine influenza viruses emerged in January 1979 in Belgium (Pensaert *et al.*, 1981), and in the winter of 1979/80, similar viruses appeared in Germany and France (Krumbholz *et al.*, 2014). In the winter of 1989 and spring of 1990, there were large outbreaks of respiratory disease in two swine herds in southern Japan. Such seasonal pattern diminished by the fact that respiratory viruses become

more and more enzootic due to the intensification of the swine production (such as larger farms and higher pig density).

The reasons for the higher incidence of respiratory viral infections in winter remain controversial. Low temperature has been suggested to be causally linked to the winter peak respiratory infections (Makinen *et al.*, 2009; Malcolm *et al.*, 2001). Laboratory and clinical evidence in humans suggests that inhalation of cold air, cooling of the body surface and/or cold stress cause pathophysiological responses, increasing susceptibility to respiratory infections (Eccles, 2002). In addition, an experimental study with an animal model demonstrated that cold temperatures are favorable to the spread of influenza (Lowen *et al.*, 2007). It is also assumed that cold temperatures per se could account for the increased susceptibility of respiratory tract viral infections (Mourtzoukou & Falagas, 2007). However, the mechanisms behind these phenomena remain unclear.

During infection, the first barrier the virus encounters is the mucus layer, a crucial constituent of the innate immune system. Mucus is a biopolymer-based hydrogel that lines all moist mucosa of humans and animals. The protective functions of mucus have been described in a number of studies. We previously described that PrV was highly inhibited by the respiratory mucus in its mobility (Yang *et al.*, 2012). Other viruses such as human immunodeficiency virus (HIV), herpes simplex virus (HSV), human papilloma virus and influenza virus have also been found to be blocked by mucus or mucin reconstituted mucus (Lai *et al.*, 2009; Lai *et al.*, 2010; Lieleg *et al.*, 2012; Shukair *et al.*, 2013; Yang *et al.*, 2014). Although these viruses are highly immobilized or blocked in mucus experimentally, they eventually succeed in infecting the host. The behavior of virus in mucus may thus be dependent on certain host factors or mucus defects. Provided that most respiratory diseases are seasonal and most have a higher incidence during winter season, the effect of temperature on the interaction between PrV and airway mucus was investigated in this study.

3.3.3. Materials and methods

3.3.3.1. Tissues and explants

Immediately after euthanasia of six-week-old piglets, the tracheas were isolated and dissected. The tissues were cut into 8 mm × 8 mm pieces. The explants were cultured on gauzes in an air-liquid interface manner, in DMEM/F12 supplemented with 100 U/ml penicillin (Continental Pharma), 0.1 mg/ml streptomycin (Certa) and 1 µg/ml gentamycin (Gibco), according to a protocol adapted from Glorieux (Glorieux *et al.*, 2007).

3.3.3.2. Porcine respiratory mucus and mucin solution

Porcine respiratory mucus was collected from pig tracheas and was stored as previously described (Yang *et al.*, 2012). Type III porcine gastric mucin lyophilized powder (Sigma) was dissolved in MEM at the concentration of 4% (w/v), buffer calibrated to pH 7, and the mucin solution was kept overnight at 4 ^{o}C for reconstitution.

3.3.3.3. Immunofluorescence staining

For mucin staining, the sections were incubated with mouse anti-MUC5AC monoclonal IgG1 antibody (45M1, LifeSpan Biosciences, 1:100) for 1 h at 37 °C. After two washings with PBS (10 min/each), the sections were incubated for 1 h with goat anti-mouse IgG polyclonal antibody labeled with FITC. For PrV visualization, the sections were incubated with FITC conjugated swine anti-PrV purified serum. The sections were then washed 2 times, mounted in glycerin-DABCO with coverslips.

3.3.3.4. Effects of temperature on PrV binding to porcine respiratory mucus

Mucus cyrosections (20 µm) were made, and incubated with 30 µl suspension containing 10^6 $TCID_{50}$ semi-purified PrV at 4, 18 and 37 ^{o}C. At 0.5, 1 and 2 h post inoculation, the mucus cryosections were washed twice to remove unbound virions. The sections were then fixed with 4% paraformaldehyde (PF) for 20 min, followed by permeabilization in 0.1% Triton X-100 for 10 min. Immunofluorescence staining was performed using FITC conjugated swine anti-PrV purified serum. Fluorescence images were acquired on randomly selected regions with a confocal microscope

system, and bound virions on the mucus were calculated with ImageJ.

3.3.3.5. Effect of temperature on PrV penetration through porcine respiratory mucus

The penetration of PrV through porcine respiratory mucus was analyzed with a virus trakcing model, so as referred to in-capsule-mucus penetration system (Fig. 1). Briefly, a gelatin capsule was filled up with 150 µl of pig mucus, and kept at 4, 18 and 37 ^{o}C for 10 min. Afterwards, 8 µl of semi-purified PrV were brought onto the mucus surface. The virus together with the mucus and gelatin capsule was embedded in methyl cellulose and snap-frozen in a bath containing dry ice with ethanol immediately after addition (designated as 2 min) or at 30 min post virus addition at the corresponding temperatures. Cryosections were made and immunofluorescence staining was performed to visualize PrV and mucins, and the virus penetration depths at different temperatures were measured from mucus surface to the deepest point of the viral signal as shown by yellow arrows.

3.3.3.6. Effect of temperature on the interaction between respiratory mucus and PrV attachment to/infection in tracheal explant

The effect of temperature on the ability of PrV to overcome the porcine respiratory mucus was analyzed with respect to the virus attachment to and infection in tracheal explants. After adaptation at 37 °C for 24 h to retrieve the mucus layer, twelve tracheal explants were divided into three groups for three different temperatures (4, 18 and 37 °C). For each group, before inoculation, two explants were washed to remove the mucus by gently pipetting up and down for 15 times, and the other two explants were left unwashed. Afterwards, the four tracheal explants (two washed and two unwashed) were kept at 4, 18 or 37 °C, for 10 min, and were then inoculated with $10^{7.3}$ $TCID_{50}$ PrV Becker in 20 µl suspension, as previously described in **Chapter 3.2**, at the corresponding temperatures. One hour after inoculation, the explants were washed by gently pipetting up and down for 15 times. Hereafter, two explants (one washed and one unwashed) were then immediately embedded and frozen in methyl

cellulose for attachment analysis, while the other two were further cultured for 24 h before snap-freezing for infection assay. For the detection of PrV attachment to the mucosal surface, 10 sections (20 µm) were made with a trimming of 400 µm between each section. To detect PrV plaques in the tissues, 100 serial sections (20 µm) were made with 1 mm trimming between the first and second 50 sections. Three independent experiments were performed.

3.3.3.7. Effect of temperature on recovery of PrV from mucus *in vitro*

To detect if PrV may be released from mucus to infect the host cells, porcine respiratory mucus and porcine gastric mucin solution were tested for the interaction with PrV infection in swine testicle (ST) cells at different temperatures. The pig mucus and mucin solution were placed at 4, 18 and 37 °C for 10 min. Meanwhile, PrV Becker was diluted to $10^{4.3}$ $TCID_{50}$/ml, and was aliquoted and kept at 4, 18 and 37 °C for 10 min. The virus suspension was mixed with an equal volume of pig mucus and mucin solution, respectively, resulting in 10^4 $TCID_{50}$/ml PrV in 50% (v/v) of pig mucus or 2% (w/v) of mucin solution. The mixtures were further incubated at the corresponding temperatures for 30 min before being inoculated to ST cells. The virus incubated with MEM at different temperatures was used as mock controls. Afterwards, 50 µl of mixture were inoculated to previously equilibrated ST cells in 96-well plates at the above temperatures. One hour post inoculation, the inoculum was removed and the cells were overlaid with medium containing carboxymethylcellulose (CMC) (1%) and cultured at 37 °C for 24 h. Subsequently, the overlay medium was removed, and cells were washed and were then fixed with 4% PF. Afterwards, an immunoperoxidase monolayer assay (IPMA) was performed as previously described (Ficinska *et al.*, 2005) to determine the number of PrV plaques.

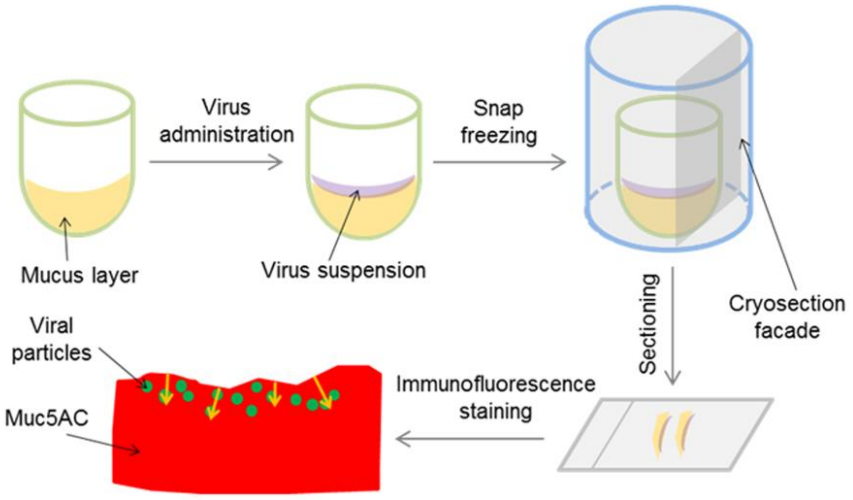

Figure 1. Schematic procedure of virus in-capsule-mucus penetration system. (1) 150 µl of mucus were brought at the bottom of a gelatin capsule. (2) 8 µl of PrV suspension were added on top of the surface of the mucus. (3) Mucus together with virus was embedded and snap-frozen. (4) Cryosections were made vertically to the mucus surface. (5) Immunofluorescence staining was performed to visualize the Muc5AC (representing the mucus) and viral particles. (6) Penetration depth (shown by yellow arrows) was measured from the surface of mucus to the furthest point of the viral signal.

3.3.4. Results

3.3.4.1. Thermo-dependent PrV binding to porcine respiratory mucus

Virions bound to the mucus cryosections were visualized by immunofluorescence staining to PrV using FITC conjugated swine anti-PrV purified serum. The virus bound to 5 mucus cryosections was analyzed, 2 images (360 µm × 360 µm) were taken for each section and in total 10 images were obtained for each condition. The average number of virions attached to an approximate region of 1.3×10^5 μm^2 was calculated. In general, the number of virions bound to the pig mucus increased with time and temperature (Fig. 2). At 30 min post inoculation, the virions bound to mucus at 37 ^oC and 18 ^oC were almost 5 and 2-fold more than those at 4 ^oC, respectively. At 2 h post inoculation, when the virus attachment was assumed to be complete, the number of virions bound to the mucus at 37 ^oC was the highest among the temperatures measured (Fig. 2). Taken together, the attachment of PrV to porcine respiratory mucus was thermo-dependent, and it indicates that low temperature may allow the virus to detach from the respiratory mucus.

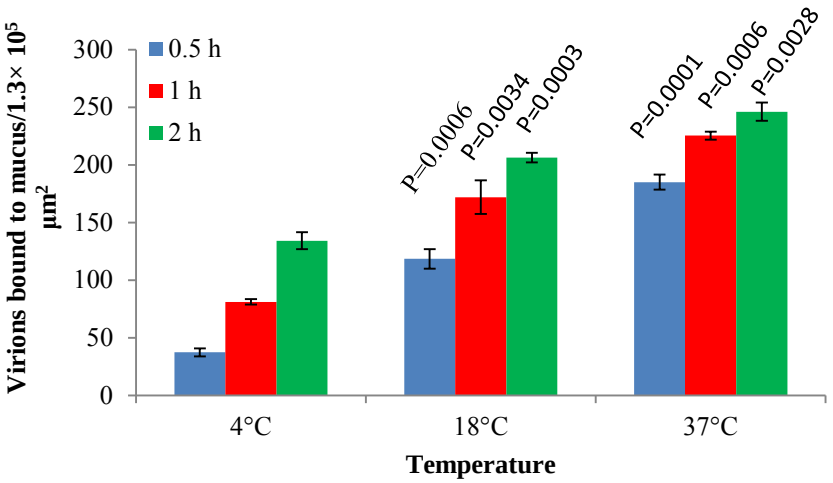

Figure 2. Effect of temperature on PrV binding to porcine respiratory mucus. PrV was inoculated to mucus cryosections at 4, 18 and 37 °C. At 0.5, 1 and 2 h post inoculation, the bound virions, together with mucus cryosections, were fixed and immunofluorescence staining was performed to visualize PrV. The virion attachment was analyzed with ImageJ. Error bars show the standard deviation of three independent experiments. The P value shows the statistical significance of the difference between particles attached to the mucus cryosections at 18 and 37 °C and those at 4 °C at the same time point (by Student's *t-test*).

3.3.4.2. PrV penetrates the porcine respiratory mucus at low temperature

The depth of PrV penetration was visualized by double immunofluorescence staining for both MUC5AC and virions. The distance from the surface down to the deepest point of virus translocation was measured and designated as the depth of virus penetration. Immediately after virus addition, the virions rapidly entered the mucus layer and reached a depth of 35 µm within 2 min, due to a passive diffusion effect (Fig. 3). At 30 min post virus addition, the virions did not spread further in the mucus at 37 °C, while the penetration was increased at lower temperature (Fig. 3). At 4 °C, the virions penetrated 12 µm further 30 min after addition onto the mucus surface, which indicates that low temperature indeed allows PrV particles to penetrate deeper through the porcine respiratory mucus.

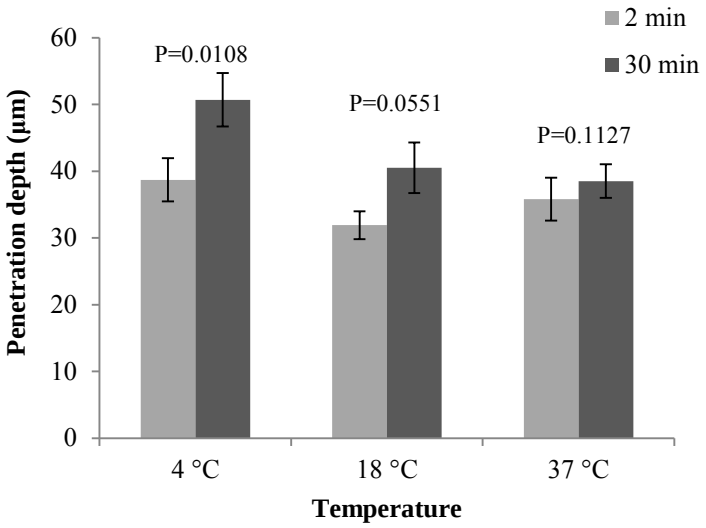

Figure 3. Effect of temperature on PrV penetration through the porcine respiratory mucus. Three experiments were performed. The error bars show the standard deviation. The P value shows statistical significance of the difference between penetration depths at 2 and 30 min at a certain temperature (by Student's *t-test*).

3.3.4.3. Temperature-dependent inhibition of PrV attachment to/infection in tracheal explant by respiratory mucus

The inhibition of mucins on PrV infection in porcine tracheal explants was temperature dependent. After the washing steps, the presence or absence of mucin above the apical face of the epithelium was confirmed by immunofluorescence staining for MUC5AC (**Chapter 3.2**). Virions attached to washed and unwashed explants were determined by immunofluorescence staining using FITC conjugated swine anti-PrV purified serum. Ten images were acquired by confocal microscopy from 10 sections. For each image, PrV particles attached to the apical epithelium (20 µm thick and 100 µm long) were measured. The total number of virions that attached to a region of 2×10^4 μm^2 of the apical epithelium was calculated and represents the capability of PrV to overcome the mucus layer. As shown in Fig. 4A, although more virions bound to the explants without a mucus layer at 37 ^oC than at 4 ^oC, the number of virions that bound to mucus coated explants was inversely lower. Only 35% of the virions overcame the porcine tracheal mucus and attached to the apical epithelium at 37 ^oC, while in contrast, the mucus almost did not prevent the virus from binding to the apical epithelium at 4 ^oC (Fig. 4B). Concerning PrV infections, the plaques

formed in the mucus-coated explants remained similar at different temperatures, while plaque number increased from 4 to 37 ^{o}C (Fig. 4C). The relative infection, determined by percentage of PrV plaques formed in the mucus coated explants related to that formed in washed explants, declined gradually with rise of temperature (Fig. 4D), suggesting that low temperature indeed allowed more virions to overcome the respiratory mucus for subsequent invasion.

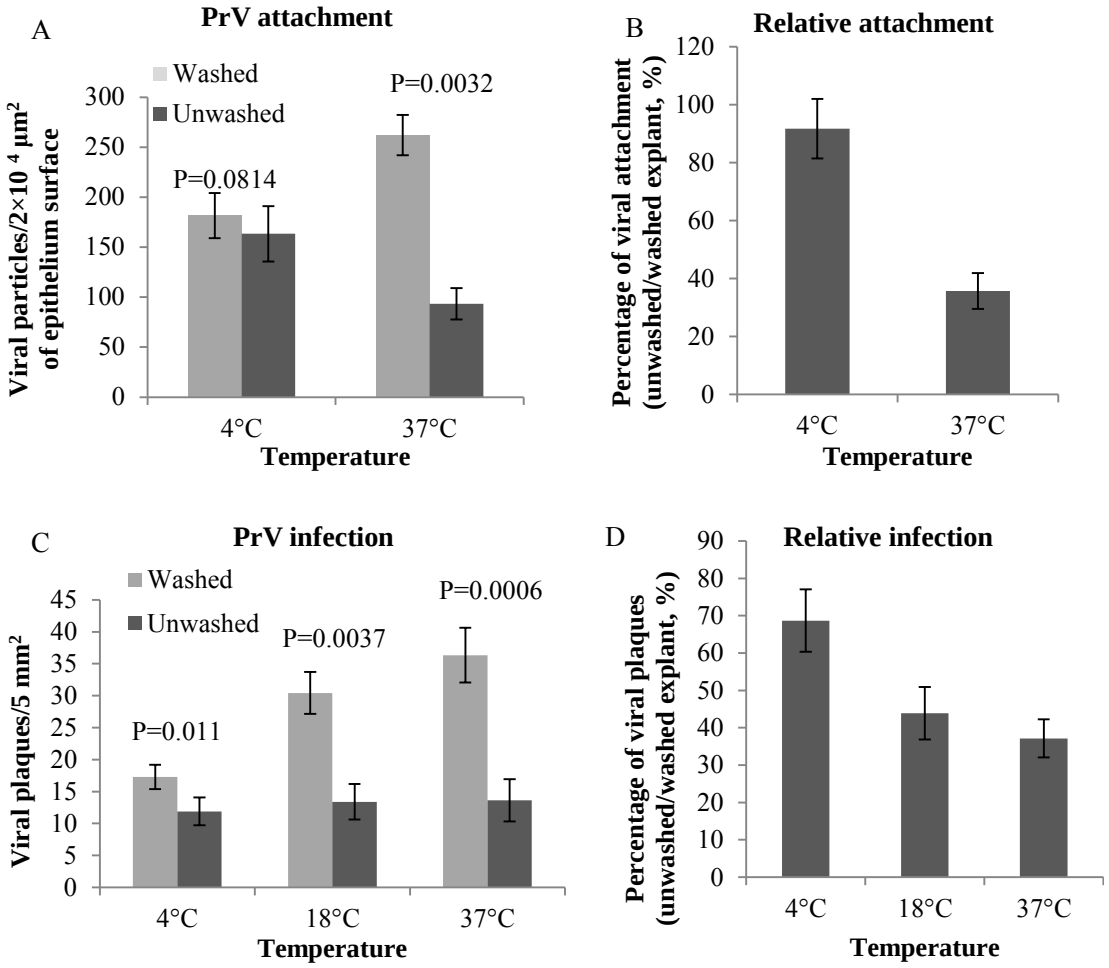

Figure 4. Effect of temperature on pig mucus blocking PrV attachment to/infection in tracheal explant. (A) The number viral particles attached to unwashed and washed explants at 4 and 37 ^{o}C. (B) Relative viral attachment to tracheal explant. The percentage of viral particles attached to unwashed explant was relative to that attached to the washed explant. (C) The number of PrV plaques formed in the unwashed explant and washed explants at different temperatures. (D) The percentage of viral plaques formed in unwashed explant was relative to that formed in washed explant. Three experiments were performed and error bar represents the standard deviation. P value (by Student's *t-test*) shows the statistical significance of the difference of viral attachment or infection between the unwashed and washed explant at the respective temperature.

3.3.4.4. Thermo-dependent mucus blocking of PrV infection *in vitro*

Both native pig mucus and reconstituted mucin solution exhibited thermo-dependent inhibition of PrV infection in ST cells. Before being inoculated to ST cells, the virus was preincubated with pig mucus and mucin solution, respectively, at 4, 18, and 37 ^{o}C for 30 min. Twenty-four hours post inoculation, PrV plaque forming units (PFU) were determined by IPMA. Both the native mucus and mucin solution showed inhibition to PrV infection in ST cells. The mock treated virus caused an increased number of plaques with the rise of temperature, but the mucus/mucin incubated virus formed similar numbers of plaques. The remained PrV infectivity was determined as the percentage of PrV plaques formed by mucus or mucin incubated virus relative to the ones formed by mock controls. The virions released from both pig mucus and mucin solution decreased with rise of the temperature (Fig. 5). Additionally, the pig mucus showed higher inhibition on PrV infection compared to the mucin solution at all temperatures. These findings not only further confirm that low temperature helped PrV to penetrate the pig mucus, but also imply a major but not exclusive contribution of mucins to the inhibitory effect of the whole mucus.

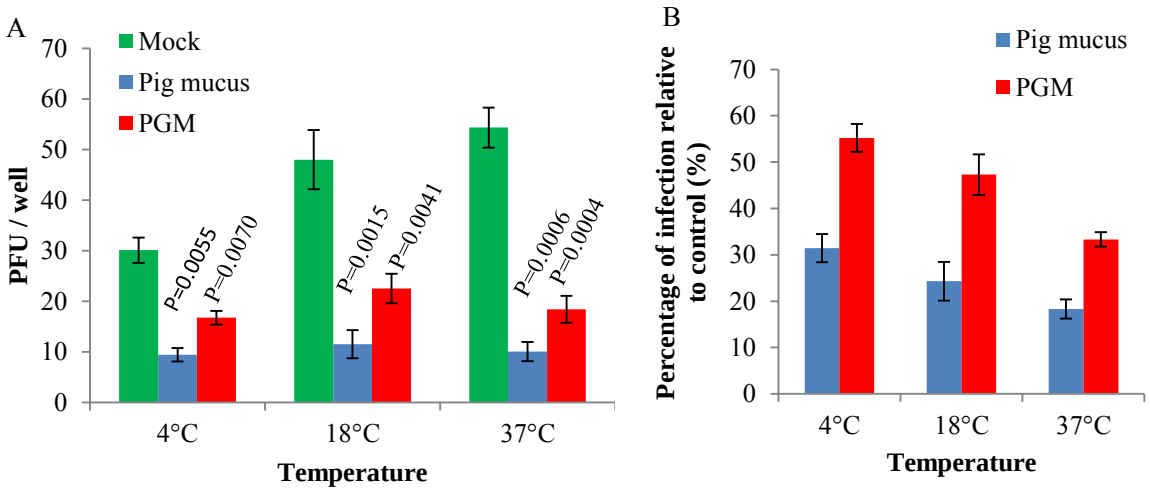

Figure 5. Effect of temperature on mucus/mucin blocking PrV infection in ST cells. (A) Absolute number of plaque forming units released from incubation with pig mucus, mucin solution and mock at 4, 18 and 37 ^{o}C was determined as PFU. (B) Percentage of PrV infection relative to mock control of respective temperature. Error bars show the standard deviation of three independent measurements. The P value (by Student's *t-test*) shows statistical significance of difference between infection formed by mucus/mucin treated virus and that by mock treated virus at the respective temperature.

3.3.5. Discussion

Mucus is a porous biopolymer matrix that coats all wet epithelia of the human and animal body and serves as the first line of defense against pathogenic bacteria and viruses. In many cases, the hosts rely on the innate immune system to repel viral infections. A crucial part of the innate immune system is constituted by mucus, which provides a physical barrier to prevent microbial pathogens from reaching the underlying epithelial cells.

A large number of studies have shown that different types of mucus, such as airway mucus, cervical mucus and porcine gastric mucus, can trap under physiological conditions various types of viruses, including PrV, HSV-1, HIV-1, human papilloma virus type 16 (HPV-16), and influenza H1N1 virus (Lai *et al.*, 2009; Lai *et al.*, 2010; Lieleg *et al.*, 2012; Shukair *et al.*, 2013; Yang *et al.*, 2012; Yang *et al.*, 2014). These viruses get obstructed in mucus probably not due to physical hindrance as the pore size of the above mucus was mostly larger than the virus particles. It is assumed that virus may overcome the mucus layer when there are physiological or pathological changes of the host mucosa or defects in the mucus. For instance, HIV is entrapped in acidic, healthy cervicovaginal mucus, whereas it moves freely in neutralized mucus which is present during bacteriovaginosis (Lai *et al.*, 2009). It has been shown that high salt concentrations increase particle mobility in the mucin hydrogel (Lieleg *et al.*, 2010). This may be due to the fact that the strength of the attractive or repulsive forces between virus particles and the hydrogel depends on the salt content. As the respiratory tract is subjected to changes of the environmental temperature, respiratory viruses may have evolved to use (misuse) this effect to overcome the mucus layer. Our findings support the latter view.

In the present study, we demonstrate that the inhibitory effect of the mucus on PrV invasion is temperature dependent. PrV attached more efficiently to pig mucus cryosections at high temperature compared to low temperature. Consistently, PrV was not able to penetrate the porcine respiratory mucus at body temperature, while at 4 ^{o}C, the virus seemed to move through the mucus. At 30 min post virus addition, the virus

spread averagely 12 μm further. Thus, we suggest that low temperature allows PrV to move through the porcine respiratory mucus. In the next experiment, we were able to confirm that low temperature helped the virus to overcome the mucus barrier and eventually cause more infection. The inhibitory effect of mucus concerning PrV attachment and infection was studied by maintaining a mucus layer on top of the apical epithelium of tracheal explants, using explants that were not coated by mucus as a mock control. We found that the mucus layer inhibited the majority of the virions to reach the apical epithelium at 37 ^{o}C, which is in contrast to the minimal effect of mucus at 4 ^{o}C (Fig. 4A and B). Decreasing the temperature seemed to increase the relative PrV attachment and infection to/in porcine tracheal explants. These data suggest that cooling of mucosal surface may increase virus moving through or releasing from mucus, thereby facilitate viral infection and spread in the respiratory tract.

From a virological point of view, the virus may be bound to decoy receptors which exist in the mucus. It is known for PrV that the virions bind to heparan sulfate via gC glycoprotein for viral attachment, which is followed by a stable interaction between gD and its cellular receptor. Up till now, heparan sulphate, nectin-1, nectin-2 and CD155 were described as receptors for PrV (Campadelli-Fiume *et al.*, 2000; Nixdorf *et al.*, 1999; Spear *et al.*, 2000; Spear & Longnecker, 2003). These PrV receptors, except the secretory heparan sulfate (Emery *et al.*, 1995), have not been found in the airway secretions. Moreover, our previous data were not able to correlate the immobilization of PrV in the pig mucus to virus-heparan sulphate interaction (Yang *et al.*, 2012). Therefore, the direct binding of PrV to mucus cryosections indicates that this attachment was probably not due to specific virus-receptor binding. Instead, we assume that mucins here may play an important role in this process via their sticky glycans. These intermolecular mucus-protein interactions are non-covalent and increase with temperature in a manner characteristic of an entropically driven reaction (Snary *et al.*, 1973). Thus lowering temperature may allow release of PrV, which otherwise have been trapped in the mucus constitution. Additionally, our study is in

agreement with a recent report which demonstrated that low temperature favors the influenza virus transmission in ferret (Lowen *et al.*, 2007). Therefore, the effects of lower temperature on virus penetration through mucus may be a generic phenomenon.

The relationship between exposure to cold and increased respiratory infections may be based on a complex interaction, and many efforts have been made in order to clarify the mechanisms behind this association. It was first proposed by Mudd and Grant that chilling of the body surface could predispose to viral infection of the airway by causing vasoconstriction in the mucous membranes lining the airway, as cooling of the skin caused a pronounced ischaemia of the nasal mucosal surface that was measured via thermistor (Mudd & Grant, 1919). Some available data also suggest that exposure to cold environment increases the risk of respiratory infections (Makinen *et al.*, 2009; Tseng *et al.*, 2013). Some other factors, such as host physiological susceptibility (Dowell, 2001), immune function (Brenner *et al.*, 1999), and crowding behavior (Lofgren *et al.*, 2007) may also be the causal links between cold temperature and higher incidence of respiratory viral infection.

To our best knowledge, it is the first demonstration which is able to directly link the increased viral susceptibility of the respiratory tract with the functionality of airway mucus. The results demonstrated in this study may not be practically applied to pig farming as the temperature is normally maintained thanks to the refinement of pig housing. However, the model setup in the present study may benefit the investigation of the seasonality of human viral infections, such as human influenza and respiratory syncytial virus infection. Furthermore, this study may provide a scientific indication for maintaining the environmental temperature at a higher level and preventing the adverse effects of cold air, during the period of low environmental temperatures.

3.3.5. Acknowledgements

This research was supported by the Concerted Research Action 01G01311 of the Research Council of Ghent University, Belgium. HJN is a member of BELVIR consortium (IAP, phase VII) sponsored by Belgian Science Policy (BELSPO). The

authors would like to express their gratitude to Zeger Vandenabeele and Loes Geypen for their help in preparing all the trachea samples. Special thanks to Lieve Sys the help in the experiments and discussion.

3.3.6. References

Borchers, A. T., Chang, C., Gershwin, M. E. & Gershwin, L. J. (2013). Respiratory syncytial virus--a comprehensive review. *Clin Rev Allergy Immunol* **45**, 331-379.

Brenner, I. K., Castellani, J. W., Gabaree, C., Young, A. J., Zamecnik, J., Shephard, R. J. & Shek, P. N. (1999). Immune changes in humans during cold exposure: effects of prior heating and exercise. *J Appl Physiol (1985)* **87**, 699-710.

Campadelli-Fiume, G., Cocchi, F., Menotti, L. & Lopez, M. (2000). The novel receptors that mediate the entry of herpes simplex viruses and animal alphaherpesviruses into cells. *Rev Med Virol* **10**, 305-319.

Christensen, L. S. (1995). The population biology of suid herpesvirus 1. *APMIS Suppl* **48**, 1-48.

Christensen, L. S., Mortensen, S., Botner, A., Strandbygaard, B. S., Ronsholt, L., Henriksen, C. A. & Andersen, J. B. (1993). Further evidence of long distance airborne transmission of Aujeszky's disease (pseudorabies) virus. *Vet Rec* **132**, 317-321.

Dowell, S. F. (2001). Seasonal variation in host susceptibility and cycles of certain infectious diseases. *Emerg Infect Dis* **7**, 369-374.

Eccles, R. (2002). An explanation for the seasonality of acute upper respiratory tract viral infections. *Acta Otolaryngol* **122**, 183-191.

Edwards, T. A. (2010). Control methods for bovine respiratory disease for feedlot cattle. *Vet Clin North Am Food Anim Pract* **26**, 273-284.

Emery, N., Place, G. A., Dodd, S., Lhermitte, M., David, G., Lamblin, G., Perini, J. M., Page, A. M., Hall, R. L. & Roussel, P. (1995). Mucous and serous secretions of human bronchial epithelial cells in secondary culture. *Am J Respir Cell Mol Biol* **12**, 130-141.

Ficinska, J., Van Minnebruggen, G., Nauwynck, H. J., Bienkowska-Szewczyk, K. & Favoreel, H. W. (2005). Pseudorabies virus glycoprotein gD contains a functional endocytosis motif that acts in concert with an endocytosis motif in gB to drive internalization of antibody-antigen complexes from the surface of infected monocytes. *J Virol* **79**, 7248-7254.

Finkelman, B. S., Viboud, C., Koelle, K., Ferrari, M. J., Bharti, N. & Grenfell, B. T. (2007). Global patterns in seasonal activity of influenza A/H3N2, A/H1N1, and B from 1997 to 2005: viral coexistence and latitudinal gradients. *PLoS One* **2**, e1296.

Gilca, R., De Serres, G., Tremblay, M., Vachon, M. L., Leblanc, E., Bergeron, M. G., Dery, P. & Boivin, G. (2006). Distribution and clinical impact of human respiratory syncytial virus genotypes in hospitalized children over 2 winter seasons. *J Infect Dis* **193**, 54-58.

Glorieux, S., Van den Broeck, W., van der Meulen, K. M., Van Reeth, K., Favoreel, H. W. & Nauwynck, H. J. (2007). In vitro culture of porcine respiratory nasal mucosa explants for studying the interaction of porcine viruses with the respiratory tract. *J Virol Methods* **142**, 105-112.

Griffin, D. (1997). Economic impact associated with respiratory disease in beef cattle. *Vet Clin North Am Food Anim Pract* **13**, 367-377.

Hope-Simpson, R. E. (1981). The role of season in the epidemiology of influenza. *J Hyg (Lond)* **86**, 35-47.

Jestin, A., Blanchard, P., Garbar-Chenon, A., Vannier, P. & Nicolas, J. C. (1990). Restriction fragment pattern analysis of genomes from French isolates of suis herpes virus 1 (Aujeszky's disease virus). *Arch Virol* **112**, 149-167.

Krumbholz, A., Lange, J., Sauerbrei, A., Groth, M., Platzer, M., Kanrai, P., Pleschka, S., Scholtissek, C., Buttner, M., Durrwald, R. & Zell, R. (2014). Origin of the European avian-like swine influenza viruses. *J Gen Virol* **95**, 2372-2376.

Lai, S. K., Hida, K., Shukair, S., Wang, Y. Y., Figueiredo, A., Cone, R., Hope, T. J. & Hanes, J. (2009). Human immunodeficiency virus type 1 is trapped by acidic but not by neutralized human cervicovaginal mucus. *J Virol* **83**, 11196-11200.

Lai, S. K., Wang, Y. Y., Hida, K., Cone, R. & Hanes, J. (2010). Nanoparticles reveal that human cervicovaginal mucus is riddled with pores larger than viruses. *Proc Natl Acad Sci U S A* **107**, 598-603.

Lieleg, O., Lieleg, C., Bloom, J., Buck, C. B. & Ribbeck, K. (2012). Mucin Biopolymers As Broad-Spectrum Antiviral Agents. *Biomacromolecules* **13**, 1724-1732.

Lieleg, O., Vladescu, I. & Ribbeck, K. (2010). Characterization of particle translocation through mucin hydrogels. *Biophys J* **98**, 1782-1789.

Lofgren, E., Fefferman, N. H., Naumov, Y. N., Gorski, J. & Naumova, E. N. (2007). Influenza seasonality: underlying causes and modeling theories. *J Virol* **81**, 5429-5436.

Lowen, A. C., Mubareka, S., Steel, J. & Palese, P. (2007). Influenza virus transmission is dependent on relative humidity and temperature. *PLoS Pathog* **3**, 1470-1476.

Maes, L. & Pensaert, M. (1984). [Persistence of virus in swine stock and breeding farms following an outbreak of Aujeszky's disease]. *Tijdschr Diergeneeskd* **109**, 439-445.

Makinen, T. M., Juvonen, R., Jokelainen, J., Harju, T. H., Peitso, A., Bloigu, A., Silvennoinen-Kassinen, S., Leinonen, M. & Hassi, J. (2009). Cold temperature and low humidity are associated with increased occurrence of respiratory tract infections. *Respir Med* **103**, 456-462.

Malcolm, E., Arruda, E., Hayden, F. G. & Kaiser, L. (2001). Clinical features of patients with acute respiratory illness and rhinovirus in their bronchoalveolar lavages. *J Clin Virol* **21**, 9-16.

Mourtzoukou, E. G. & Falagas, M. E. (2007). Exposure to cold and respiratory tract infections. *Int J Tuberc Lung Dis* **11**, 938-943.

Mudd, S. & Grant, S. B. (1919). Reactions to Chilling of the Body Surface: Experimental Study of a Possible Mechanism for the Excitation of Infections of the Pharynx and Tonsils. *J Med Res* **40**, 53-101.

Nixdorf, R., Schmidt, J., Karger, A. & Mettenleiter, T. C. (1999). Infection of Chinese hamster ovary cells by pseudorabies virus. *J Virol* **73**, 8019-8026.

Pensaert, M., Ottis, K., Vandeputte, J., Kaplan, M. M. & Bachmann, P. A. (1981). Evidence for the natural transmission of influenza A virus from wild ducts to swine and its potential importance for man. *Bull World Health Organ* **59**, 75-78.

Shukair, S. A., Allen, S. A., Cianci, G. C., Stieh, D. J., Anderson, M. R., Baig, S. M., Gioia, C. J., Spongberg, E. J., Kauffman, S. M., McRaven, M. D., Lakougna, H. Y., Hammond, C., Kiser, P. F. & Hope, T. J. (2013). Human cervicovaginal mucus contains an activity that hinders HIV-1 movement. *Mucosal Immunol* **6**, 427-434.

Snary, D., Allen, A. & Pain, R. H. (1973). The effect of temperature on gel formation in pig-gastric mucus. *Eur J Biochem* **36**, 72-75.

Snowder, G. D., Van Vleck, L. D., Cundiff, L. V. & Bennett, G. L. (2006). Bovine respiratory disease in feedlot cattle: environmental, genetic, and economic factors. *J Anim Sci* **84**, 1999-2008.

Spear, P. G., Eisenberg, R. J. & Cohen, G. H. (2000). Three classes of cell surface receptors for alphaherpesvirus entry. *Virology* **275**, 1-8.

Spear, P. G. & Longnecker, R. (2003). Herpesvirus entry: an update. *J Virol* **77**, 10179-10185.

Tseng, C. M., Chen, Y. T., Ou, S. M., Hsiao, Y. H., Li, S. Y., Wang, S. J., Yang, A. C., Chen, T. J. & Perng, D. W. (2013). The effect of cold temperature on increased exacerbation of chronic obstructive pulmonary disease: a nationwide study. *PLoS One* **8**, e57066.

Valarcher, J. F. & Taylor, G. (2007). Bovine respiratory syncytial virus infection. *Vet Res* **38**, 153-180.

Van der Poel, W. H., Kramps, J. A., Middel, W. G., Van Oirschot, J. T. & Brand, A. (1993). Dynamics of bovine respiratory syncytial virus infections: a longitudinal epidemiological study in dairy herds. *Arch Virol* **133**, 309-321.

Yang, X., Forier, K., Steukers, L., Van Vlierberghe, S., Dubruel, P., Braeckmans, K., Glorieux, S. & Nauwynck, H. J. (2012). Immobilization of pseudorabies virus in porcine tracheal respiratory mucus revealed by single particle tracking. *PLoS One* **7**, e51054.

Yang, X., Steukers, L., Forier, K., Xiong, R., Braeckmans, K., Van Reeth, K. & Nauwynck, H. (2014). A beneficiary role for neuraminidase in influenza virus penetration through the respiratory mucus. *PLoS One* **9**, e110026.

Chapter 4

4. A beneficiary role for neuraminidase in influenza virus penetration through the respiratory Mucus

Xiaoyun Yang, Lennert Steukers, Katrien Forier, Ranhua Xiong, Kevin Braeckmans, Kristien Van Reeth, Hans Nauwynck

PLoS ONE 9(10): e110026. doi:10.1371/journal.pone.0110026 (2014)

4.1. Abstract

Swine influenza virus (SIV) has a strong tropism for pig respiratory mucosa, which consists of a mucus layer, epithelium, basement membrane and lamina propria. Sialic acids present on the epithelial surface have long been considered to be determinants of influenza virus tropism. However, mucus which is also rich in sialic acids may serve as the first barrier of selection. It was investigated how influenza virus interacts with the mucus to infect epithelial cells. Two techniques were applied to track SIV H1N1 in porcine mucus. The microscopic diffusion of SIV particles in the mucus was analyzed by single particle tracking (SPT), and the macroscopic penetration of SIV through mucus was studied by a virus in-capsule-mucus penetration system, followed by visualizing the translocation of the virions with time by immunofluorescence staining. Furthermore, the effects of neuraminidase on SIV getting through or binding to the mucus were studied by using zanamivir, a neuraminidase inhibitor (NAI), and *Arthrobacter ureafaciens* neuraminidase. The distribution of the diffusion coefficient shows that 70% of SIV particles were entrapped, while the rest diffused freely in the mucus. Additionally, SIV penetrated the porcine mucus with time, reaching a depth of 65 μm at 30 min post virus addition, 2 fold of that at 2 min. Both the microscopic diffusion and macroscopic penetration were largely diminished by NAI, while they were clearly increased by addition of exogenous neuraminidase. Moreover, the exogenous neuraminidase sufficiently prevented the binding of SIV to mucus which was inversely enhanced by effect of NAI. These findings clearly show that the neuraminidase helps SIV move through the mucus, which is important for the virus to reach and infect epithelial cells and eventually become shed into the lumen of the respiratory tract.

4.2. Introduction

Pigs are naturally susceptible to three subtypes of influenza A viruses: H1N1, H3N2 and H1N2, all of which have a strong tropism for the pig respiratory tract mucosa (Crisci *et al.*, 2013; Medina & Garcia-Sastre, 2011; Webster *et al.*, 1992). Swine

influenza virus particles are transmitted by direct contact and through the air in large droplets or as aerosols (Crisci *et al.*, 2013; Tellier, 2009; Torremorell *et al.*, 2012). During the transmission from pig to pig, the virus first encounters mucus, the first barrier of the respiratory tract. After overcoming this barrier, the virus reaches the target cells in the mucosal epithelium. Influenza virus infects host cells by binding to cellular receptors via one of the major viral glycoproteins, hemagglutinin (HA). HA binds to sialic acids (SA) on the cell surface and mediates the subsequent membrane fusion leading to virus entry (Ramos & Fernandez-Sesma, 2012). Neuraminidase (NA) catalyzes the removal of terminal sialic acids on the cellular surface to release the progeny virus (Colman, 1994). It is well documented that the NA functions at the releasing stage of the virus replication (Itamura, 1997; Seto & Chang, 1969; Shtyrya *et al.*, 2009), while little is known if NA plays a role during the virus entry into host cells and even less on if it helps the virus overcome the mucus layer.

Mucus consists of a complex mixture of mucous glycoproteins (mucins), proteins, proteases and protease inhibitors, lipids and water (Lillehoj & Kim, 2002; Thornton *et al.*, 2008). Mucins, the major component of mucus, are highly o-glycosylated with glycans covalently linked via N-acetylgalactosamine (GalNAc) to the hydroxyl groups of serine or threonine residues of the mucin backbone (Cone, 2009; Thornton *et al.*, 2008). Most of the sugar chains of mucin monomers are terminated with sialic acid, which is also known to be the cellular receptor of influenza viruses. It is hypothesized that influenza viruses bind to these extracellular receptors, get entrapped in the mucus and then are removed by ciliary clearance (Fazekas De, 1952; Linden *et al.*, 2008; Matrosovich & Klenk, 2003). Several studies have shown that interaction of influenza virus with mucus results in competitive inhibition of the virus. Roberts *et al.* (Roberts *et al.*, 2011) showed that pre-incubation of human H3N2 virus strain A/Victoria/3/75 with ferret nasal washes containing mucus clearly reduced the virus infectivity, and this inhibition was correlated to competitive binding of the virus with alpha 2,3 and 2,6 linked sialic acids (α2,3- and α2,6-SA) present in the mucus secretions. The protective effect of the mucus barrier was confirmed by a recent study

using a transgenic mouse model that overexpressed SA α2-3 Gal rich Muc5AC. Transgenic mice challenged with A/PR8/34 H1N1, which preferentially binds α2,3-SA showed significant less infection than the normal mice (Ehre *et al.*, 2012). These studies suggest that mucus or mucins block the influenza virus infection by competitively inhibiting HA-mediated cell adsorption.

Despite this inhibitory function of the mucus, the virus is ultimately able to reach the susceptible epithelial cells. It has long been assumed that NA promotes virus access to target cells in the airway by mucus degradation. However, this concept is scarcely supported by experimental data. Cohen *et al.* (Cohen *et al.*, 2013) incubated A/PR/8/34 H1N1 and A/Aichi/2/68 H3N2 virus with human salivary mucins which were previously coated on magnetic beads, and after extensive washings, detected the remaining Neu5AC on the mucins. They showed that these human influenza viruses had cleaved away 40-60% of Neu5AC content of the mucins by their viral neuraminidase. The effective cleavage may allow the efficient release of virus from the mucus. This contrasts with the findings of Ehre *et al.* (Ehre *et al.*, 2012) who demonstrated a strong protection of Muc5AC up-regulated mice against A/PR/8/34 H1N1 virus infection. Hence, the purified human salivary mucins may not fully reflect the natural mucus as these mucins had been highly modified after attaching to magnetic beads. Unraveling the mechanism behind the penetration of viruses across the mucosal barriers has potentially significant implications for the development of novel antiviral strategies. Therefore, an *in vitro* model resembling the *in vivo* situation is needed and the interactions of influenza virus with natural mucus should be studied in depth. In the present study, we aimed to address the following questions:

(1) Is the virus entrapped or able to penetrate through the native respiratory mucus?

(2) Can viral neuraminidase use mucin sialic acids as substrates and catalyze their cleavage?

(3) Is this cleavage sufficient to liberate the virions and allow them to penetrate through the mucus layer?

To this purpose, we applied swine influenza virus to a model we previously set up

using porcine respiratory mucus, pseudorabies virus (PrV) and single particle tracking (SPT) (Yang *et al.*, 2012). In addition, the penetration of SIV was studied by the use of a mucus layer on which an appropriate amount of virus particles was added. The microscopic diffusion and macroscopic translocation were evaluated. Next, the effects of neuraminidase on the virus mobility in mucus were examined.

4.3. Materials and methods

4.3.1. Mucus sample collection

Tracheas were collected from 6-month-old pigs which were negative for swine influenza A viruses as shown by a Hemagglutination Inhibition (HI) test. Using of tracheas from euthanized animals was approved by the Ethical and Animal Welfare Committee of the Faculty of Veterinary Medicine of Ghent University. Two days before euthanization, the pigs were treated intramuscularly with ceftiofur (Naxcel, Pfizer-1 ml/20 kg body weight) to clear the respiratory tract from possible bacterial infections. The tracheas were dissected and the mucus was gently scraped with a spoon, collected with a syringe, and the mucus samples were stored separately at -70 °C until use. These samples were negative for neuraminidase determined by NA assay using fluorescent NA substrate (4-methylumbelliferyl-N-acetylneuraminic acid [MU-NANA]).

4.3.2. Fluorescence lectin staining of α2,3- and α2,6-SA in mucus

Freshly collected mucus was filled in a gelatin capsule (2.3 cm × 0.8 cm), snap-frozen in methyl cellulose (Fluka) using a bath containing dry ice with ethanol. Cryosections of 20 µm were made with a trimming interval of 400 µm between each section. The mucus cryosections were blocked in 1% (w/v) bovine serum albumin for 1 h, followed by incubation with biotin conjugated *Sambucus nigra* lectin (SNA-I) (EY laboratory, CA, USA; 1:100) that recognizes SAα2,6-Gal/GalNAc for 1 h, at room temperature. After 2 washings in phosphate buffered saline (PBS), the sections were incubated with Streptavidin-Texas Red (Invitrogen, 1:200) and FITC labeled *Maackia amurensis* lectin (MAA) (EY laboratory, CA, USA; 1:25) that recognizes SAα2,3-Gal

for 1 h, at room temperature. Afterwards, the cryosections were washed, and mounted in 90% glycerin containing 2.5% 1,4-diazobicyclo-(2,2,2)-octane (DABCO). Images of the fluorescence staining were acquired using a confocal microscope (Leica TCS SP2 Laser scanning spectral confocal system, Leica microsystems GmbH) and the fluorescence signal was analyzed with ImageJ. The coverage of either SA was calculated by ratio of fluorescence signal to the region of interest (ROI).

4.3.3. Cells and virus

Madin Darby Canine Kidney (MDCK) cells were maintained in Minimum Essential Medium (MEM, Gibco) supplemented with 10% fetal calf serum (Gibco), 100 µg/ml of streptomycin and 100 units/ml of penicillin (Invitrogen). The avian-like H1N1 swine influenza virus Sw/Belgium/1/98 was used at the third passage on MDCK cells. The virus was propagated in MDCK cells in MEM supplemented with 5 µg/ml trypsin (Gibco), 100 µg/ml of streptomycin and 100 units/ml of penicillin (Gibco).

4.3.4. Purification of SIV

Confluent MDCK cells were inoculated with SIV at a multiplicity of infection (m.o.i) of 0.01 in MEM. Twenty hours post inoculation, the supernatant was harvested. The cellular debris was removed by ultracentrifugation at 7 000 ×g for 20 min at 4 °C in a Type 35 rotor (Beckman, Fullerton, CA, USA) and the suspension was clarified by filtration with a 0.45 µm filter (Millipore). Afterwards, the virus was pelleted at 75 000 ×g for 2 h at 4 ℃ in a type 35 rotor. Following resuspension in PBS (1/100 of the original volume), the virus suspension was brought on a discontinuous OptiPrep (Sigma) gradient containing 10-30% (w/v) of iodixanol and centrifuged at 100 000 ×g for 3 h at 4 °C in an SW41Ti rotor (Beckman, Fullerton, CA, USA). The visible opalescent virus bands at the interfaces were harvested separately. The buffer was exchanged with HNE (5 mM HEPES, 150 mM NaCl, 0.1 mM EDTA, pH 7.4) buffer by the use of a 50 kDa filter device (Millipore).

4.3.5. Verification of the viral purity by lipophilic labeling and immunofluorescence staining of SIV antigens

To verify the purity of the virus from each band, double staining was performed by using 3,3′-Dioctadecyloxacarbocyanine perchlorate (Dio) and hyperimmune swine serum directed to influenza Sw/Belgium/1/98 virus, followed by Texas Red-conjugated goat anti-swine IgG antibody. Hyperimmune swine serum was diluted (1:50) and mixed with the virus suspension (1:1, v/v). After 2 h incubation on ice, Texas Red-conjugated goat anti-swine IgG secondary antibody (1:50, Invitrogen) was added and incubated further on ice for 2 h. Afterwards, the resulting mixture containing virus, hyperimmune serum, and secondary antibody was equilibrated to room temperature. Dio solution (1 mM in DMSO) was mixed with virus suspension (1:100, v/v) by fierce vortexing, followed by incubation at room temperature for 20 min. The resulting suspension was ultracentrifuged at 100 000 ×g for 1.5 h in a type 35 rotor to remove the free antibodies and dyes. After resuspension in PBS, the virions were clarified by a further ultracentrifugation at 100 000 ×g for 1.5 h. The staining was analyzed with confocal microscope by randomly selecting 10 regions. The ratio of viral antigen positive particles (virions) versus Dio positive particles was calculated, which is referred to as the degree of viral purity.

4.3.6. Characteristic analysis of the Dio-labeled SIV

The band containing the most purified virus was obtained and the buffer was exchanged with HNE buffer. After incubation with Dio solution as previously described, the virus suspension was filtered by the use of a Sephadex G-50 column (GE Healthcare, Belgium) to remove unbound dye. The unlabeled virus that was eluted through the Sephadex G-50 column was used as negative control. Dio is a lipophilic dye which integrates into the lipid components of the viral envelope. To determine that the integration of the Dio dye into the viral envelope does not change the biophysical properties of the virus, the size and surface charge (*zeta* potential) of the labeled and unlabeled virions were measured by dynamic light scattering and laser Doppler anemometry as previously described (Yang *et al.*, 2012). Infectivity and hemagglutination activity of the Dio-labeled viral particles were tested by virus titration and HA assay as previously described (De Vleeschauwer *et al.*, 2009). The

NA enzymatic activity was determined according to the protocol adapted from Adamo *et al.* (Adamo *et al.*, 2009). Briefly, 25 µl of fluorescent NA substrate (4-methylumbelliferyl-N-acetylneuraminic acid [MU-NANA], 100 µM in PBS, pH 7.4) was added to 25 µl of each sample containing 16 HA units. After 1 h incubation at 37 °C, reactions were stopped with 0.1 M glycine (pH 10.7) in 25% ethanol. Controls and standards were run in parallel, and the fluorescence was measured on a Victor V (Perkin Elmer, Waltham, MA) at an excitation of 360 nm and an emission of 430 nm for 0.1 s per well.

4.3.7. Microscopic diffusion of SIV in mucus determined by SPT

The trajectories of fluorescent viral particles in porcine tracheal respiratory mucus were recorded by a fast and sensitive electron-multiplying charge-coupled device (EMCCD) camera (Cascade II: 512; Roper Scientific, Tucson, AZ, USA) mounted on an inverted epifluorescence microscope (Nikon TE2000E, Nikon Belux, Brussels, Belgium) equipped with a 100x oil-immersion objective (Plan Apochromat, Nikon). Tracking experiments were performed in press-to-seal silicone isolators (20 mm diameter, 0.5 mm deep, Invitrogen, Merelbeke, Belgium). Our previous study shows that PrV was highly immobilized while 100 nm PGEylated beads were diffusive in porcine respiratory mucus, hence GFP-PrV was used as a negative control and the latter was used as a positive control (Yang *et al.*, 2012). GFP-PrV was semi-purified according to the previous protocol (Yang *et al.*, 2012). Three microliters of SIV ($10^{8.5}$ $TCID_{50}$/ml) or PrV ($10^{8.5}$ $TCID_{50}$/ml) suspension or 100 nm PEGylated beads (approximately 10^{10} particles/ml) were mixed with 100 µl of porcine tracheal respiratory mucus by gentle stirring. To determine if NA would affect SIV diffusion, the virus was added to the mucus with or without the presence of 0.02 µM zanamivir (Sigma) or 10 mU/ml *Arthrobacter ureafaciens* neuraminidase (Roche Applied Science). The mixture was placed in a custom made glass chamber. The samples were incubated at 37°C for 10 min on the microscope using a stage-top incubator (Tokai Hit, Fujinomiya, Japan) before SPT measurement. Movies were captured with the EMCCD camera at a temporal resolution of 33 ms for 5 s and analyzed with the NIS

Elements AR software (Nikon). The illumination time was 30 ms per frame. Trajectories of n ≥ 500 particles were analyzed for each experiment and three independent experiments were performed for each condition. Movies were analyzed with the Image Processing Software (IPS, in-house developed software) (Braeckmans K, 2010) to extract x, y positional data over time. The apparent diffusion coefficient (*Da*) was calculated as a function of the time scale (*t*) for each particle. Analysis of the movies was performed with IPS. The centroids of individual particles were identified in each frame of a movie. Based on the positions of the centroids, the trajectories of the particles can be determined by a nearest neighbor algorithm. The apparent diffusion coefficient *Da* corresponding to the first time lag *Δt* was calculated according to the classical formula: $Da = MSD/4\Delta t$ (Saxton & Jacobson, 1997). Afterwards, the distribution of diffusion coefficient of the particles was obtained by maximum entropy method (MEM) analysis (Braeckmans *et al.*, 2010).

4.3.8. Penetration of SIV in porcine respiratory mucus

SIV penetration was performed in a virus in-capsule-mucus penetration system as previously described (Chapter 3.3). Briefly, mucus sample (150 µl) was added to a gelatin capsule to create a mucus "layer" at the bottom. Afterwards, eight microliter of virus suspension containing approximately $10^{6.5}$ $TCID_{50}$ purified SIV were brought in the form of 5 droplets onto the surface of the mucus. Immediately, 10 min and 30 min after virus addition, the capsules were snap-frozen in methyl cellulose using a bath containing dry ice with ethanol. Due to a delay of freezing process, the time point "immediately after addition" was designated as 2 min. To determine if the NA would influence the SIV penetration, the virus was added with or without the presence of 0.1 µM Zanamivir (Sigma) or 50 mU/ml *Arthrobacter ureafaciens* neuraminidase onto the mucus, followed by snap-freezing at 30 min post virus addition. Cryosections of 12 µm were made with a trimming interval of 400 µm between each section. Double immunofluorescence staining was performed using mouse anti-Muc5AC IgG1 (45M1, LifeSpan Biosciences, 1:100) and mouse anti-NP IgG2a (HB-65, ATCC, 1:50) monoclonal antibodies, followed by Texas Red conjugated goat anti-mouse IgG1 and

Alexa Fluor 488 conjugated goat anti-mouse IgG2a secondary antibodies (Invitrogen), respectively. Ten sections were made for each condition, then 10 images were taken, and finally translocations of the virions was measured from the top of the mucus layer until the deepest point of the viral signal.

4.3.9. Effects of NA on SIV binding to porcine respiratory mucus

Mucus cryosections (12 μm) were made, and incubated with 30 μl suspension containing 10^6 $TCID_{50}$ SIV in the presence or absence of 0.1 μM zanamivir or 50 mU/ml *Arthrobacter ureafaciens* neuraminidase at 37°C, for 1 h. The sections were then fixed with 4% paraformaldehyde for 20 min, followed permeabilization in 0.1% (v/v) Triton X-100 for 10 min. Immunofluorescence staining was performed using a mouse IgG antibody to SIV NP, followed by Goat anti-mouse IgG antibody conjugated with FITC to visualize the virions. Fluorescence images were acquired on randomly selected regions with a confocal microscope, and the bound virions on the mucus were calculated with ImageJ.

4.4. Results

4.4.1. SAs distribution in porcine respiratory mucus

Five sections were examined for each mucus sample for the semi-quantification of α2,3- and α2,6-SA coverage in the mucus. For each section, 2 images were taken and thus 10 images were obtained for each sample. As shown in Fig. 1, the mucus consisted of mixed and heterogeneous α2,3- and α2,6-SA. The SA coverage was calculated by the ratio of the pixels of positive signal to the total pixels measured. The α2,6-SA covered over 50% the region of interest (ROI), while merely 11% of the region was constituted by α2,3-SA.

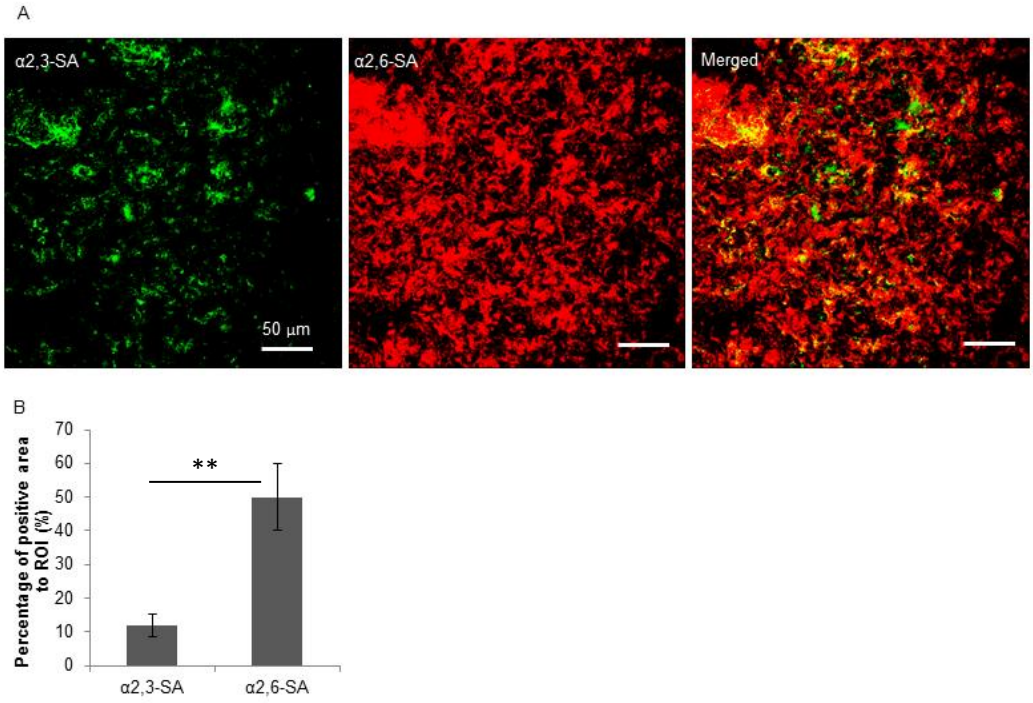

Figure 1. Expression of α2,3- and α2,6-SA on porcine respiratory mucus determined by fluorescence lectin staining. (A) Representative confocal microscopy images. Green color shows α2,3-SA staining and red color represents α2,6-SA staining. The scale bars indicate 50 μm. (B) Semi-quantification of the sialic acids. Three independent mucus samples were analyzed and error bars indicate the standard deviation. The asterisks (**) indicate statistical significance ($P<0.01$, Student's *t*-test).

4.4.2. SIV purity assessed by double staining

After ultracentrifugation over a discontinuous OptiPrep gradient containing 10% to 30% of iodixanol, three visible opalescent bands were collected, named Band 1, Band 2 and Band 3, respectively, from top to bottom (Fig. 2B). The purity of virus from each band was assessed by confocal microscopy following Dio lipophilic dye labeling and SIV immunofluorescence staining. As Dio integrates into the lipophilic components of virus and cellular debris, Dio staining was used as a total-particle assessment. The red color visualized the viral particles, and the green color represented Dio-labeled particles (Fig. 2A). The percentage of double positive particles versus Dio positive particles represents the virus purity in a ratio extent. Consequently, the highest viral purity (over 0.9 for the ratio of double positive particles/Dio positive particles) was found in Band 2 (Fig. 2C). Therefore, the virus preparation from Band 2 was used for

further analysis.

4.4.3. Characterization of Dio-labeled SIV

After incubation with 10 μM Dio dye at room temperature, followed by elution in a Sepharose G-50 column, the labeled and unlabeled SIV were analyzed for different characteristics. The results show that the hemagglutination activity and infectivity were not altered by labeling. The neuraminidase activity of Dio-labeled SIV was 91% of that of unlabeled SIV. Measured by dynamic light scattering and laser Doppler anemometry, the size and surface charge of the labeled virions were not significantly altered (Table 1).

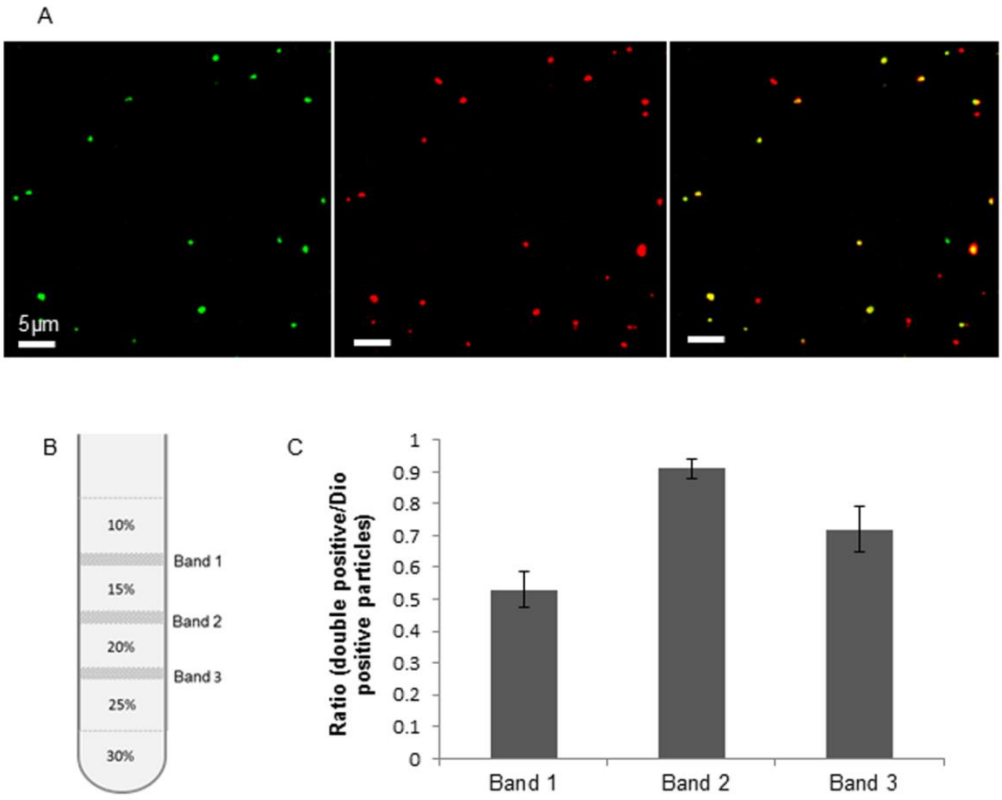

Figure 2. Purity of SIV determined by Dio labeling and immunofluorescence staining. (A) Confocal microscopy of the double staining of the virus preparations. Green represents Dio labeled particles; viral antigens are shown in red. Merged signals represent virus particles which are also labeled with Dio. (B) Bands form in the discontinuous iodixanol gradient separation. Three bands were identified, named Band 1, Band 2 and Band 3 from up downwards. (C) Ratio of double positive particles versus Dio positive particles for the particles from three different bands. Three independent experiments were performed and error bars indicate the standard deviation.

Table 1. Characteristics of SIV and Dio-labeled SIV

	Zeta potential (mV)	Diameter (nm)	Infectivity ($TCID_{50}$ lg/ml)	HA titer	NA activity (RFU*)
SIV	-24.2±3.8	101.8±2.9	8.7±0.43	256	34017±3250
Dio-Labeled SIV	-28.1±5.1	113.5±2.5	8.5±0.23	256	30950±4172

*RFU= Relative Fluorescence Units

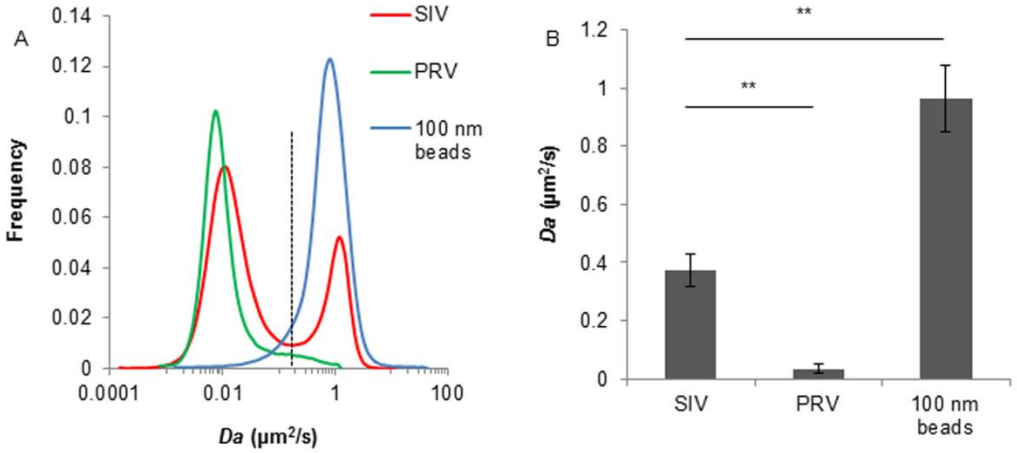

Figure 3. Diffusion coefficient of SIV in mucus and comparison with PrV and 100 nm PEGylated beads. (A) Distributions of the apparent diffusion coefficient of SIV, PrV and 100 nm PEGylated beads in porcine respiratory mucus. Trajectories of 8 steps were analyzed for each of the 1500 diffusion coefficients. Distributions were refined with MEM. Dashed line indicates the boundary of mobile and immobile diffusion. (B) Average diffusion coefficient of SIV, PrV and 100 nm PEGylated beads. Data were obtained from three independent experiments, and error bars indicate the standard deviation. The asterisks (**) indicate statistical significance ($P<0.01$, by Student's *t*-test).

4.4.4. SIV was partially diffusive in porcine respiratory mucus

The motion of SIV in porcine respiratory mucus was investigated and compared with the diffusion of PrV and 100 nm PEGylated beads. Trajectories of 8 steps were analyzed, from which a distribution of the apparent diffusion coefficients was obtained. Similar to our previous data, PrV was highly hindered in the porcine respiratory mucus, while the 100 nm PEGylated beads diffused freely. The

distribution of diffusion coefficient clearly demonstrated that, compared to one immobile fraction for PrV or a mobile fraction for the 100 nm beads, SIV experienced two diffusion patterns in porcine respiratory mucus, with 70% of viral particles being trapped while the rest of particles moving rapidly (Fig. 3A). The average diffusion coefficient of SIV in mucus was 11-fold higher than that of PrV (Fig. 3B). The similar size 100 nm PEGylated beads are muco-inert which indicates that these particles did not interact with any type of the mucus moieties. Thus to the opposite, the viral particles were immobilized probably due to binding interactions with the mucus. These data suggest that binding and releasing effects were present in the interactions of SIV with porcine respiratory mucus.

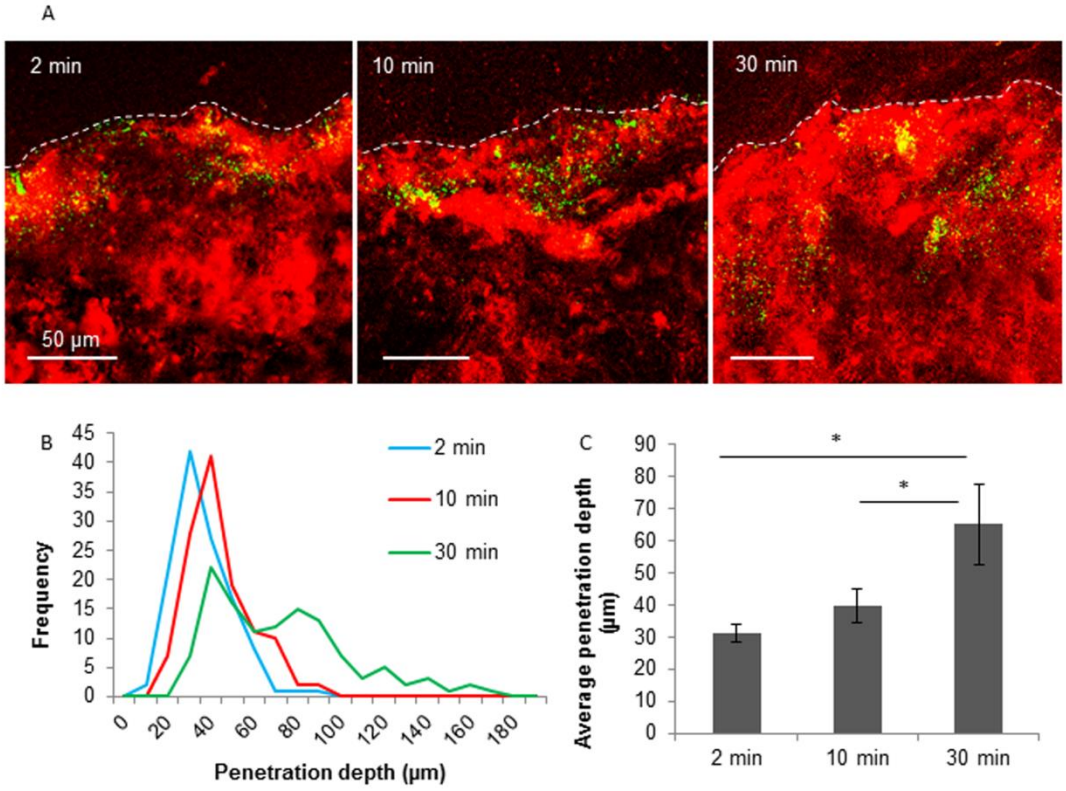

Figure 4. Penetration of SIV through porcine respiratory mucus. (A) Confocal microscopic analysis of the virus penetration. Representative confocal photomicrographs of the penetration of SIV at 2, 10 and 30 min post virus addition. Mucin 5AC and SIV antigens were visualized by red and green color, respectively. (B) Penetration depths of SIV with time. Hundred and twenty measurements were obtained from three independent mucus samples. (C) Average penetration depth of SIV at 2, 10 and 30 min post virus addition. Three independent experiments were performed. Error bars indicate the standard deviation. The asterisk (*) indicates statistical significance ($P<0.05$, by Student's *t*-test).

4.4.5. Penetration of SIV through the mucus layer

The depth of SIV penetration could be visualized by double immunofluorescence staining of the MUC5AC and SIV nucleoprotein (NP). The distance from the surface down to the deepest point of virus translocation was measured and designated as the depth of virus penetration. Three independent experiments were performed and in total 120 measurements were conducted. Distribution of the penetration depth for each condition was eventually obtained. Immediately after virus addition, the virions rapidly entered the mucus layer and reached a depth of 31 μm within 2 min, due to a passive diffusion effect (Fig. 4A). Incubated at 37°C, the virions spread further in the mucus with time. The distribution of penetration depth shows that the majority of SIV particles travelled 10 μm further in the mucus from 2 until 10 min after virus addition and reached a depth of up to 180 μm at 30 min after addition (Fig. 4A). Similarly to the microscopic diffusion, the distribution of SIV penetration clearly shows two fractions at 30 min after virus addition (Fig. 4B). About 65% of the viral particles penetrated at 30 min more than 2-fold further than 2 min post virus addition (Fig. 4B). The average depth of virus penetration at 30 min was significantly higher than that of earlier time points (Fig. 4C), suggesting that the SIV virions were able to actively penetrate the mucus layer.

4.4.6. Neuraminidase mediated the diffusion and penetration of SIV in respiratory mucus

Movies were captured with SPT software, and the SIV microscopic diffusion in mucus in the presence or absence of zanamivir or exogenous neuraminidase was analyzed with IPS. As shown in Fig. 5A, the mobile fraction of SIV diffusion was severely diminished by NAI treatment, while it was elevated by the addition of *Arthrobacter ureafaciens* neuraminidase. Approximately 55% of the mobile viral particles (with *Da* larger than 0.2 $\mu m^2/s$) became stuck by the effect of zanamivir whereas the exogenous neuraminidase increased the mobile particles by approximately 15% (Fig. 5B). Consistently, the presence of zanamivir in virus suspension almost completely inhibited the SIV macroscopic penetration which

contrasts the further penetration by the effect of exogenous neuraminidase (Fig. 5C). The average penetration of mock treated SIV was significantly higher than that of NAI treated virus, while the rise of average penetration from mock to neuraminidase treated virus was also significant (Fig. 5D). These data imply that neuraminidase helped SIV penetrate through the porcine respiratory mucus.

4.4.7. Effects of NA on SIV binding to the porcine respiratory mucus

Virus attaching to the mucus cryosections was visualized by immunofluorescence staining to the SIV NP. The virus binding to 5 mucus cryosections was analyzed, 2 images were taken for each section and in total 10 images were obtained for virions quantification. The number of virions that attached to a mucus region of 10^5 μm^2 was calculated. Three independent experiments were performed. The representative confocal photomicrographs show that zanamivir clearly enhanced the attachment of SIV to the mucus. In contrast, the exogenous neuraminidase depleted the virus binding to the mucus by 2-fold (Fig. 6). These data clearly demonstrated that NA was able to release the SIV particles which may have been bound by interaction of HA with mucins, moving the virions through the mucus.

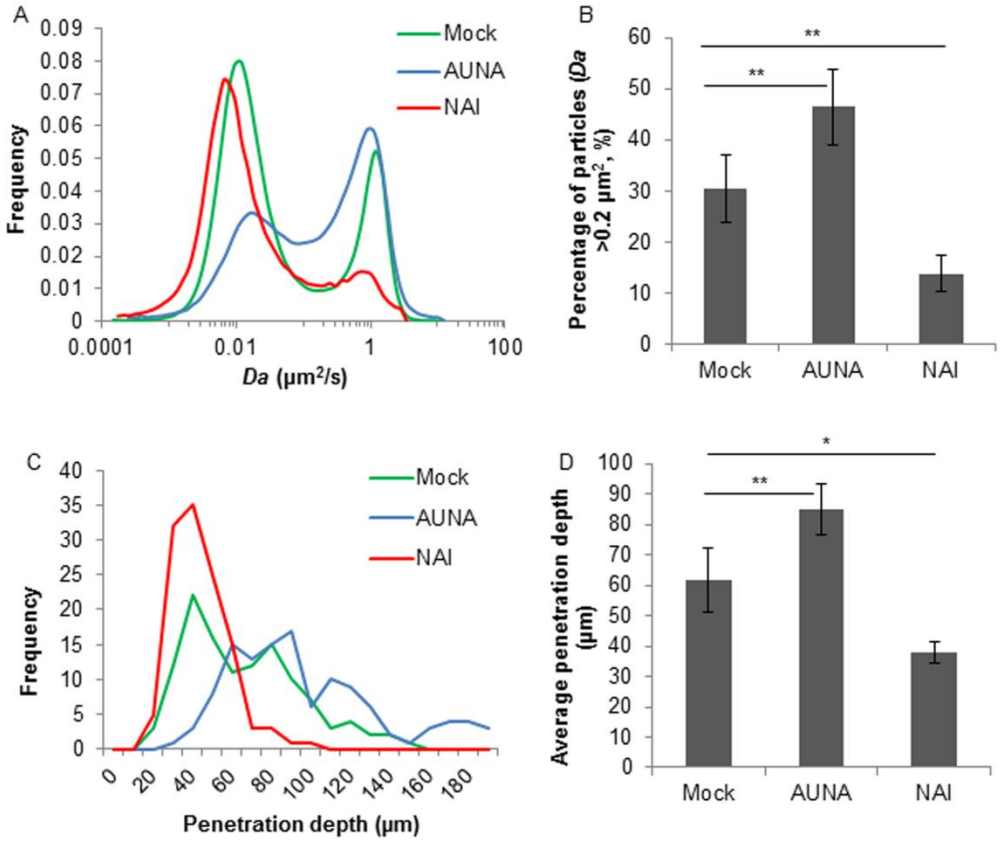

Figure 5. Effects of NAI and *Arthrobacter ureafaciens* neuraminidase (AUNA) on microscopic diffusion and macroscopic penetration of SIV in porcine respiratory mucus. (A) Distribution of diffusion coefficient of NAI, AUNA and mock treated SIV in mucus. 1500 trajectories were analyzed. Distributions were refined with MEM. (B) Proportion of mobile fraction (*Da* >0.2 μm^2/s) of NAI, AUNA and mock treated SIV in mucus. Error bars represent the standard deviation from three independent experiments. The asterisks (**) indicate statistical significance (P<0.01, by Student's *t*-test) (C) Distribution of the penetration depth of NAI, AUNA and mock treated SIV through mucus at 30 min post virus addition. Hundred and twenty measurements were performed on three independent mucus samples. (D) Average penetration depth of NAI, AUNA and mock treated SIV through mucus at 30 min post virus addition. Three independent samples were performed, and error bars indicate the standard deviation. The asterisks (** and *) indicate statistical significance (P<0.01, and P<0.05, respectively, by Student's *t*-test).

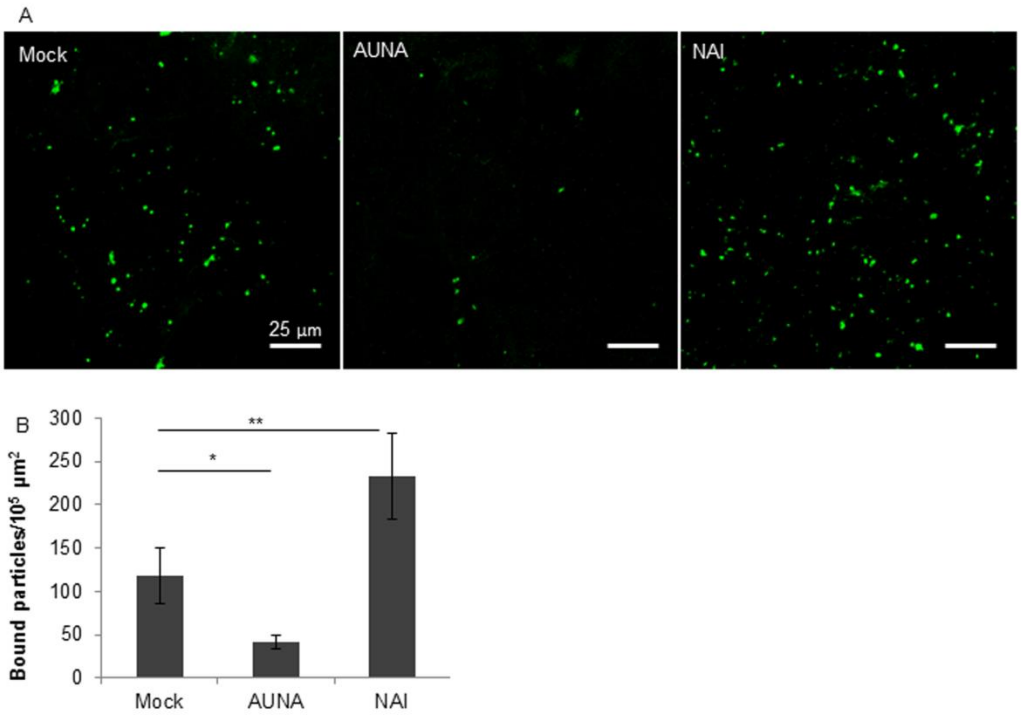

Figure 6. Effects of NA on SIV binding to porcine respiratory mucus shown by confocal microscopy. (A) Virions (white) bound to mucus cryosections in the presence or absence (Mock) of Zanamivir (NAI) or *Arthrobacter ureafaciens* neuraminidase (AUNA). (B) Quantification of viral particles bound to mucus (per 10^5 μm^2). The error bars indicate the standard deviation from 3 independent experiments. The asterisks (** and *) show the significance difference ($P<0.01$, and $P<0.05$ by Student's *t*-test).

4.5. Discussion

Influenza viruses are highly contagious and readily spread by aerosol transmission. The mucus is the first barrier for the small aerosol droplets to settle and overcome. In the present study, we applied SPT technique and a custom made virus in-capsule-mucus penetration system to visualize the microscopic diffusion and macroscopic penetration of SIV in porcine respiratory mucus.

SPT is a unique model for rigorous analysis of virus-mucus interactions from the mobility point of view. The virus in-capsule-mucus penetration system allows the visualization of virus penetration in mucus layer thereby mimicking the natural conditions. By the use of these models, we were able to track the diffusion of SIV in natural respiratory mucus. In the SPT assay, there were two fractions based on the virus diffusion coefficient, a mobile and an immobile fraction. The ability of SIV to

detach from mucus was attributed to the NA activities, as inhibiting NA by the use of zanamivir significantly suppressed the liberation of the virus from the mucus network (Fig. 5A, 5B). This is also in line with a previous report by Matrosovich *et al.* (Matrosovich *et al.*, 2004), which describes that blocking of the NA activities by oseltamivir efficiently inhibited influenza A viruses from infecting the differentiated human airway epithelium cultures which were probably covered by mucin secretions. Furthermore, exogenous neuraminidase was shown to promote both the microscopic diffusion and macroscopic penetration detected by the SPT and virus in-capsule-mucus penetration system (Fig. 5). This does not only confirm the beneficial effect of neuraminidase on releasing SIV from respiratory mucus, but also highlights bidirectional synergistic interactions between influenza virus and bacterial infections. The influenza virus predisposition to secondary bacterial infections has been thoroughly studied (Peltola *et al.*, 2005; Pittet *et al.*, 2010), however, little information exists regarding the impact of bacterial neuraminidase on influenza virus entry and transmission, and further research is needed.

Neuraminidase was indicated to play a role in the SIV releasing from mucus, however, two fractions of viral motion in the mucus lead to a discussion of the way that the virus binds to the mucus. Mucins are the major constitute of mucus and are highly decorated by glycans terminated by sialic acids, thus they are likely to be attributed to the immobilization of SIV in porcine respiratory mucus. Mucins may play direct and indirect roles in host defense distinct from their ability to form adhesion decoys. In addition to mucins, the aqueous mucus layer consists of a great number of host defense agents including lysozyme, lactoferrin, secretory IgA (sIgA), collectins, defensins, cathelicidins, histatins and surfactant proteins (Schicht *et al.*, 2013; Tjabringa *et al.*, 2005; Vareille *et al.*, 2011). These molecules may function by binding the virions in a receptor-independent pattern. It has been shown that surfactant protein D (SP-D) binds via a carbohydrate recognition domain in a Ca^{2+}-dependent manner to N-linked high-mannose carbohydrates present on the HA and NA of the influenza viruses (Hartshorn *et al.*, 1994). In addition, sIgA is retained at high concentrations in

mucus where it can efficiently trap the pathogens. Last but not least, defensins are of great interest with respect to respiratory viral infection. Human defensins have been shown to bind several types of viruses and inhibit the entry of the viruses to target cells (Daher *et al.*, 1986; Doss *et al.*, 2009). These components may be retained in mucus by direct binding with mucins or by the biophysical properties of mucus and thus become part of the gel network and provide an immobilized reservoir of protective effectors. Alternatively, it is possible that the viral particles that were immobilized in the mucus were actually incomplete or defective virions or became inactive while being prepared. The production of defective particles has been reported for influenza A viruses (Brooke *et al.*, 2013; Nayak *et al.*, 2009). However, the approach of distinguishing active and inactive virions in an entity has not been readily achieved, and will be further examined.

While vaccination remains the primary option for the prevention and control of influenza, anti-influenza virus drugs are considered as a complementary approach, as vaccine production may not be rapidly achieved. Our findings provide experimental evidence for the essential role of NA in influenza virus penetration through the respiratory mucus. Blocking the NA activities clearly suppressed the movement of virus in mucus (Fig. 5), illustrating that NA played a role in removing the sialic acids on mucins, which may enable the virus to gain access to the cellular receptors. This suggests the usefulness of neuraminidase inhibitors as prophylactic treatment for influenza. On the other hand, preventative treatment with oseltamivir (Tamiflu) failed to protect the lung from virus replication or inflammation in an *in vivo* influenza infection study in pigs despite reduced clinical symptoms and virus shedding (Duerrwald *et al.*, 2013). This highlights the complexity of the *in vivo* situation and the minimal benefits neuraminidase inhibitors may have.

The ability of an influenza virus passing through the mucus may serve as a determinant for influenza virus transmission in addition to efficient virus attachment, high potential of replication and low infectious dose required (Sorrell *et al.*, 2011; Tellier, 2009; Yassine *et al.*, 2010). Combining the study of Cohen *et al.* (Cohen *et al.*,

2013), it can be noticed that human influenza viruses could bind and be released from human salivary mucins but not from porcine submaxillary mucins, whereas, swine influenza virus was able to escape from porcine airway mucus, suggesting there may be different interactions between different influenza viruses and the mucus of different species. A balance of binding to and releasing from the mucin sialic acids, which is determined by the functional balance of HA and NA, may influence how efficiently the virus avoids sticking to mucus. Fluorescence lectin staining on mucus cryosection showed that both α2,3- and α2,6-SA were present in the porcine respiratory mucus, with distinct predominance for the latter (Fig. 1). The binding profile of the SIV strain was not investigated in this study, however, it has been well documented that swine influenza virus isolates, especially those with the avian-like H1 and H3 hemagglutinins showed receptor specificity for both α2,3- and α2,6-sialylated glycans (Bradley *et al.*, 2011; Chen *et al.*, 2011; Gambaryan *et al.*, 2005). Probably the mucus provides sufficient amount of receptors for SIV binding. The binding of SIV via HA to the porcine respiratory mucus was proved in the present study, and the amount of viral or exogenous NA indeed modulated the extent of viral binding to and releasing from the porcine mucus (Fig. 6). Concerning the releasing effect, NA which mediates the process also has a substrate preference. It was demonstrated that NA of human and swine influenza viruses have a preferential specificity for α2,3-SA although they cleave both linked sialylated glycans (Couceiro & Baum, 1994; Kobasa *et al.*, 1999). Therefore, we assume that the sialic acids in respiratory mucus secretions may exert an effect on influenza virus transmission.

Since the majority of viral particles were incapable of penetrating through the mucus layer, why do influenza viruses invade the respiratory tract of the animals after all (Crisci *et al.*, 2013; Thacker & Janke, 2008; Webster *et al.*, 1992)? Based on our experimental findings and present literature, we propose several strategies that influenza viruses may use to overcome the mucus barrier and find their way to establish infection:

(1) Production of enzymes that aid the virus movement through the mucus.

Influenza virus binds to and uses sialic acid-containing molecules as receptors. It is because of this capability that influenza virus has evolved a second viral surface protein, neuraminidase, as a receptor-destroying enzyme that cleaves sialic acid, allowing the virus to be released after binding to sialic acid-containing molecules that do not lead to viral infection. A similar strategy is utilized by many other microbes, such as *E. histolytica* (Frederick & Petri, 2005; Leitch *et al.*, 1988), *Vibrio cholerae* (Silva *et al.*, 2003), *Helicobacter pylori* (Celli *et al.*, 2009), reovirus (Bisaillon *et al.*, 1999) and coronavirus (Schwegmann-Wessels & Herrler, 2006), to subvert or avoid the mucus barrier. The production of enzymes, including mucinase, sialidase, glycosidase, elastase, and hydrolase, which are capable of degrading mucin core proteins and mucin carbohydrates facilitates microbes to swim through the mucus layer. Furthermore, the enzymes that the microbes produce may also facilitate the invasion of other pathogens. In women with bacterial vaginosis, the overgrowth of anaerobic gram-negative bacteria that produce sialidase, glycosidases and other mucin-degrading enzymes causes a breakdown in the barrier properties of cervicovaginal mucus, thereby destroying the mucus gel and helping other sexually transmitted pathogens such as human immunodeficiency virus (HIV) to invade (Olmsted *et al.*, 2003).

(2) The use of abundant and ubiquitous molecules as receptors. Although there may be a risk of binding to decoy receptors, the use of abundant and ubiquitous molecules as receptors provides the apparent advantage to the virus for allowing infection of multiple cell types and species. This can result in a low minimal infectious dose for initial infection. Based on the data of diffusion and penetration, the effects of the mucus network that virions encounter are so extreme that only a part of the particles can escape and reach susceptible target cells ultimately. Thus the viruses which require lower minimal infectious doses for the same tissues may gain higher chance to establish an infection.

(3) Spread via aerosol. The slow settle of aerosols in the air can cause prolonged contact of the virus with the respiratory tract which benefits the virus penetration

through the mucus layer. Furthermore, aerosol droplets can travel much more efficiently to the lower respiratory tract and the mucociliary apparatus may need a longer time to transport and exclude the virions out of the respiratory tract, which increases the chance of these viruses to penetrate through the mucus layer and reach the target cells eventually.

The issues if SIV is able to penetrate through the porcine respiratory mucus and if the neuraminidase contributes to move the virus through the mucus layer have been addressed. However, the ability of the viral neuraminidase to cleave sialic acid from mucus has not been investigated due to technical limitation. The viscous property impedes the separation of the free sialic acids from the mucus even if they would have been cleaved by the viral neuraminidase. Investigating the role of influenza virus neuraminidase in the cleavage of sialic acid from mucus may shed some light on unravelling the mechanism of influenza pneumonia. Hence the effect of influenza virus neuraminidase on mucus needs to be studied.

4.6. Acknowledgements

The authors would like to express their gratitude to Lieve Sys for the technical guidance and discussions on influenza viruses. Thanks go to Zeger Vandenabeele and Loes Geypen for their help in preparing the trachea samples, and Nele Dennequin for preparing cell samples.

4.7. References

Adamo, J. E., Liu, T., Schmeisser, F. & Ye, Z. (2009). Optimizing viral protein yield of influenza virus strain A/Vietnam/1203/2004 by modification of the neuraminidase gene. *J Virol* **83**, 4023-4029.

Bisaillon, M., Senechal, S., Bernier, L. & Lemay, G. (1999). A glycosyl hydrolase activity of mammalian reovirus sigma1 protein can contribute to viral infection through a mucus layer. *J Mol Biol* **286**, 759-773.

Bradley, K. C., Jones, C. A., Tompkins, S. M., Tripp, R. A., Russell, R. J., Gramer, M. R., Heimburg-Molinaro, J., Smith, D. F., Cummings, R. D. & Steinhauer, D. A. (2011). Comparison of the receptor binding properties of contemporary swine isolates and early human pandemic H1N1 isolates (Novel 2009 H1N1). *Virology* **413**, 169-182.

Braeckmans, K., Buyens, K., Bouquet, W., Vervaet, C., Joye, P., De Vos, F., Plawinski, L.,

Doeuvre, L., Angles-Cano, E., Sanders, N. N., Demeester, J. & De Smedt, S. C. (2010). Sizing nanomatter in biological fluids by fluorescence single particle tracking. *Nano Lett* **10**, 4435-4442.

Braeckmans K, V. D., Demeester J, De Smedt SC (2010). Single particle tracking. In: Diaspro A, editor. Nanoscopy multidimensional optical fluorescence microscopy. *Sci-Tech News* **64**, 92-92.

Brooke, C. B., Ince, W. L., Wrammert, J., Ahmed, R., Wilson, P. C., Bennink, J. R. & Yewdell, J. W. (2013). Most influenza a virions fail to express at least one essential viral protein. *J Virol* **87**, 3155-3162.

Celli, J. P., Turner, B. S., Afdhal, N. H., Keates, S., Ghiran, I., Kelly, C. P., Ewoldt, R. H., McKinley, G. H., So, P., Erramilli, S. & Bansil, R. (2009). Helicobacter pylori moves through mucus by reducing mucin viscoelasticity. *Proc Natl Acad Sci U S A* **106**, 14321-14326.

Chen, L. M., Rivailler, P., Hossain, J., Carney, P., Balish, A., Perry, I., Davis, C. T., Garten, R., Shu, B., Xu, X., Klimov, A., Paulson, J. C., Cox, N. J., Swenson, S., Stevens, J., Vincent, A., Gramer, M. & Donis, R. O. (2011). Receptor specificity of subtype H1 influenza A viruses isolated from swine and humans in the United States. *Virology* **412**, 401-410.

Cohen, M., Zhang, X. Q., Senaati, H. P., Chen, H. W., Varki, N. M., Schooley, R. T. & Gagneux, P. (2013). Influenza A penetrates host mucus by cleaving sialic acids with neuraminidase. *Virol J* **10**, 321.

Colman, P. M. (1994). Influenza virus neuraminidase: structure, antibodies, and inhibitors. *Protein Sci* **3**, 1687-1696.

Cone, R. A. (2009). Barrier properties of mucus. *Adv Drug Deliv Rev* **61**, 75-85.

Couceiro, J. N. & Baum, L. G. (1994). Characterization of the hemagglutinin receptor specificity and neuraminidase substrate specificity of clinical isolates of human influenza A viruses. *Mem Inst Oswaldo Cruz* **89**, 587-591.

Crisci, E., Mussa, T., Fraile, L. & Montoya, M. (2013). Review: influenza virus in pigs. *Mol Immunol* **55**, 200-211.

Daher, K. A., Selsted, M. E. & Lehrer, R. I. (1986). Direct inactivation of viruses by human granulocyte defensins. *J Virol* **60**, 1068-1074.

De Vleeschauwer, A., Atanasova, K., Van Borm, S., van den Berg, T., Rasmussen, T. B., Uttenthal, A. & Van Reeth, K. (2009). Comparative pathogenesis of an avian H5N2 and a swine H1N1 influenza virus in pigs. *PLoS One* **4**, e6662.

Doss, M., White, M. R., Tecle, T., Gantz, D., Crouch, E. C., Jung, G., Ruchala, P., Waring, A. J., Lehrer, R. I. & Hartshorn, K. L. (2009). Interactions of alpha-, beta-, and theta-defensins with influenza A virus and surfactant protein D. *J Immunol* **182**, 7878-7887.

Duerrwald, R., Schlegel, M., Bauer, K., Vissiennon, T., Wutzler, P. & Schmidtke, M. (2013). Efficacy of influenza vaccination and tamiflu(R) treatment--comparative studies with Eurasian Swine influenza viruses in pigs. *PLoS One* **8**, e61597.

Ehre, C., Worthington, E. N., Liesman, R. M., Grubb, B. R., Barbier, D., O'Neal, W. K., Sallenave, J. M., Pickles, R. J. & Boucher, R. C. (2012). Overexpressing mouse model demonstrates the protective role of Muc5ac in the lungs. *Proc Natl Acad Sci U S A* **109**, 16528-16533.

Fazekas De, S. G. S. (1952). Nasal mucus and influenza viruses. I. The haemagglutinin inhibitor in nasal secretions. *J Hyg (Lond)* **50**, 471-490.

Frederick, J. R. & Petri, W. A., Jr. (2005). Roles for the galactose-/N-acetylgalactosamine-binding lectin of Entamoeba in parasite virulence and differentiation. *Glycobiology* **15**, 53R-59R.

Gambaryan, A. S., Karasin, A. I., Tuzikov, A. B., Chinarev, A. A., Pazynina, G. V., Bovin, N. V., Matrosovich, M. N., Olsen, C. W. & Klimov, A. I. (2005). Receptor-binding properties of swine influenza viruses isolated and propagated in MDCK cells. *Virus Res* **114**, 15-22.

Hartshorn, K. L., Crouch, E. C., White, M. R., Eggleton, P., Tauber, A. I., Chang, D. & Sastry, K. (1994). Evidence for a protective role of pulmonary surfactant protein D (SP-D) against influenza A viruses. *J Clin Invest* **94**, 311-319.

Itamura, S. (1997). [Structure and function of influenza virus neuraminidase]. *Nihon Rinsho* **55**, 2570-2574.

Kobasa, D., Kodihalli, S., Luo, M., Castrucci, M. R., Donatelli, I., Suzuki, Y., Suzuki, T. & Kawaoka, Y. (1999). Amino acid residues contributing to the substrate specificity of the influenza A virus neuraminidase. *J Virol* **73**, 6743-6751.

Leitch, G. J., Harris-Hooker, S. A. & Udezulu, I. A. (1988). Movement of Entamoeba histolytica trophozoites in rat cecum and colon intact mucus blankets and harvested mucus gels. *Am J Trop Med Hyg* **39**, 282-287.

Lillehoj, E. R. & Kim, K. C. (2002). Airway mucus: its components and function. *Arch Pharm Res* **25**, 770-780.

Linden, S. K., Sutton, P., Karlsson, N. G., Korolik, V. & McGuckin, M. A. (2008). Mucins in the mucosal barrier to infection. *Mucosal Immunol* **1**, 183-197.

Matrosovich, M. & Klenk, H. D. (2003). Natural and synthetic sialic acid-containing inhibitors of influenza virus receptor binding. *Rev Med Virol* **13**, 85-97.

Matrosovich, M. N., Matrosovich, T. Y., Gray, T., Roberts, N. A. & Klenk, H. D. (2004). Neuraminidase is important for the initiation of influenza virus infection in human airway epithelium. *J Virol* **78**, 12665-12667.

Medina, R. A. & Garcia-Sastre, A. (2011). Influenza A viruses: new research developments. *Nat Rev Microbiol* **9**, 590-603.

Nayak, D. P., Balogun, R. A., Yamada, H., Zhou, Z. H. & Barman, S. (2009). Influenza virus morphogenesis and budding. *Virus Res* **143**, 147-161.

Olmsted, S. S., Meyn, L. A., Rohan, L. C. & Hillier, S. L. (2003). Glycosidase and proteinase activity of anaerobic gram-negative bacteria isolated from women with bacterial vaginosis. *Sex Transm Dis* **30**, 257-261.

Peltola, V. T., Murti, K. G. & McCullers, J. A. (2005). Influenza virus neuraminidase contributes to secondary bacterial pneumonia. *J Infect Dis* **192**, 249-257.

Pittet, L. A., Hall-Stoodley, L., Rutkowski, M. R. & Harmsen, A. G. (2010). Influenza virus infection decreases tracheal mucociliary velocity and clearance of Streptococcus pneumoniae. *Am J Respir Cell Mol Biol* **42**, 450-460.

Ramos, I. & Fernandez-Sesma, A. (2012). Cell receptors for influenza a viruses and the innate immune response. *Front Microbiol* **3**, 117.

Roberts, K. L., Shelton, H., Scull, M., Pickles, R. & Barclay, W. S. (2011). Lack of transmission of a human influenza virus with avian receptor specificity between ferrets is not due to decreased virus shedding but rather a lower infectivity in vivo. *J Gen Virol* **92**, 1822-1831.

Saxton, M. J. & Jacobson, K. (1997). Single-particle tracking: applications to membrane dynamics. *Annu Rev Biophys Biomol Struct* **26**, 373-399.

Schicht, M., Knipping, S., Hirt, R., Beileke, S., Sel, S., Paulsen, F. & Brauer, L. (2013). Detection of surfactant proteins A, B, C, and D in human nasal mucosa and their regulation in chronic rhinosinusitis with polyps. *Am J Rhinol Allergy* **27**, 24-29.

Schwegmann-Wessels, C. & Herrler, G. (2006). Sialic acids as receptor determinants for coronaviruses. *Glycoconj J* **23**, 51-58.

Seto, J. T. & Chang, F. S. (1969). Functional significance of sialidase during influenza virus multiplication: an electron microscope study. *J Virol* **4**, 58-66.

Shtyrya, Y. A., Mochalova, L. V. & Bovin, N. V. (2009). Influenza virus neuraminidase: structure and function. *Acta Naturae* **1**, 26-32.

Silva, A. J., Pham, K. & Benitez, J. A. (2003). Haemagglutinin/protease expression and mucin gel penetration in El Tor biotype Vibrio cholerae. *Microbiology* **149**, 1883-1891.

Sorrell, E. M., Schrauwen, E. J., Linster, M., De Graaf, M., Herfst, S. & Fouchier, R. A. (2011). Predicting 'airborne' influenza viruses: (trans-) mission impossible? *Curr Opin Virol* **1**, 635-642.

Tellier, R. (2009). Aerosol transmission of influenza A virus: a review of new studies. *J R Soc Interface* **6 Suppl 6**, S783-790.

Thacker, E. & Janke, B. (2008). Swine influenza virus: zoonotic potential and vaccination strategies for the control of avian and swine influenzas. *J Infect Dis* **197 Suppl 1**, S19-24.

Thornton, D. J., Rousseau, K. & McGuckin, M. A. (2008). Structure and function of the polymeric mucins in airways mucus. *Annu Rev Physiol* **70**, 459-486.

Tjabringa, G. S., Vos, J. B., Olthuis, D., Ninaber, D. K., Rabe, K. F., Schalkwijk, J., Hiemstra, P. S. & Zeeuwen, P. L. (2005). Host defense effector molecules in mucosal secretions. *FEMS Immunol Med Microbiol* **45**, 151-158.

Torremorell, M., Allerson, M., Corzo, C., Diaz, A. & Gramer, M. (2012). Transmission of Influenza A Virus in Pigs. *Transbound Emerg Dis*.

Vareille, M., Kieninger, E., Edwards, M. R. & Regamey, N. (2011). The airway epithelium: soldier in the fight against respiratory viruses. *Clin Microbiol Rev* **24**, 210-229.

Webster, R. G., Bean, W. J., Gorman, O. T., Chambers, T. M. & Kawaoka, Y. (1992). Evolution and ecology of influenza A viruses. *Microbiol Rev* **56**, 152-179.

Yang, X., Forier, K., Steukers, L., Van Vlierberghe, S., Dubruel, P., Braeckmans, K., Glorieux, S. & Nauwynck, H. J. (2012). Immobilization of pseudorabies virus in porcine tracheal respiratory mucus revealed by single particle tracking. *PLoS One* **7**, e51054.

Yassine, H. M., Lee, C. W., Gourapura, R. & Saif, Y. M. (2010). Interspecies and intraspecies transmission of influenza A viruses: viral, host and environmental factors. *Anim Health Res Rev* **11**, 53-72.

Chapter 5

5. General discussion

Pseudorabies virus (PrV) and swine influenza virus (SIV) are two important porcine viruses which both primarily replicate in the respiratory mucosa (Glorieux *et al.*, 2007; Nauwynck *et al.*, 2007; Van Reeth, 2007), however with different patterns. PrV primarily targets the epithelial cells of nasal mucosa and rapidly traverses the basement membrane (Glorieux *et al.*, 2009; Kritas *et al.*, 1994). Between 2 and 5 days post inoculation, virus spreads over the whole mucosa and further into the submucosa. In contrast, SIV infection is generally limited to the epithelial cells of the whole respiratory tract. The infection is very efficient in the lower respiratory tract, and the virus load can reach high levels (Heinen *et al.*, 2000; Van Reeth *et al.*, 1999). The primary mean of transmission of PrV among swine herds is direct contact between infected and susceptible pigs, whereas SIV is shed via nasal secretions and is efficiently transmitted via air (Van Gucht *et al.*, 2006). SIV is cleared within 1 week after infection (Van Reeth, 2007), whereas PrV may replicate for 10-14 days (Nauwynck *et al.*, 2007; Nauwynck, 1997). Hence a fast and intensive infection of the mucosal epithelium is crucial for SIV. In order to invade the host mucosa, both viruses may have evolved different mechanisms to reach and infect the respiratory tract.

5.1. Significance of virus mobility in mucus

The first barrier for a respiratory virus to encounter is the mucus layer. Together with the submucosal glands, epithelial mucus-producing cells secrete high molecular weight mucins, which comprise the respiratory mucus and maintain the biochemical and biophysical properties of mucus (Turner & Jones, 2009). In order to study virus-mucus interactions, we first set up a model using single particle tracking, which was used to study the mobility of particles in solution. The path travelled by each particle over time was recorded and the mean squared displacement and diffusion coefficient of the particles through the mucus gel were calculated (Braeckmans K, 2010) (**Chapter 3.1**). Both PrV and SIV were found with single particle tracking to be immobilized in the porcine respiratory mucus, though the extent of hindrance was different. PrV experienced a significant obstruction in porcine tracheal respiratory

mucus, with approximately 96% of the viral particles being entrapped (**Chapter 3.1**). Seventy percent of the SIV virions, which were previously assumed to move freely in respiratory mucus, were entrapped (**Chapter 4**). Two major mechanisms may prevent particles from diffusing through mucus. Particles can adhere to mucus constituents or they can be hindered by the size of the mesh spacing between the mucin fibers. Measured with different sized polyethylene glycol coupled (PEGylated) nanoparticles and atomic force microscope, the pore size of porcine tracheal respiratory mucus ranged from 80 to 1500 nm, with an average diameter of 455 nm. Therefore, these viruses were entrapped in mucus due to adhesive interactions rather than size exclusion.

The hindrance of these viruses was also confirmed by the penetration depth measured in a virus-capsule-mucus penetration system. PrV was almost completely trapped in the porcine respiratory mucus shown by this model (**Chapter 3.3**). On the other hand, some SIV particles remained stuck in mucus, while the rest were able to penetrate further with time (**Chapter 4**). These findings further demonstrate that the porcine respiratory mucus almost completely blocked PrV entry, while it seemed only to delay SIV from reaching the epithelial cells.

It should be noted that strongly charged (positively or negatively) nanoparticles also showed a hindered motion similar to PrV which is negatively charged. Neutral PEGylated nanoparticles diffused freely in mucus (**Chapter 3.1**). Similarly, Lieleg *et al.* analyzed the diffusion of amine-, carboxyl-terminated and PEGylated particles (1 μm) in extracellular matrix (ECM) purified from the Engelbreth-Holm-Swarm sarcoma of mice, and found that the diffusion of charged particles was extremely suppressed compared to the neutral PEG modified particles (Lieleg *et al.*, 2009). The net surface charge of SIV was also found to be negative. Thus we hypothesize that the obstruction of PrV and SIV in the porcine respiratory mucus was at least partly due to charge interactions. As influenza virus is known to bind to negative sialic acids (SAs) via the pocket of the globular head of HA1 (Skehel & Wiley, 2000; Stevens *et al.*, 2006), immobility of SIV in the porcine mucus may involve more complicated

interactions. Immobilization is likely responsible for the majority of the inhibitory activity of mucus against a virus. Hindering the virus in mucus can prevent it from reaching the target cells in the epithelium.

Movement in mucus may be a prerequisite for a virus to invade the mucus coated mucosa. PrV was almost completely immobilized in mucus, while SIV moved partially through mucus. Movement allows virus to penetrate through the respiratory mucus, as well to become released into the lumen after infection. In summary, PrV remains trapped in porcine respiratory mucus. PrV particles are mostly immobilized, and the particles may be bound to mucin fibers via interactions with mucin glycans (Fig. 1A and B). PrV has difficulties in crossing the mucus layer, which may explain why most infections occur subclinically (Martinez-Lopez *et al.*, 2009; Newby *et al.*, 2002). It may depend on defects of mucus to be able to subvert the protective mucus barrier. On the other hand, SIV is partially moving in the mucus. Despite having chance of binding to SAs which are abundantly present in mucin glycans, the SIV particles are much more actively diffusing in the respiratory mucus. The NA of SIV constantly clips away the SAs that may be or may have been bound to the virus, thus helping the virus to drill through the respiratory mucus (Fig. 2A). The easy approach of influenza viruses to the target epithelial cells, may aid to explain why they may cause high morbidity during influenza virus outbreaks.

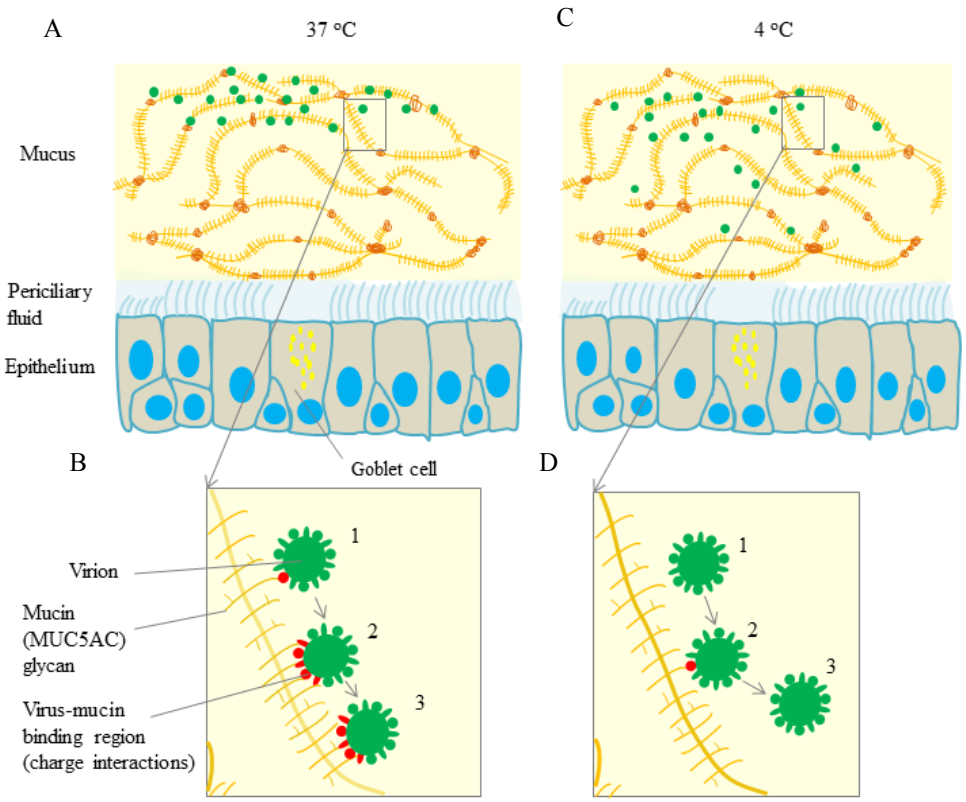

Figure 1. Schematic interactions of PrV with porcine respiratory mucus and the effect of temperature. (A) At body temperature (37 °C), PrV quickly enters after encountering the respiratory mucus due to passive concentration-dependent diffusion. PrV is highly trapped in mucus and remains trapped with time. (B) The immobilization may be mediated by binding of PrV to mucin (especially MUC5AC) glycans via charge interactions as the following process: (1) the PrV virion encounters and quickly binds to a mucin glycan; (2) the binding becomes stronger by involving more virus-mucin glycan interactions; (3) the attachment remains overtime. (C) At cold temperature (4 °C), PrV quickly enters after encountering the respiratory mucus due to passive concentration-dependent diffusion. PrV is partially diffusive, with some particles penetrating through the mucus layer. (D) The interactions may occur as follows: (1) the virion encounters a mucin glycan, while binding does not occur; (2) binding may occur when optimal interaction is achieved; (3) the virus may then be detached due to the weak bonding between the virus and glycan(s) at low temperature.

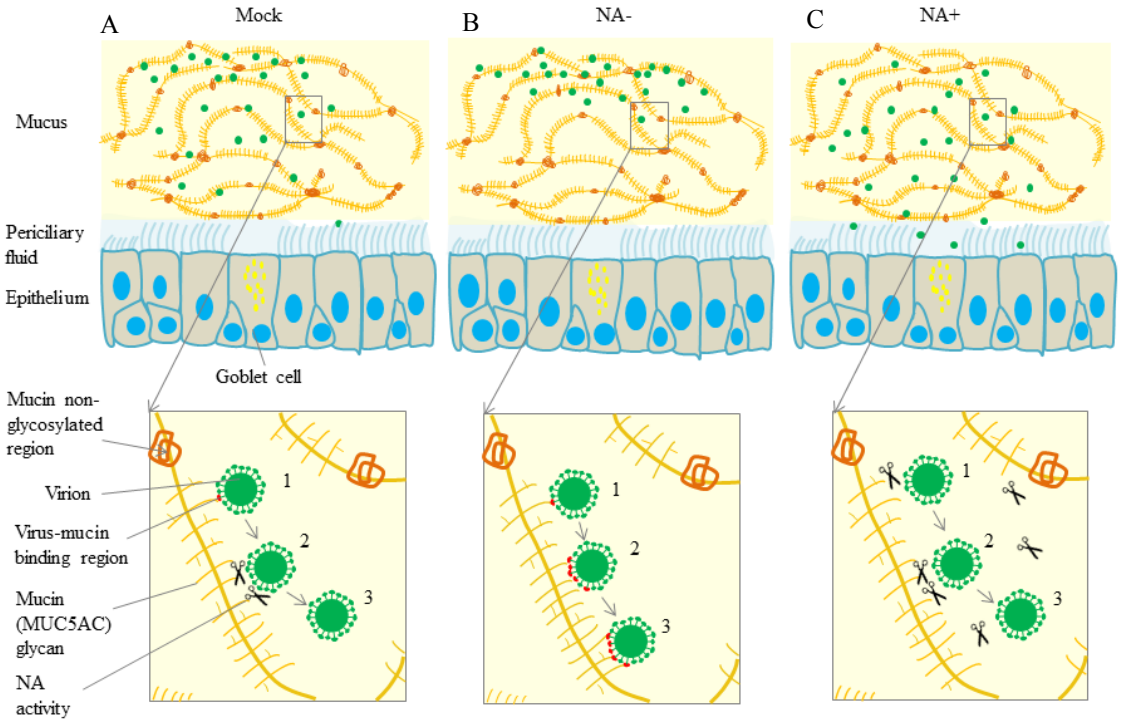

Figure 2. Schematic interactions of SIV with porcine respiratory mucus and the effect of NA. SIV quickly enters after encountering the respiratory mucus due to passive concentration-dependent diffusion. (A) SIV is partially diffusive, with particles being immobilized or moving variably. Some particles remain immobilized in mucus, and some have overcome the mucus layer and are approaching to the target epithelial cells. Interactions of a SIV virion with mucins may occur as follows: (1) the virion encounters and quickly binds to a mucin glycan, probably via SA; (2) NA functions to cleave the SA linkage; (3) the virion is released from the mucin glycan. (B) In the presence of NA inhibitor, SIV is mostly trapped in mucus, which may occur in the following process: (1) the virion meets with and quickly binds to a mucin glycan via SA; (2) the binding becomes more tightly by involving more virus-mucin interactions; (3) no NA functioning, hence the virion remained attached to the mucins. (C) In the presence exogenous NA, the SIV penetration increases, with more virions penetrating further into the mucus layer. More virions may have overcome the mucus layer and are approaching to the target cells. The interactions may occur as follows: the virion meets with a mucin glycan, but does not bind to it because the SA has been cleaved by the exogenous NA; (2) the virion avoids attaching to mucin glycans; (3) the virion moves freely.

5.2. Binding of PrV and SIV to porcine respiratory mucus

Immobilization of virus in mucus may be the result of virus binding to specific component(s) of mucus. Both PrV and SIV were indeed found to bind to the mucus cryosections (**Chapter 3.3** and **Chapter 4**). Mucins, the major component of mucus, may play a crucial role in this reaction.

It was demonstrated in this thesis that mucin glycans seem to bind PrV, thereby entrapping the virus in the porcine respiratory mucus. It is known for PrV that the virions bind to heparan sulfate via glycoprotein C (gC) for viral attachment, which is followed by a stable interaction between gD and its cellular receptor (Spear *et al.*, 2000; Trybala *et al.*, 1998). Up till now, heparan sulphate, nectin-1, nectin-2 and CD155 were described as receptors for PrV (Campadelli-Fiume *et al.*, 2000; Nixdorf *et al.*, 1999; Spear *et al.*, 2000; Spear & Longnecker, 2003). These PrV receptors, except the secretory heparan sulphate (Emery *et al.*, 1995), have not been identified in the airway secretions. However, we were not able to correlate the immobilization of PrV in the pig mucus to virus-heparan sulphate interaction by using anti-PrV antibodies (**Chapter 3.1**). Therefore, we hypothesize that PrV may not bind to mucus via virus-receptor interactions. Instead, we assume that mucins could play an important role in adhering PrV via their sticky glycans (**Fig. 1B**). The inverse correlation between the presence of the dominant respiratory mucin, MUC5AC, and PrV infection in both tracheal explant and primary epithelial cells may support this assumption (**Chapter 3.2**). Furthermore, O-glycans seem to mediate the inhibitory activity of mucin, as removing the glycans elevated the infection of PrV in the MUC5AC-producing cells (**Chapter 3.2**). Our finding is in concert with some other studies which describe that O-glycosylated oligosaccharides present in human milk can block the binding and infection of viruses to epithelial cells (Etzold & Bode, 2014; Morrow *et al.*, 2005; Ruiz-Palacios *et al.*, 2003). In summary, mucin O-glycans possess antiviral activity that is related to a direct block of viral infection, providing an indication to a novel antiviral strategy.

Binding of SIV to the respiratory mucins seemed to be more evident compared to PrV. SA, the well-known receptor for influenza virus, comprises most of the termini of mucin side chain glycans (Thornton *et al.*, 2008). Fluorescence lectin staining on mucus cryosections showed that an abundant amount of SAs were present in the porcine respiratory mucus (mucins) (**Chapter 4**). The binding profile of SIV strain was not investigated in this study. However, it has been well documented that SIV

isolates, especially those with the avian-like H1 and H3 hemagglutinins can bind both a2,3- and a2,6-sialylated glycans without distinct preference (Bradley *et al.*, 2011; Chen *et al.*, 2011; Gambaryan *et al.*, 2005). The porcine respiratory mucins, which contain both α2,3- and α2,6-linked SAs, provide sufficient receptors for SIV to attach. Binding of SIV via HA to the mucins was firmly proved in this thesis, because the amount of viral or exogenous NA indeed modulated the extent of viral binding to and releasing from the porcine mucus (**Chapter 4**). Taken together, mucins are responsible for the major adhesive effects of the respiratory mucus. In accordance with our findings, isolated human salivary mucins have also been suggested to directly interact with HIV-1 (Bergey *et al.*, 1994; Habte *et al.*, 2006) and to reduce HSV-1 infectivity at the early stage of infection (adsorption and penetration) (Bergey *et al.*, 1993). In addition, purified gastric mucins have been described to inhibit the infectivity of various types of viruses, including human papillomavirus (HPV), Merkel cell polyomavirus (MCV), and influenza A virus (Lieleg *et al.*, 2012).

Mucin glycans also bind a variety of bacteria and parasites. It is well documented that *Staphylococcus aureus,* a frequently occurring community- as well as hospital-acquired pathogen, binds to several types of mucins, including bovine submaxillary mucin (Sanford *et al.*, 1989; Thomas *et al.*, 1993), salivary mucin (Biesbrock *et al.*, 1991) and human nasal mucin (Shuter *et al.*, 1996). In addition, *Lactobacillus reuteri* binds to mucin glycans via its mucin-binding protein, MUB (Mackenzie *et al.*, 2010). *Tritrichomonas foetus*, a potent veterinary pathogen, and *Entamoeba histolytica*, predominantly infecting humans and other primates, are both found to express a SA-specific lectin, which enables them to attach to colonic mucins (Chadee *et al.*, 1987; Hicks *et al.*, 2000). This lectin-mediated binding to mucus is one of the initial steps in colonization. Unlike bacteria and parasites, which colonize upon binding to mucins (Lee *et al.*, 1986; Macfarlane *et al.*, 2005; Tse & Chadee, 1991), viruses that are bound to the respiratory mucins may be cleared by mucociliary beating and enventually inactivated in the stomach.

In addition to mucins, a great number of host defense molecules including defensins,

lactoferrin, secretory IgA (sIgA), collectins, cathelicidins, histatins and surfactant proteins (Schicht *et al.*, 2013; Tjabringa *et al.*, 2005; Vareille *et al.*, 2011) are present in the airway secretions. Surfactant proteins D (SP-D) is a C-type lectin (collectin) found in the airway secretions of the pig. It is well documented that both purified and recombinant porcine SP-D possess antiviral activities against influenza A viruses (Hartshorn *et al.*, 1994; Hillaire *et al.*, 2013; LeVine *et al.*, 2001). In addition, defensins have been shown to bind several viruses, including influenza virus and HSV, and to inhibit the entry of these viruses into target cells (Daher *et al.*, 1986; Doss *et al.*, 2009; Hazrati *et al.*, 2006). Secretory IgA, which is retained at high concentrations in mucus, can efficiently trap diverse pathogens (Jacquot *et al.*, 1992). Lastly, the syndecan family of proteoglycans can be produced by ectodomain shedding of the epithelial cells (Fitzgerald *et al.*, 2000; Ramani *et al.*, 2012). Thus, it may be abundantly present in the respiratory mucus. These molecules may function by binding the virions in a receptor-independent pattern. They may be retained in mucus by direct binding to mucins or by the biophysical retard of mucus, resulting in inactivation and/or indirect entrapment of virus in the mucus barrier.

5.3. Different mechanisms for mucus invasion of PrV and SIV

Most viruses initiate their infection at the mucosal surface of the respiratory tract, gastrointestinal tract, eye and/or cervical vagina which are coated with mucus (McChlery *et al.*, 2009; Moon & Stappenbeck, 2012; Newman & Gooding, 2013; Slots, 2009; Steukers *et al.*, 2012). Different viruses may have evolved different mechanisms to overcome the mucus barrier.

Influenza virus binds via hemagglutinin to SA to initiate its entry into a host cell. After assembly, the newly formed virions need to be released from the cell surface, which is mediated by neuraminidase. Neuraminidase cleaves the linkage between SA and the penultimate galactose, which is abundantly present in mucin glycans. Thus, it is assumed that neuraminidase functions to detach influenza virions from SA-containing mucin glycans. SIV was demonstrated in **Chapter 4** to utilize this

enzymatic strategy to get through the mucus layer. We found that 30% of SIV particles were diffusing freely in the porcine respiratory mucus as determined by single particle tracking. In addition, there was a fraction of viral particles that actively penetrated the respiratory mucus, as shown by the virus in-capsule-mucus penetration system. This movement of SIV particles was found to be mediated by the effects of neuraminidase, as the virus mobility was suppressed by the use of a neuraminidase inhibitor, whereas the movement was increased when exogenous neuraminidase was added (Fig. 2B and C). These findings suggest that neuraminidase helped to release the SIV particles which may have been bound to mucins, and rendered the virions to move through the mucus, resulting in traversal penetration through the mucus layer. A similar strategy is also employed by a great number of microbes, such as *Entamoeba histolytica* (Frederick & Petri, 2005; Leitch *et al.*, 1988), *Vibrio cholerae* (Silva *et al.*, 2003), *Helicobacter pylori* (Celli *et al.*, 2009), reovirus (Bisaillon *et al.*, 1999) and coronavirus (Schwegmann-Wessels & Herrler, 2006). These mibrobes produce several kinds of enzymes, such as mucinase, sialidase, glycosidase, elastase, and hydrolase, which are able to degrade mucin core proteins or mucin carbohydrates, facilitating microbes to pave their way through the mucus layer.

Unlike SIV, PrV was highly stuck in mucus. It seems to have difficulties in crossing the mucus barrier. Hence, the invasion of the virus may depend on defects or physiological changes of the mucus. We hypothesize that PrV was not able to penetrate through porcine respiratory mucus at body temperature (37 ^{o}C), while at 4 ^{o}C, the virus moved more easily through the mucus (Fig. 1). Consistently, the number of virions attached to mucus increased with rise of temperature. This was further confirmed by using tracheal explant models, for which we found that the percentage of PrV which overcomes the mucus barrier and eventually causes infection in the epithelium was higher at 4 ^{o}C than that at 37 ^{o}C (**Chapter 3.3**). We therefore suggest that PrV may benefit from low temperature regarding its penetration through the porcine respiratory mucus. To be specific, PrV interacts with mucus, especially mucins, with weak bonding. The weak affinity interactions may be thermo-dependent,

thus be reduced with decline of temperature. A similar reasoning was made to the beneficial role of low temperature in influenza virus transmission in ferrets (Lowen *et al.*, 2007). Hence, this effect may be general for the invasion of viruses, and contribute to the relationship between cold temperature and higher incidence of respiratory viral infections. In addition, pH appears also to be crucial in maintaining the physiological functions of mucus. Alterations of it may cause mucus deficiencies. For instance, HSV and HIV are only able to penetrate the cervicovaginal mucus at a pH that is increased from acid to neutral by bacterial vaginosis (Ensign *et al.*, 2014; Lai *et al.*, 2009).

Compared to PrV, SIV seems to have evolved more sophisticated mechanisms to invade the respiratory tract. This may be related to the restricted epithelial infection of influenza virus. SIV hits and runs in a very short time and its skills to cross the mucus in a very efficient way and spread in the air fully fit in this concept. In contrast with SIV which exclusively infects the epithelial cells, PrV crosses rapidly the basement membrane upon primary infection and infects all sorts of cells in the underlying tissue in a very cell-associated way for 10-14 days and finally disseminates through the whole body (Nauwynck *et al.*, 2007; Nauwynck, 1997). PrV is spreading from cell-to-cell without using the apical extracellular route, where it may risk being trapped in the respiratory mucus.

Another mechanism, although not examined in this thesis, may be applied to small and capsid viruses to get through the mucus. Human papilloma virus (55 nm) and Norwalk virus (38 nm) (Olmsted *et al.*, 2001) have been found to belong to this category. These capsid viruses may have developed a strategy to penetrate mucus by being small in size, neutral in net surface charge, and/or coated densely with equal amounts of positively and negatively charged moieties. Densely coated with equal densities of positive and negative charges, capsid viruses expose no or few hydrophobic patches on the surface, an adhesion-preventing mechanism present on the surface of most soluble proteins (Wada & Nakamura, 1981). Furthermore, surfaces densely coated with net neutral surface charge will neither be repelled nor

attracted to the negatively charged glycan domains of mucins.

Lastly, the view of the mucus as a continuous layer that moves in bulk may not be correct for all areas of the respiratory tract. Our hypothesis is that mucus may form a discontinuous layer with dynamic attachments to the surface. For instance, a scanning electron micrograph of mucus on the surface of a trachea was described as forming "rafts" and "strands" (Rogers, 2007). Another recent study using three-dimensional cell culture demonstrated that mucus can form discontinuous layers with temporary attachments to the epithelial surface (Sears *et al.*, 2011). This is due to the fact that the mucus does not flow evenly but preferentially concentrates along troughs or grooves (Agarwal *et al.*, 1994). These observations indicate that there are some epithelial regions that are coated with thin or no mucus at all and these areas may be more susceptible to virus invasion.

In summary, we set up two models, virus particle tracking and a virus in-capsule-mucus penetration system, and tracked the movement of PrV and SIV in porcine respiratory mucus. We found that they behaved differently in mucus and this difference was due to neuraminidase activity in influenza virus. Finally, we propose several mechanisms for different respiratory viruses invading the airway mucus.

i) Producing enzymes enabling the virions to avoid from attaching to decoy receptors.

ii) Viruses, especially the large, enveloped viruses, which lack enzymatic functions, may have evolved to get through the mucus layer depending on the defects, physiological changes and/or discontinuous property of mucus.

iii) By being small and neutral in the surface charge, virus may avoid adhesive interactions with mucins.

5.4. Reference

Agarwal, M., King, M. & Shukla, J. B. (1994). Mucous gel transport in a simulated cough machine: effects of longitudinal grooves representing spacings between arrays of cilia. *Biorheology* **31**, 11-19.

Bergey, E. J., Cho, M. I., Blumberg, B. M., Hammarskjold, M. L., Rekosh, D., Epstein, L. G. & Levine, M. J. (1994). Interaction of HIV-1 and human salivary mucins. *J Acquir Immune*

Defic Syndr **7**, 995-1002.

Bergey, E. J., Gu, M., Collins, A. R., Bradway, S. D. & Levine, M. J. (1993). Modulation of herpes simplex virus type 1 replication by human salivary secretions. *Oral Microbiol Immunol* **8**, 89-93.

Biesbrock, A. R., Reddy, M. S. & Levine, M. J. (1991). Interaction of a salivary mucin-secretory immunoglobulin A complex with mucosal pathogens. *Infect Immun* **59**, 3492-3497.

Bisaillon, M., Senechal, S., Bernier, L. & Lemay, G. (1999). A glycosyl hydrolase activity of mammalian reovirus sigma1 protein can contribute to viral infection through a mucus layer. *J Mol Biol* **286**, 759-773.

Bradley, K. C., Jones, C. A., Tompkins, S. M., Tripp, R. A., Russell, R. J., Gramer, M. R., Heimburg-Molinaro, J., Smith, D. F., Cummings, R. D. & Steinhauer, D. A. (2011). Comparison of the receptor binding properties of contemporary swine isolates and early human pandemic H1N1 isolates (Novel 2009 H1N1). *Virology* **413**, 169-182.

Braeckmans K, V. D., Demeester J, De Smedt SC (2010). Single particle tracking. In: Diaspro A, editor. Nanoscopy multidimensional optical fluorescence microscopy. *Sci-Tech News* **64**, 92-92.

Campadelli-Fiume, G., Cocchi, F., Menotti, L. & Lopez, M. (2000). The novel receptors that mediate the entry of herpes simplex viruses and animal alphaherpesviruses into cells. *Reviews in Medical Virology* **10**, 305-319.

Celli, J. P., Turner, B. S., Afdhal, N. H., Keates, S., Ghiran, I., Kelly, C. P., Ewoldt, R. H., McKinley, G. H., So, P., Erramilli, S. & Bansil, R. (2009). Helicobacter pylori moves through mucus by reducing mucin viscoelasticity. *Proc Natl Acad Sci U S A* **106**, 14321-14326.

Chadee, K., Petri, W. A., Jr., Innes, D. J. & Ravdin, J. I. (1987). Rat and human colonic mucins bind to and inhibit adherence lectin of Entamoeba histolytica. *J Clin Invest* **80**, 1245-1254.

Chen, L. M., Rivailler, P., Hossain, J., Carney, P., Balish, A., Perry, I., Davis, C. T., Garten, R., Shu, B., Xu, X., Klimov, A., Paulson, J. C., Cox, N. J., Swenson, S., Stevens, J., Vincent, A., Gramer, M. & Donis, R. O. (2011). Receptor specificity of subtype H1 influenza A viruses isolated from swine and humans in the United States. *Virology* **412**, 401-410.

Daher, K. A., Selsted, M. E. & Lehrer, R. I. (1986). Direct inactivation of viruses by human granulocyte defensins. *J Virol* **60**, 1068-1074.

Doss, M., White, M. R., Tecle, T., Gantz, D., Crouch, E. C., Jung, G., Ruchala, P., Waring, A. J., Lehrer, R. I. & Hartshorn, K. L. (2009). Interactions of alpha-, beta-, and theta-defensins with influenza A virus and surfactant protein D. *J Immunol* **182**, 7878-7887.

Emery, N., Place, G. A., Dodd, S., Lhermitte, M., David, G., Lamblin, G., Perini, J. M., Page, A. M., Hall, R. L. & Roussel, P. (1995). Mucous and serous secretions of human bronchial epithelial cells in secondary culture. *Am J Respir Cell Mol Biol* **12**, 130-141.

Ensign, L. M., Lai, S. K., Wang, Y. Y., Yang, M., Mert, O., Hanes, J. & Cone, R. (2014). Pretreatment of Human Cervicovaginal Mucus with Pluronic F127 Enhances Nanoparticle Penetration without Compromising Mucus Barrier Properties to Herpes Simplex Virus. *Biomacromolecules* **15**, 4403-4409.

Etzold, S. & Bode, L. (2014). Glycan-dependent viral infection in infants and the role of human milk oligosaccharides. *Curr Opin Virol* **7**, 101-107.

Fitzgerald, M. L., Wang, Z., Park, P. W., Murphy, G. & Bernfield, M. (2000). Shedding of

syndecan-1 and -4 ectodomains is regulated by multiple signaling pathways and mediated by a TIMP-3-sensitive metalloproteinase. *J Cell Biol* **148**, 811-824.

Frederick, J. R. & Petri, W. A., Jr. (2005). Roles for the galactose-/N-acetylgalactosamine-binding lectin of Entamoeba in parasite virulence and differentiation. *Glycobiology* **15**, 53R-59R.

Gambaryan, A. S., Karasin, A. I., Tuzikov, A. B., Chinarev, A. A., Pazynina, G. V., Bovin, N. V., Matrosovich, M. N., Olsen, C. W. & Klimov, A. I. (2005). Receptor-binding properties of swine influenza viruses isolated and propagated in MDCK cells. *Virus Res* **114**, 15-22.

Glorieux, S., Favoreel, H. W., Meesen, G., de Vos, W., Van den Broeck, W. & Nauwynck, H. J. (2009). Different replication characteristics of historical pseudorabies virus strains in porcine respiratory nasal mucosa explants. *Vet Microbiol* **136**, 341-346.

Glorieux, S., Van den Broeck, W., van der Meulen, K. M., Van Reeth, K., Favoreel, H. W. & Nauwynck, H. J. (2007). In vitro culture of porcine respiratory nasal mucosa explants for studying the interaction of porcine viruses with the respiratory tract. *J Virol Methods* **142**, 105-112.

Habte, H. H., Mall, A. S., de Beer, C., Lotz, Z. E. & Kahn, D. (2006). The role of crude human saliva and purified salivary MUC5B and MUC7 mucins in the inhibition of Human Immunodeficiency Virus type 1 in an inhibition assay. *Virol J* **3**, 99.

Hartshorn, K. L., Crouch, E. C., White, M. R., Eggleton, P., Tauber, A. I., Chang, D. & Sastry, K. (1994). Evidence for a protective role of pulmonary surfactant protein D (SP-D) against influenza A viruses. *J Clin Invest* **94**, 311-319.

Hazrati, E., Galen, B., Lu, W., Wang, W., Ouyang, Y., Keller, M. J., Lehrer, R. I. & Herold, B. C. (2006). Human alpha- and beta-defensins block multiple steps in herpes simplex virus infection. *J Immunol* **177**, 8658-8666.

Heinen, P. P., van Nieuwstadt, A. P., Pol, J. M., de Boer-Luijtze, E. A., van Oirschot, J. T. & Bianchi, A. T. (2000). Systemic and mucosal isotype-specific antibody responses in pigs to experimental influenza virus infection. *Viral Immunol* **13**, 237-247.

Hicks, S. J., Theodoropoulos, G., Carrington, S. D. & Corfield, A. P. (2000). The role of mucins in host-parasite interactions. Part I-protozoan parasites. *Parasitol Today* **16**, 476-481.

Hillaire, M. L., Haagsman, H. P., Osterhaus, A. D., Rimmelzwaan, G. F. & van Eijk, M. (2013). Pulmonary surfactant protein D in first-line innate defence against influenza A virus infections. *J Innate Immun* **5**, 197-208.

Jacquot, J., Hayem, A. & Galabert, C. (1992). Functions of proteins and lipids in airway secretions. *Eur Respir J* **5**, 343-358.

Kritas, S. K., Pensaert, M. B. & Mettenleiter, T. C. (1994). Invasion and spread of single glycoprotein deleted mutants of Aujeszky's disease virus (ADV) in the trigeminal nervous pathway of pigs after intranasal inoculation. *Vet Microbiol* **40**, 323-334.

Lai, S. K., Hida, K., Shukair, S., Wang, Y. Y., Figueiredo, A., Cone, R., Hope, T. J. & Hanes, J. (2009). Human immunodeficiency virus type 1 is trapped by acidic but not by neutralized human cervicovaginal mucus. *J Virol* **83**, 11196-11200.

Lee, A., O'Rourke, J. L., Barrington, P. J. & Trust, T. J. (1986). Mucus colonization as a determinant of pathogenicity in intestinal infection by Campylobacter jejuni: a mouse cecal model. *Infect Immun* **51**, 536-546.

Leitch, G. J., Harris-Hooker, S. A. & Udezulu, I. A. (1988). Movement of Entamoeba histolytica trophozoites in rat cecum and colon intact mucus blankets and harvested mucus gels. *Am J*

Trop Med Hyg **39**, 282-287.

LeVine, A. M., Whitsett, J. A., Hartshorn, K. L., Crouch, E. C. & Korfhagen, T. R. (2001). Surfactant protein D enhances clearance of influenza A virus from the lung in vivo. *J Immunol* **167**, 5868-5873.

Lieleg, O., Baumgartel, R. M. & Bausch, A. R. (2009). Selective filtering of particles by the extracellular matrix: an electrostatic bandpass. *Biophys J* **97**, 1569-1577.

Lieleg, O., Lieleg, C., Bloom, J., Buck, C. B. & Ribbeck, K. (2012). Mucin Biopolymers As Broad-Spectrum Antiviral Agents. *Biomacromolecules* **13**, 1724-1732.

Lowen, A. C., Mubareka, S., Steel, J. & Palese, P. (2007). Influenza virus transmission is dependent on relative humidity and temperature. *PLoS Pathog* **3**, 1470-1476.

Macfarlane, S., Woodmansey, E. J. & Macfarlane, G. T. (2005). Colonization of mucin by human intestinal bacteria and establishment of biofilm communities in a two-stage continuous culture system. *Appl Environ Microbiol* **71**, 7483-7492.

Mackenzie, D. A., Jeffers, F., Parker, M. L., Vibert-Vallet, A., Bongaerts, R. J., Roos, S., Walter, J. & Juge, N. (2010). Strain-specific diversity of mucus-binding proteins in the adhesion and aggregation properties of Lactobacillus reuteri. *Microbiology* **156**, 3368-3378.

Martinez-Lopez, B., Carpenter, T. E. & Sanchez-Vizcaino, J. M. (2009). Risk assessment and cost-effectiveness analysis of Aujeszky's disease virus introduction through breeding and fattening pig movements into Spain. *Prev Vet Med* **90**, 10-16.

McChlery, S., Ramage, G. & Bagg, J. (2009). Respiratory tract infections and pneumonia. *Periodontol 2000* **49**, 151-165.

Moon, C. & Stappenbeck, T. S. (2012). Viral interactions with the host and microbiota in the intestine. *Curr Opin Immunol* **24**, 405-410.

Morrow, A. L., Ruiz-Palacios, G. M., Jiang, X. & Newburg, D. S. (2005). Human-milk glycans that inhibit pathogen binding protect breast-feeding infants against infectious diarrhea. *J Nutr* **135**, 1304-1307.

Nauwynck, H., Glorieux, S., Favoreel, H. & Pensaert, M. (2007). Cell biological and molecular characteristics of pseudorabies virus infections in cell cultures and in pigs with emphasis on the respiratory tract. *Vet Res* **38**, 229-241.

Nauwynck, H. J. (1997). Functional aspects of Aujeszky's disease (pseudorabies) viral proteins with relation to invasion, virulence and immunogenicity. *Vet Microbiol* **55**, 3-11.

Newby, T. J., Carter, D. P., Yoon, K. J., Jackwood, M. W. & Hawkins, P. A. (2002). Assessment of replication and virulence of attenuated pseudorabies virus in swine. *J Vet Sci* **3**, 61-66.

Newman, H. & Gooding, C. (2013). Viral ocular manifestations: a broad overview. *Rev Med Virol* **23**, 281-294.

Nixdorf, R., Schmidt, J., Karger, A. & Mettenleiter, T. C. (1999). Infection of Chinese hamster ovary cells by pseudorabies virus. *J Virol* **73**, 8019-8026.

Olmsted, S. S., Padgett, J. L., Yudin, A. I., Whaley, K. J., Moench, T. R. & Cone, R. A. (2001). Diffusion of macromolecules and virus-like particles in human cervical mucus. *Biophys J* **81**, 1930-1937.

Ramani, V. C., Pruett, P. S., Thompson, C. A., DeLucas, L. D. & Sanderson, R. D. (2012). Heparan sulfate chains of syndecan-1 regulate ectodomain shedding. *J Biol Chem* **287**, 9952-9961.

Rogers, D. F. (2007). Physiology of airway mucus secretion and pathophysiology of hypersecretion. *Respir Care* **52**, 1134-1146; discussion 1146-1139.

Ruiz-Palacios, G. M., Cervantes, L. E., Ramos, P., Chavez-Munguia, B. & Newburg, D. S. (2003). Campylobacter jejuni binds intestinal H(O) antigen (Fuc alpha 1, 2Gal beta 1, 4GlcNAc), and fucosyloligosaccharides of human milk inhibit its binding and infection. *J Biol Chem* **278**, 14112-14120.

Sanford, B. A., Thomas, V. L. & Ramsay, M. A. (1989). Binding of staphylococci to mucus in vivo and in vitro. *Infect Immun* **57**, 3735-3742.

Schicht, M., Knipping, S., Hirt, R., Beileke, S., Sel, S., Paulsen, F. & Brauer, L. (2013). Detection of surfactant proteins A, B, C, and D in human nasal mucosa and their regulation in chronic rhinosinusitis with polyps. *Am J Rhinol Allergy* **27**, 24-29.

Schwegmann-Wessels, C. & Herrler, G. (2006). Sialic acids as receptor determinants for coronaviruses. *Glycoconj J* **23**, 51-58.

Sears, P. R., Davis, C. W., Chua, M. & Sheehan, J. K. (2011). Mucociliary interactions and mucus dynamics in ciliated human bronchial epithelial cell cultures. *Am J Physiol Lung Cell Mol Physiol* **301**, L181-186.

Shuter, J., Hatcher, V. B. & Lowy, F. D. (1996). Staphylococcus aureus binding to human nasal mucin. *Infect Immun* **64**, 310-318.

Silva, A. J., Pham, K. & Benitez, J. A. (2003). Haemagglutinin/protease expression and mucin gel penetration in El Tor biotype Vibrio cholerae. *Microbiology* **149**, 1883-1891.

Skehel, J. J. & Wiley, D. C. (2000). Receptor binding and membrane fusion in virus entry: the influenza hemagglutinin. *Annu Rev Biochem* **69**, 531-569.

Slots, J. (2009). Oral viral infections of adults. *Periodontol 2000* **49**, 60-86.

Spear, P. G., Eisenberg, R. J. & Cohen, G. H. (2000). Three classes of cell surface receptors for alphaherpesvirus entry. *Virology* **275**, 1-8.

Spear, P. G. & Longnecker, R. (2003). Herpesvirus entry: an update. *J Virol* **77**, 10179-10185.

Steukers, L., Glorieux, S., Vandekerckhove, A. P., Favoreel, H. W. & Nauwynck, H. J. (2012). Diverse microbial interactions with the basement membrane barrier. *Trends Microbiol* **20**, 147-155.

Stevens, J., Blixt, O., Tumpey, T. M., Taubenberger, J. K., Paulson, J. C. & Wilson, I. A. (2006). Structure and receptor specificity of the hemagglutinin from an H5N1 influenza virus. *Science* **312**, 404-410.

Thomas, V. L., Sanford, B. A. & Ramsay, M. A. (1993). Calcium- and mucin-binding proteins of staphylococci. *J Gen Microbiol* **139**, 623-629.

Thornton, D. J., Rousseau, K. & McGuckin, M. A. (2008). Structure and function of the polymeric mucins in airways mucus. *Annu Rev Physiol* **70**, 459-486.

Tjabringa, G. S., Vos, J. B., Olthuis, D., Ninaber, D. K., Rabe, K. F., Schalkwijk, J., Hiemstra, P. S. & Zeeuwen, P. L. (2005). Host defense effector molecules in mucosal secretions. *FEMS Immunol Med Microbiol* **45**, 151-158.

Trybala, E., Bergstrom, T., Spillmann, D., Svennerholm, B., Flynn, S. J. & Ryan, P. (1998). Interaction between pseudorabies virus and heparin/heparan sulfate. Pseudorabies virus mutants differ in their interaction with heparin/heparan sulfate when altered for specific glycoprotein C heparin-binding domain. *J Biol Chem* **273**, 5047-5052.

Tse, S. K. & Chadee, K. (1991). The interaction between intestinal mucus glycoproteins and enteric infections. *Parasitol Today* **7**, 163-172.

Turner, J. & Jones, C. E. (2009). Regulation of mucin expression in respiratory diseases. *Biochem*

Soc Trans **37**, 877-881.

Van Gucht, S., Atanasova, K., Barbe, F., Cox, E., Pensaert, M. & Van Reeth, K. (2006). Effect of porcine respiratory coronavirus infection on lipopolysaccharide recognition proteins and haptoglobin levels in the lungs. *Microbes Infect* **8**, 1492-1501.

Van Reeth, K. (2007). Avian and swine influenza viruses: our current understanding of the zoonotic risk. *Vet Res* **38**, 243-260.

Van Reeth, K., Labarque, G., Nauwynck, H. & Pensaert, M. (1999). Differential production of proinflammatory cytokines in the pig lung during different respiratory virus infections: correlations with pathogenicity. *Res Vet Sci* **67**, 47-52.

Vareille, M., Kieninger, E., Edwards, M. R. & Regamey, N. (2011). The airway epithelium: soldier in the fight against respiratory viruses. *Clin Microbiol Rev* **24**, 210-229.

Wada, A. & Nakamura, H. (1981). Nature of the Charge-Distribution in Proteins. *Nature* **293**, 757-758.

Chapter 6

6. Summary

Pseudorabies virus (PrV) and swine influenza virus (SIV), which both initiate infection in the respiratory mucosa, are two of the most important causative agents of pig respiratory disease. The viruses enter the respiratory tract, make contact with the mucosal surface and infect the epithelial cells. Before reaching the epithelium, the viruses need to overcome the mucus barrier, which outlines the respiratory mucosa. Crossing the mucus layer may be a crucial step for the mucosal invasion of PrV and SIV. Therefore, we aimed to study the interactions of PrV and SIV with porcine respiratory mucus, and to unravel the association between viral behavior in mucus and viral pathogenesis.

In **Chapter 1**, a brief introduction is given on the classification, the virion structure and the pathogenesis of PrV and SIV. The second part focused on the characteristics, composition of mucus and the interactions between different classes of pathogens and mucus.

In **Chapter 2**, the aims are given.

Chapter 3 describes the investigation of PrV-mucus interactions by the use of single particle tracking, a virus in-capsule-mucus penetration system, and explant models. We demonstrated that PrV has difficulties in crossing the mucus barrier, and the inhibition was attributed to mucins, especially MUC5AC. However, the mucus barrier could be overcome by PrV at low temperature (4 ^{o}C), which reflects the epidemiology of PrV and potentially other respiratory viruses.

In **Chapter 3.1**, we measured the barrier properties of porcine respiratory mucus, and investigated the mobility of PrV particles in mucus. First, the pore size of the porcine respiratory mucus was measured with atomic force microscopy as well as by fitting polyethylene glycol coupled (PEGylated) nanoparticles to the mucus. In addition, the mobility of PrV in porcine respiratory mucus was examined and compared with that of negatively charged, positively charged and PEGylated nanoparticles. We found that the pore size of the respiratory mucus ranged between 80 and 1500 nm, and the

majority of the pores were larger than the size of the virus. In contrast to the free diffusion of neutral PEGylated nanoparticles, PrV, which is negative in net surface charge, experienced a severe obstruction in the porcine respiratory mucus, with 96% of the viral particles being immobilized. Additionally, the highly negatively and positively charged nanoparticles were significantly trapped. Taken together, mobility of the particles was related to their surface charge. These findings indicate that the mobility of PrV was significantly hindered in porcine respiratory mucus, and that the obstruction of PrV was at least partly due to charge interactions rather than size exclusion.

In **Chapter 3.2**, we investigated the distribution of the major mucin types, MUC5AC and MUC5B, along the respiratory tract and the anti-PrV activity of MUC5AC. First, the expression of MUC5AC and MUC5B in the porcine respiratory mucosa, including nasal mucosa, trachea, bronchus and the lungs, was examined by double immunofluorescence staining. We found that both MUC5AC and MUC5B were widely expressed in the whole respiratory tract. MUC5AC was mainly expressed in the apical epithelium and the MUC5B expression was almost exclusively located in the submucosal glands. The content of MUC5AC on the apical epithelium was inversely related to the attachment and infection of PrV to/in porcine tracheal explant, suggesting a dominant role of MUC5AC in blocking PrV to reach the epithelium. Furthermore, the enhancement of PrV infection in MUC5AC-producing cells treated with O-glycosidase indicated that O-glycans may mediate the anti-PrV activity of mucins. In summary, we suggest that MUC5AC is the dominant mucin type in the porcine respiratory tract, and may serve as a major contributor to PrV entrapment via its O-glycans to the inhibitory effects of the airway mucus.

Since most clinical outbreaks of PrV infection occur during winter season, the effect of low temperature on interactions of PrV with porcine respiratory mucus was investigated in **Chapter 3.3**. First, the effect of temperature on the binding of PrV to porcine respiratory mucus was examined by confocal microscopy. Next to that, the penetration depth of PrV through the respiratory mucus was analyzed with the virus

in-capsule-mucus penetration system at different temperatures. Furthermore, the effect of temperature on the ability of PrV to overcome the mucus barrier was studied in a well-established respiratory mucosa explant system (*ex vivo*) as well as in a culture system, where virus was first incubated with pig mucus and mucin solution (*in vitro*) and afterwards brought on top of the susceptible cells. We found that less virions were bound to the respiratory mucus at low temperature, which is in line with the observation that viral particles penetrated further in the mucus at 4 ^{o}C, but not at 37 ^{o}C. Additionally, the mucus almost did not prevent the virus from binding to the tracheal apical epithelium at 4 ^{o}C, but blocked the viral attachment by 65% at 37 ^{o}C. Lastly, the percentage of PrV that overcame the mucus and caused infection in tracheal explants and cell cultures increased with decline of temperature. Altogether, these findings indicate a beneficial role of low temperature in helping PrV to thwart the porcine respiratory mucus, which may shed new light on the interactions between exposure to cold and high incidence of respiratory viral infections.

Chapter 4 demonstrated a crucial role of neuraminidase in helping the influenza virus to move through the respiratory mucus. Two techniques were applied to track SIV H1N1 in porcine mucus. The microscopic diffusion of SIV particles in the mucus was analyzed by single particle tracking, and the macroscopic penetration of SIV through mucus was studied with a virus in-capsule-mucus penetration system, followed by visualizing the translocation of the virions by immunofluorescence staining. Furthermore, the effects of neuraminidase on SIV getting through or binding to the mucus were studied by using zanamivir, a neuraminidase inhibitor, and *Arthrobacter ureafaciens* neuraminidase. Results showed that 70% of SIV particles were entrapped, while the rest diffused freely in the mucus. Additionally, SIV was able to penetrate the respiratory mucus with time, and travelled a distance of 65 μm at 30 min post virus addition. Both the microscopic diffusion and macroscopic penetration were enhanced by exogenous neuraminidase treatment, while they were in contrast diminished by the use of neuraminidase inhibitor. Moreover, the exogenous neuraminidase suppressed binding of SIV to mucus which was inversely enhanced by the addition of the

neuraminidase inhibitor. These findings demonstrated that the neuraminidase helps SIV to move through the mucus, which is important for the virus to reach and infect epithelial cells as well as to eventually become shed into the lumen of the respiratory tract.

Chapter 5 summarizes the overall results of this thesis and presents a general discussion regarding the different interactions of PrV and SIV with porcine respiratory mucus, and proposes possible strategies for both viruses to overcome the mucus. Both PrV and SIV were found with single particle tracking to be immobilized in the porcine respiratory mucus, though the extent of hindrance was different. PrV experienced a significant obstruction in porcine tracheal respiratory mucus, with approximately 96% of the viral particles being entrapped. Seventy percent of the neuraminidase-producing SIV was entrapped in the mucus. Mucins, especially MUC5AC, were responsible for the entrapment of PrV in the respiratory mucus, as shown by binding of the virions to mucus cryosections and the inverse relation between MUC5AC content and PrV release. Thus, the virus likely depends on mucus defects, which for example may be caused by low temperature to invade the mucus barrier. On the other hand, SIV has evolved to produce neuraminidase which is able to release the SIV particles which may be bound to mucins, thereby enabling the virus to move through the respiratory mucus. The in-depth investigation of mucus invasion of these viruses may provide novel insights into the study of prophylactic treatment of swine influenza, Aujeszky's disease and other related and perhaps unrelated viruses.

Samenvatting

Pseudorabies virus (PrV) en swine influenza virus (SIV), welke allebei de bovenste luchtwegen van varkens infecteren, zijn twee van de meest belangrijke oorzaken van ademhalingsstoornissen bij varkens. De virussen worden geïnhaleerd, maken contact met de mucosa en infecteren vervolgens epitheelcellen. Vooraleer ze tot bij deze epitheelcellen geraken, moeten ze echter de overliggende mucusbarrière overwinnen. Aangezien dit een cruciale stap kan zijn in de mucosale invasie van PrV en SIV, was de doelstelling in deze thesis om de interactie van beide virussen met respiratoire mucus te bestuderen. Op deze manier konden we eveneens mogelije verbanden leggen tussen de gedragingen van het virus in de mucus en hun pathogenese achterhalen.

In **Hoofdstuk 1** werd er eerst een korte introductie gegeven over de classificatie, structuur en pathogenese van PrV en SIV. In het tweede deel ligt de focus op de karakteristieken en samenstelling van mucus. Bijkomend worden ook de interacties tussen verschillende soorten pathogenen en mucus besproken.

In **Hoofdstuk 2** worden de algemene doelstellingen van het onderzoek uiteengezet.

Hoofdstuk 3 beschrijft het onderzoek van PrV-mucus interacties door gebruik te maken van *single particle tracking*, het virus-in-capsule-mucus penetratie systeem en explantmodellen. We hebben aangetoond dat dit virus moeite had om de mucusbarrière te doorbreken. Mucines, waaronder vooral MUC5AC, droegen bij tot deze inhibitie. De mucusbarrière kon echter wel overwonnen worden bij een lage temperatuur (4 °C), wat overeenkomt met de epidemiologie van PrV en mogelijks andere respiratoire virussen.

In **Hoofdstuk 3.1** hebben we naast de eigenschappen van porciene respiratoire mucus, ook de mobiliteit van PrV in deze mucus onderzocht. Eerst werd de poriegrootte van de mucus gemeten met "*atomic force*" microscopie en met het inbrengen van polyethyleen glycol gekoppelde (*PEGylated*) nanopartikels in de mucus. Bijkomend werd de beweging van PrV in porciene respiratoire mucus onderzocht en vergeleken

met die van negatief geladen, positief geladen en *PEGylated* nanopartikels. We hebben aangetoond dat de poriegrootte van deze mucus varieert tussen 80 en 1500 nm en dat de meerderheid van deze poriën dus groter zijn dan de grootte van het virus. In tegenstelling tot neutrale *PEGylated* nanopartikels, welke vrij in de mucus konden bewegen, werden de negatief geladen PrV partikels tegengehouden in de mucus. Ongeveer 96% van de viruspartikels werd hierin immers geïmmobiliseerd. De negatief en positief geladen nanopartikels werden eveneens gecapteerd in de mucus. Hieruit besloten we dat de mobiliteit van partikels afhangt van hun oppervlaktelading. Deze bevindingen suggereren dat de obstructie van PrV in porciene respiratoire mucus vooral veroorzaakt wordt door ladinginteracties en niet zozeer door hun grootte.

In **Hoofdstuk 3.2** werd enerzijds de distributie van de belangrijkste mucines (MUC5AC en MUC5B) in het ademhalingssysteem en anderzijds het antiviraal effect van MUC5AC op PrV onderzocht. Eerst werd de expressie van MUC5AC en MUC5B d.m.v. fluorescentiekleuringen onderzocht in de verschillende delen van het ademhalingsstelsel, nl. de nasale mucosa, de trachea, de bronchiën en de longen. Mucines bleken omnipresent te zijn in het porcien ademhalingssysteem, alhoewel de verdeling type-afhankelijk is. Zo komt MUC5AC sterk tot expressie in het apicaal epitheel en is MUC5B voornamelijk aanwezig in de submucosale klieren. Daarnaast werd in het porcien explantsysteem een omgekeerd evenredig verband vastgesteld tussen de graad van PrV-infectie en de expressie van MUC5AC. Dit suggereert dat MUC5AC een blokkerende rol speelt in het bereiken van en aanhechten van PrV aan het epitheel. Meer specifiek werd, door gebruik van O-glycosidase, aangetoond dat deze obstructie door MUC5AC te wijten is aan O-gelinkte glycanen. Er werd dus aangetoond door MUC5AC het dominante type van mucines is in het porcien ademhalingsstelsel en dat O-gelinkte glycanen een belangrijke rol spelen in het inhiberend effect van mucus op PrV infectie.

Aangezien de meeste klinische uitbraken van PrV zich voordoen in de winter, werd in **Hoofdstuk 3.3** de interactie van PrV met de porciene respiratoire mucus bij een lage temperatuur onderzocht. Initieel werd er met behulp van confocale microscopie het effect van de temperatuur op de binding van PrV aan de porciene respiratoire mucus onderzocht. Vervolgens werd de penetratiediepte van PrV t.h.v. de respiratoire mucus op verschillende temperaturen geanalyseerd met het virus-in-capsule-mucus penetratie systeem. De interactie tussen PrV, temperatuur en migratie efficiëntie doorheen de mucus werd onderzocht met zowel het respiratoir mucosa explant systeem (*ex vivo*) als in een *in vitro* cultuursysteem. In dit *in vitro* systeem werd het virus eerst geïncubeerd met varkensmucus en een mucine oplossing of vervolgens werd het aangebracht op gevoelige cellen.

Hierbij werd waargenomen dat bij een lage temperatuur minder viruspartikels binden aan de respiratoire mucus. Dit komt overeen met de observatie dat viruspartikels dieper in de mucus penetreren bij 4 °C, dan bij 37 °C. Bovendien verhinderde de mucus niet dat het virus bindt aan het tracheale apicale epitheel bij 4 °C, terwijl bij 37 ^{o}C de aanhechting van 65% van de virions geblokkeerd werd.

Tot slot werd in de tracheale explanten en celculturen waargenomen dat het percentage van PrV-virions dat de mucus overwon en infectie veroorzaakte, toenam bij een dalende temperatuur.

Deze resultaten wijzen erop dat de lage temperatuur PrV helpt om de respiratoire mucus te overwinnen. Dit geeft nieuwe inzichten in de interacties tussen koude temperaturen en de hogere incidentie van respiratoire virale infecties.

In **Hoofstuk 4** werd er dieper ingegaan op de cruciale helpende rol van neuraminidase bij het migreren van het influenzavirus doorheen de respiratoire mucus. Twee technieken werden toegepast om SIV H1N1 te lokaliseren in de porciene mucus.

De diffusie van SIV-partikels werd microscopisch geanalyseerd met ‘single particle tracking’ en de microscopische penetratie van SIV doorheen de mucus werd geanalyseerd met een virus-in-capsule-mucus penetratie systeem, gevolgd door het visualiseren van de viriontranslocatie met immunofluorescentiekleuring. Vervolgens

werd het effect van neuraminidase op de SIV-binding en translocatie doorheen de mucus bestudeerd met zanamivir, een neuraminidase-inhibitor, en *Arthrobacter ureafaciens* neuraminidase. Hierbij werd 70% van de SIV-partikels gevangen in de mucus, terwijl het overige percentage zich vrij in de mucus bevond. Bovendien was SIV, mits de nodige tijd, in staat de respiratoire mucus te penetreren en een afstand van 65 µm af te leggen binnen de 30 minuten nadat het virus was toegevoegd. Zowel de microscopische diffusie als de macroscopische penetratie verhoogden door het behandelen met een exogeen neuraminidase, terwijl ze afnamen na behandeling met een neuraminidase inhibitor. Bovendien verhinderde het exogene neuraminidase de binding van SIV aan de mucus, terwijl de neuraminidase inhibitor deze binding bevorderde. Deze resultaten tonen dat het neuraminidase SIV helpt doorheen de mucus te migreren, wat belangrijk is voor het virus om de epitheelcellen te bereiken en te infecteren, om uiteindelijk uitgescheiden te worden in het lumen van de luchtwegen.

In **Hoofdstuk 5** worden alle resultaten, bekomen in deze thesis op een rijtje gezet en besproken. De interacties van PrV en SIV met mucus worden hierbij vergeleken en verscheidene hypotheses werden opgesteld om het effect van mucus op het virus te omzeilen. Zowel PrV als SIV worden sterk geremd in hun migratie doorheen de mucus, de grootte-orde van dit effect was echter virus-afhankelijk. Zo wordt PrV bijna volledig geblokkeerd in de tracheale mucus, daar 96% van de PrV viruspartikels geïmmobiliseerd raken. Voor SIV bleek dit slechts voor 70% van de viruspartikels op te gaan. De mucines, en meer specifiek MUC5AC, zijn verantwoordelijk voor het inhiberen van de migratie van viruspartikels door de mucus. Dit werd enerzijds aangetoond door de rechtstreekse binding van viruspartikels aan mucus en anderzijds door het omgekeerd evenredig verband tussen MUC5AC-expressie en PrV-infectie. Hieruit kunnen we concluderen dat het virus afhankelijk is van onregelmatigheden in de mucus, deze kunnen o.a. veroorzaakt worden door lagere temperaturen. In tegenstelling tot PrV, heeft SIV een mechanisme ontwikkeld om zijn virion opnieuw los te maken van de mucines. SIV produceert namelijk neuraminidase, dat in staat is

de binding tussen viruspartikel en mucines te verbreken, waardoor het virus zich kan voortbewegen door de mucus. Dit onderzoek naar invasie van virussen doorheen de mucus kan nieuwe inzichten opleveren voor de ontwikkeling van profylactische behandelingen voor zowel varkensgriep als de ziekte van Aujeszky en mogelijks andere (verwante) virussen.

7. Curriculum vitae

Xiaoyun Yang was born in 1983, in Guangxi Province, China.

In 2002, she was admitted to Northwest Agriculture and Forestry University in China and studied Biological Science for her bachelor's degree. After graduation in 2006, she was enrolled as a master student in Northwest Agriculture and Forestry University, where she was involved in two projects on recombinant vaccine development and cell line establishment in the Laboratory of Epidemic Disease Prevention and Control. In 2010, she was admitted to Ghent University, and undertook a project on mucosal invasion of respiratory viruses with an emphasis on interactions of alphaherpesviruses and influenza viruses with porcine respiratory mucus. She has mainly focused on whether and how the respiratory viruses penetrate through the mucus barrier. During her Ph.D. study, she published two papers as first-author and two papers as a co-author in peer reviewed journals, and her results were presented in several international conferences.

Publications

- Yang X, Steukers L, Forier K, Xiong R, Braeckmans K, Van Reeth K, Nauwynck HJ. A beneficiary role for neuraminidase in influenza virus penetration through the respiratory mucus. PLoS ONE. 2014 Oct 15. [Epub ahead of print]. .
- Steukers L, Weyers S, Yang X, Vandekerckhove AP, Glorieux S, Cornelissen M, Van den Broeck W, Temmerman M, Nauwynck HJ. Mimicking herpes simplex virus 1 and herpes simplex virus 2 mucosal behavior in a well characterized human genital organ culture. J Infect Dis. 2014, 210(2):209-13.
- Yang X, Forier K, Steukers L, Van Vlierberghe S, Dubruel P, et al. (2012) Immobilization of Pseudorabies Virus in Porcine Tracheal Respiratory Mucus Revealed by Single Particle Tracking. PLoS ONE 7(12): e51054.
- Glorieux S, Vandekerckhove AP, Goris N, Yang X, Steukers L, Van de Walle GR, Croubels S, Neyts J, Nauwynck HJ. Evaluation of the antiviral activity of (1'S,2'R)-9-[[1',2'-bis(hydroxymethyl)cycloprop-1'-yl]methyl]guanine(A-5021) against equine herpesvirus type 1 in cell monolayers and equine nasal mucosal explants. Antiviral Res. 2012, 93(2):234-8.
- He Lei, Zhang Yanming, Xiang Hua, Tang Qinghai, Xu Yanzhao, Yang Xiaoyun, Wang Jing and Dai Chen. Construction and Immunoenhancement of a Recombinant Adenoviruses Encoding Porcine Interleukin 2. Acta Agriculturae Boreali-occidentalis Sinica, 2010, 19(11) :1-7. (Chinese)
- Wang Jing, Zhang Yanming, Tong Gang, Liu Fangning, Zhou Hongchao, He Lei, Yang Xiaoyun, Xu Yanzhao, Hong Haixia. The isolation and identification of neonatal swine intestinal epithelial cells. Acta Veterinaria Et Zootechnica Sinica. 2010, 41 (1): 92-98. (Chinese)
- He Lei, Zhang Yanming, Xu Yanzhao, Tang Qinghai, Wang Jing, Yang Xiaoyun, Dai Chen, Xiang Hua. Construction and Immunogenicity of a Recombinant Adenovirus Co-expressing the E2 Protein of Classical Swine Fever Virus and the Porcine Interleukin 2 in Rabbits. Chinese Journal of Virology, 2010, 26(5):385-391. (Chinese)

- Sun Pei, Yang Xiaoyun, Yanming Zhang, Guo Kangkang, Dang Ruyi. Research of isolation and culture of porcine tracheal epithelial cells [J]. Acta Veterinaria Et Zootechnica Sinica, 2008, 39(6): 56-64 (Chinese)
- Xu Hao, Hong Haixia, Guo Kangkang, Deng Xiaomin, Ye Guisheng, Yang Xiaoyun, Zhang Yanming. Cytopathic Effect of Classical Swine Fever Virus NS3 Protein on PK-15 Cells [J]. Intervirology, 2007, 50:433-438.

Conference abstracts

- Yang Xiaoyun, Steukers Lennert, Nauwynck Hans, Inhibitory Effects of Porcine Airway Mucus on Pseudorabies Virus. 4th ESVV Herpesvirus Symposium 2013, Zurich, Switzerland.
- Xiaoyun Yang, Katrien Forier, Lennert Steukers, Sandra Van Vlierberghe, Peter Dubruel, Kevin Braeckmans, Sarah Glorieux, Hans Nauwynck. Immobilization of Pseudorabies Virus in Porcine Respiratory Mucus Revealed by Single Particle Tracking. 37th International Herpesvirus Workshop 2012, Calgary, Canada.

8. Acknowledgements

I would like to thank my promoter, Prof. Hans Nauwyanck, for his effort to train me in scientific thinking and research skills. Also highly appreciated are the fruitful discussions, which have inspired me to look further into, and to get a better understanding in my research topic.

I would like to gratitude my co-promoter, Prof. Kristien van Reeth, for sharing her knowledge on influenza virus and her writing skills. I would like to show my sincere gratitude to my guidance committee members, Prof. Xavier Saelens and Prof. Stefaan De Smedt, for their general comments. I highly appreciate my examination committee members: Prof. Bachert Claus, Prof. Peter Delputte, Prof. Niek Sanders, Prof. Sarah Gloreux, Prof. Frank Gasthuys, Prof. Herman Favoreel, Prof. Dominiek Maes, Prof. Piet Deprez, Prof. Xavier Saelens and Prof. Stefaan De Smedt, for their critical and detailed comments, which have definitely helped to improve the quality of my thesis.

I would like to specially thank Prof. Sarah Glorieux, for helping me to initiate the collaboration with the Laboratory of General Biochemistry and Physical Pharmacy, where I acquired important research findings. Her scientific guidance and all her kind help in life are also highly appreciated.

Special thanks go to Prof. Herman Favoreel, for, besides the crucial comments on my thesis, his support in my postdoc searching.

I am highly grateful to my former colleague and best friend, Lennert Steukers, without whose help my research and life would not have gone smoothly. I highly appreciate him for his patience to listen, his effort to help me to settle down, his guidance in research and in writing, and most importantly, his friendship. Besides, I would like to thank Jasper for the nice conversations and the tasty food he made.

I am highly grateful to another best friend of mine, Hossein Bannazadeh Baghi, for his spiritual support, and for the lifts he has offered to me, especially when the bus was not running. I would like to thank his wife, Zenap, who has been sweet and kind to me, and for the good food she prepared.

I would like to show my sincere gratitude to all the technicians: Lieve Sys, Melanie Bauwens, Carine Boone, Zeger Vandenabeele, Nele Dennequin, Chantal Vanmaercke, Tim Van Gaever, Loes Geypen, who are always kind and helpful.

I would also like to thank the administrative staff: Dirk Demeulenaere, Gert Verdonck, Ann Machtelinckx and Mieke Godefroid for their financial and/or administrative arrangements.

I truly thank my former colleagues: Sabrina Vairo, Annelies Vandekerckhove, Annick Gryspeerdt, Mieke Verbeeck, Karl De Hert, Marc Geldhof, Dipongkor Saha, Jun Cao, Liping Huang, Zhongfang Wang, Wander Van Breedam, Sarah Costers, Sjouke Van Poucke and Dominique Olyslaegers, for their help in research and their friendship.

I truly acknowledge all my colleagues in the Laboratory of Virology: Jing Zhao, Ilias Frydas, Kathlyn Laval, Jolien Van Cleemput, Katrien Poelaert and Ivy Brown, for the pleasant conversations and scientific discussions we've made; Wenfeng Li, Jun Xiang, Shunchuan Zhang, Yu Qiu, Yewei Li, Tingting Cui, Ruifang Wei, Jiexiong Xie and Bo Yang, for the pleasant time we've had; José Carlos Mancera Gracia, Vishwanatha Reddy, Haileleul Negussie Dubale, Lowiese Desmarets , Sebastiaan Theuns , Inge Roukaerts , Isaura Christiaens, Delphine Acar, Ivan Trus, Vo Van Tuan, Thuong Van Khuong and Abubakar Garba for their kindness.

Special thanks go to Jolien Van Cleemput, Katrien Poelaert, Jochen Lamote, and Karl De Hert for translating the summary of my thesis, and to Melanie Bauwens and Delphine Acar for their grammatical checks.

I would like to specially thank my neighbors, Guangzhi Zhang, Yan Li, Zebao Zhang, Georges Bleyaert and Lily van de Berge for being amiable and supportive. My truly thanks go to all my Chinese friends: Baoyu Zhang, Qing Hai, Hanbo Zhang, Yufeng Niu, Feng Lan, Nan Zhang, Ming Zheng, Huaihan Cai, Shan Zhang, Liang Sun, Shaoren Deng, Minqi Wang, Wenwen Li, Ou Wang, Ranhua Xiong, Fang Wang, Qilu Zhang, Meng Bai, Yuechao Lu, Lei Guo, Cheng Liu, Shaoji Li, Jungang Liang, Miao He.

Last but not least, I'm truly grateful to my families, without whose love I would not have made it.